

UNIVERSITÀ DEGLI STUDI DI NAPOLI
“FEDERICO II”



TESI DI DOTTORATO DI RICERCA
TERAPIE AVANZATE BIOMEDICHE E CHIRURGICHE
XXXV CICLO

Coordinatore: Prof. Fabrizio Pane

**Next-generation probiotics in obesity and metabolic syndrome:
The effects of a genetically-modified lactobacillus paracasei producing
oleoyl-ethanolamide (OEA) in obese mice.**

Relatore

Ch.mo Prof. Giovanni Sarnelli

Dottoranda

Dott.ssa Marcella Pesce

ANNO ACCADEMICO 2021/2022

**NEXT-GENERATION PROBIOTICS AND THEIR THERAPEUTIC POTENTIAL
IN GASTROINTESTINAL DISORDERS**

- Engineered probiotics.....1
- Next-generation probiotics in inflammatory bowel disease: Engineered lactobacillus paracasei producing palmitoylethanolamide (PEA) prevents colitis in mice.....4
- Next-generation probiotics in infectious diseases: A Palmitoylethanolamide Producing Lactobacillus paracasei Improves Clostridium difficile Toxin A-Induced Colitis24

NEXT-GENERATION PROBIOTICS IN OBESITY AND METABOLIC SYNDROME.....47

BACKGROUND & AIM.....48

MATERIAL AND METHODS.....51

- Generation of genetically-modified strains of Lactobacillus paracasei subsp paracasei F19
- In vitro assessment of NAPE-PLD expression and quantification of bacterial-derived OEA release
- Animals and experimental design
- Evaluation of body weight and food intake
- Glucose tolerance test
- Insulin level assessment
- Homeostatic model assessment (HOMA)
- Cholesterol and triglycerides levels measurement
- Histological analysis
- Faecal microbiota community determination by shotgun sequencing
- Statistical analysis

RESULTS.....59

- Time- and oleate concentration-dependent NAPE-PLD enzyme expression and OEA release by pNAPE-LP in vitro
- The co-administration of pNAPE-LP and oleate reduces body weight and modulates satiety in obese mice via the in-situ production of OEA
- The co-administration of pNAPE-LP and oleate improves metabolic profile and reduces liver steatosis in HFD-treated mice via the in-situ production of OEA.
- Effects of pNAPE-LP and oleate treatment on gut microbiota profile in HFD-treated mice

CONCLUSIONS.....64

REFERENCES.....68

FIGURES AND LEGENDS.....78

ENGINEERED PROBIOTICS

Probiotics are living microorganisms that may confer health benefit(s) to the host by restoring mucosal barrier integrity, exerting immunomodulatory effects on the Gut Associated Lymphoid Tissue (GALT) and improving microbial diversity [1].

With the outstanding advancements in genetic engineering, we recently witnessed the development of bacterial/probiotic strains genetically engineered to either act as “intestinal biosensors” (detecting specific molecules within the gut milieu i.e. inflammatory markers) or as “resident cells’ factories” of therapeutic molecules (biotherapeutics improving drug delivery at the mucosal surface) [2, 3].

Biosensors are live bacteria engineered to respond to specific biomarkers by producing a reporter substrate that could be easily detected (like fluorescent proteins), hence limiting the need for invasive testing. To this aim, several biosensors have been recently developed to respond to markers of intestinal inflammation [3, 4] or bleeding [2]. Yet, biosensors should display high sensitivity and specificity toward the selected biomarker to be used as diagnostic tools. This approach is, therefore, currently hampered by the limited knowledge of relevant specific biomarkers and the number of characterized bacterial systems that can be reliably used as disease-responsive circuits.

Given these shortcomings, most published studies have focused on developing engineered probiotics able of expressing therapeutic molecules (biotherapeutic probiotics), either constitutively or “on-demand” through inducible systems that respond to exogenously administered substrates (commonly added to food or water) or to locally produced biomarkers (sense and respond systems) (Figure 1).

All biotherapeutic probiotics are live bacteria designed to produce in situ anti-inflammatory molecules, offering the main advantage of achieving the topical release of therapeutics. Therapeutic agents, indeed, may be released directly in situ, maximizing therapeutic concentrations in the target tissue using relatively smaller doses of the therapeutic compound, thus limiting systemic side effects.

Constitutive systems offer the unquestionable advantage of using relatively simpler genetic modifications, mostly expressed in a constitutive fashion by the chosen probiotic platform. However, this comes at a cost considering the large amount of energy required for the probiotic to constitutively express these substances, while also exposing to the risk of overproducing the therapeutic substance in unwanted sites, potentially hindering their effectiveness and safety, respectively.

Inducible probiotic systems overcome these two main concerns, by producing the therapeutic substance in a controlled fashion only upon activation of inducible promoters. Depending on the considered probiotic construct, several types of inducible expression systems have been produced, able of regulating the expression of the therapeutic molecule by adding exogenous substrates (like xylan, palmitate, xylose, etc.) to animals' food and/or water [5-7].

Sense and respond systems are an even more specific type of inducible system that combines and incorporates the technology of biosensors into live biotherapeutics to generate a more efficient and targeted delivery of the biotherapeutics only in response to a site-specific and/or disease-specific biomarker [2]. These systems do not respond to externally administered substances, rather they "sense" specific environmental stimuli within the gut milieu (such as low pH, heat shock, or nitric oxide) and

consequently release the therapeutic molecule, increasing the likelihood that its delivery is effectively site-specific and released under the most desirable circumstances [8]. Nonetheless, like with biosensors themselves, “sense and respond systems” are hampered by the lack of specificity of biomarkers produced along the GI tract and the limited number of reliable disease-responsive circuits identified in bacterial systems.

In this context, a recent pivotal study, using a synthetic memory circuit in *E. Coli*, has allowed recording environmental stimuli differentially activated as the bacteria passed through the host and to retain this information via reporter gene expression, thus effectively enabling a non-invasive readout of transient signals generated under physiological and inflammatory circumstances, respectively [9]. The different genetic libraries obtained from healthy or dextran sulfate sodium (DSS) -treated mice, indeed, detected a number of activators or repressors differentially expressed during gut inflammation. Though their identity or function is not fully understood, this study marks an important step forward in our understanding of novel biomarkers that may be indirectly activated during the inflammatory process, paving the way to construct disease-responsive circuits by combining multiple redundant sensors differentially responding based on the localization within the gut.

In the following chapters, we will illustrate three potential fields of application of a genetically modified *Lactobacillus Paracasei* F19 able to respond to exogenous substrates (fatty acids; i.e., palmitic and oleic acid, respectively) with the in-situ production and release of bioactive autacoid local injury antagonist amides (ALIAmides).

Next-generation probiotics in inflammatory bowel disease: Engineered lactobacillus paracasei producing palmitoylethanolamide (PEA) prevents colitis in mice

ABSTRACT

Palmitoylethanolamide (PEA) is an *N*-acylethanolamide produced on-demand by the enzyme *N*-acylphosphatidylethanolamine-preferring phospholipase D (NAPE-PLD). Being a key member of the larger family of bioactive autacoid local injury antagonist amides (ALIAmides), PEA significantly improves the clinical and histopathological stigmata in models of ulcerative colitis (UC). Despite its safety profile, high PEA doses are required in vivo to exert its therapeutic activity; therefore, PEA has been tested only in animals or human biopsy samples, to date. To overcome these limitations, we developed a NAPE-PLD-expressing *Lactobacillus paracasei* F19 (pNAPE-LP), able to produce PEA under the boost of ultra-low palmitate supply, and investigated its therapeutic potential in a murine model of UC. The coadministration of pNAPE-LP and palmitate led to a time-dependent release of PEA, resulting in a significant amelioration of the clinical and histological damage score, with a significantly reduced neutrophil infiltration, lower expression and release of pro-inflammatory cytokines and oxidative stress markers, and a markedly improved epithelial barrier integrity. We concluded that pNAPE-LP with ultra-low palmitate supply stands as a new method to increase the in situ intestinal delivery of PEA and as a new therapeutic able of controlling intestinal inflammation in inflammatory bowel disease.

INTRODUCTION

Palmitoylethanolamide (PEA) is a naturally-produced lipid derived from the hydrolysis of its phospholipid precursor, by *N*-acylphosphatidylethanolamine-specific phospholipase D (NAPE-PLD) [10-12]. PEA belongs to the larger family of bioactive autacoid local injury antagonist amides (ALIAMides), whose production is induced on-demand by several cells' types and tissues, during inflammatory noxae [13].

PEA exerts potent anti-inflammatory effects, and it has been shown to improve intestinal inflammation, following both intraperitoneal and oral administration [14], in animal models of colitis. More importantly, its efficacy has also been demonstrated in mucosal biopsies from patients with ulcerative colitis (UC) [15–17], with the peroxisome proliferator activated receptor α (PPAR α) being one of the key receptors mediating these effects [18].

Inflammatory bowel disease (IBD), which comprises Crohn's disease and UC, is a chronic relapsing inflammatory bowel disorder with multifactorial pathophysiology, featuring diarrhea, abdominal pain, and weight loss [19]. In IBD, an altered PEA turnover with relative down-expression of NAPE-PLD and overexpression of its degrading enzymes led to the postulation of an impairment of the acylethanolamide–PPAR α anti-inflammatory axis in patients with active UC [20].

In spite of the widespread use of PEA-based over-the-counter preparations for disorders featuring pain and hyper-inflammation [21], and the lack of recorded serious adverse drug reactions [22], its use in treating intestinal inflammatory conditions is currently limited by the high doses required to achieve its therapeutic effect, following oral administration. This strongly limits PEA use in current clinical practice, and

alternative strategies to efficiently increase PEA bioavailability are currently under development.

An innovative approach that may overcome such limitations could be the topical delivery of PEA at the colonic mucosa surface, by genetically-modified probiotics, able to achieve a controlled production of anti-inflammatory molecules. This probiotic system could adhere to the intestinal surface and produce specific bioactive metabolite(s) in response to an exogenous substrate; thus, behaving as a resident “cell factory” for intestinal therapeutics against IBD. This approach was first explored in the pioneer works by Djordjevic and Klaenhammer and Steidler et al. [23,24] in the late 1990s and early 2000s, and was proven to be feasible both in animals and in phase I clinical studies involving IBD patients.

Using *Lactobacillus paracasei* subsp. *paracasei* F19 (pLP) engineered with human *N*-acylphosphatidylethanolamine-specific phospholipase D-(NAPE-PLD) gene, we aimed at generating an in situ drug-delivery probiotic system, able to selectively release PEA in the gastrointestinal (GI) tract, under the boost of ultra-low doses of exogenous palmitate. Previous in vivo studies demonstrated that *Lactobacillus* F19 survived well through the human GI tract and was detected in reasonable numbers in stool specimens from 100% of studied subjects [25].

Given the high genetic stability of this widely used probiotic, we tested whether the transformed NAPE-expressing LP (pNAPE-LP) was able to release PEA effectively both in vitro and in vivo, and assessed the in vivo effects of orally administered pNAPE-LP on (i) colitis severity, (ii) plasmatic release of pro-inflammatory signaling molecules and cytokines (iii) mucosal inflammation and neutrophil infiltration and (iv)

epithelial barrier integrity in a well-validate murine model of acute colitis. Dextran sodium sulphate (DSS) is a widely used method to study various clinical and histopathological features that reflect those observed in human ulcerative colitis, because of its simplicity, inexpensiveness, and reproducibility [26].

MATERIAL AND METHODS

Generation of Genetically Modified Strains of *Lactobacillus paracasei* subsp. *paracasei* F19

The pTRKH3-slpGFP vector (Addgene, Watertown, MA, USA) was first modified to remove the GFP sequence at SalI/PstI restriction sites, insert T7 transcriptional terminators at BamHI/EcoRV sites, and insert linker sequences containing BsaI-BsaI at PstI/XmaI restriction sites. The cDNA of human NAPE-PLD was then inserted into the BsaI sites using the In-Fusion method (Clontech, Mountain View, CA, USA). The resulting pTRKH3-slp-NAPE-PLD and parental plasmid (not expressing NAPE-PLD gene, used as negative control) constructs were transfected into the *Lactobacillus paracasei* subsp. *paracasei* F19 strain (Arla Foods, Hoersholm, Denmark) by electroporation, and positive clones were obtained by erythromycin (5 µg/mL) selection. Both parental plasmid (pLP) and NAPE-PLD-expressing bacteria (pNAPE-LP) were amplified anaerobically in Man, Rogosa and Sharpe (MRS)-broth (Conda, Torrejón de Ardoz Madrid, Spain) and isolated in MRS agar (Conda, Torrejón de Ardoz Madrid, Spain), both supplemented with erythromycin 5 µg/mL (Sigma-Aldrich, Milan, Italy) under anaerobic conditions for 72 h at 37 °C. Bacteria viability was determined by manually counting colonies, and the colony forming units (CFU)/mL were obtained through a colonies number correction for the dilution factor.

Animals and Experimental Design

Six-week-old male C57BL/6J mice (Charles River, Lecco, Italy) were used for the experiments. This gender/strain of rodents has been widely validated and investigated in DSS-induced colitis, given high animal susceptibility and detailed course in acute colitis [27]. All experimental procedures were approved by Sapienza University's Ethics Committee. Animal care was in compliance with the IASP and European Community (EC L358/1 18/12/86) guidelines on the use and protection of animals in experimental research. Mice were randomly divided into the following groups ($n = 10$ each): (1) non-colitic (vehicle) group; (2) colitic group receiving a daily intragastric gavage with 200 μ L MRS broth without probiotic supplementation; colitic groups receiving a daily intragastric gavage with either (3) pLP or (4) pNAPE-LP combined with palmitate (0.0003 μ g/kg); and (5) colitic group receiving a daily intragastric gavage with palmitate alone (0.0003 μ g/kg), colitic groups receiving a daily intragastric gavage with pNAPE-LP combined with palmitate (0.0003 μ g/kg) in the presence of selective (6) PPAR α antagonist MK886 (10 mg/Kg) or (7) PPAR γ antagonist GW966 (1 mg/Kg), respectively. A representative figure of our experimental plan is depicted in Figure 2A.

In all groups, colitis was experimentally induced by administering dextran sulfate sodium (DSS 4% w/v , MW 36,000 to 50,000, Sigma Aldrich, Italy) in drinking water for six consecutive days (starting from day 1). Probiotic treatment was given daily from day 2 until day 6 by intragastric administration of 0.1 mL of bacteria suspension containing $0.8\text{--}1.2 \times 10^9$ CFU/mL of pLP or pNAPE-LP together with palmitate 0.0003 μ g/kg. PPAR α antagonist MK886 and PPAR γ antagonist GW966 were given

intraperitoneally from day 2 to day 6. During the whole length of the study, animal body weight, stool consistency and presence of bloody diarrhea were recorded daily to determine the disease activity index (DAI) (see Figure 2B). Animals were sacrificed at day 7 after colitis induction, spleen weight and colon length were measured after post-mortem isolation, and colonic tissues were removed to perform macroscopic, histochemical, and biochemical analyses, as described below.

In Vitro and In Vivo Quantification of Bacteria-Produced PEA by HPLC–MS Method

Specimens from the stomach, duodenum, jejunum, ileum, and distal colon from a subset of mice of the vehicle group treated with 0.1 mL of bacteria suspension containing $0.8\text{--}1.2 \times 10^9$ CFU/mL of pLP or pNAPE-LP together with palmitate $0.0003 \mu\text{g}/\text{kg}$ were isolated to evaluate PEA concentrations in vivo ($n = 12$ in total, 6 mice treated with pLP and 6 mice treated with pNAPE-LP). Tissues were processed according to the method described by the Endocannabinoid Research Group [28]. Extraction and analysis were performed according to Gachet et al. [29], with slight modifications. Firstly, samples of bacterial cultures were ultra-centrifuged at $10,956\times g$ for 10 min, obtaining a supernatant (representing the culture medium) and a pellet (representing the bacteria). An amount of $250 \mu\text{l}$ of supernatant was extracted with the same volume of acetonitrile (ACN) with 0.1% formic acid (extraction solution), vortexed for 1 min, and placed at $4 \text{ }^\circ\text{C}$ for 10 min, to facilitate the precipitation of proteins. Then, the samples were centrifuged ($10,956\times g$, $4 \text{ }^\circ\text{C}$, 5 min) and the supernatant was injected for the mass spectrometry analysis. For the lysis of the bacterial pellet, $200 \mu\text{L}$ of extraction solution were added to each sample and vortexed

for 1 min. Samples were kept to $-20\text{ }^{\circ}\text{C}$ for 10 min and then in an ultrasound bath for a total of 30 min (2 cycles of 15 min each, with 5 min of break). Subsequently, the samples were centrifuged ($10,956\times g$, $4\text{ }^{\circ}\text{C}$, 5 min) and the supernatant was injected for the mass spectrometry analysis. Analyses were run on a Jasco Extrema LC-4000 system (Jasco Inc., Easton, MD, USA) coupled to an Advion Expression mass spectrometer (Advion Inc., Ithaca, NY, USA) equipped with an electrospray (ESI) source. Mass spectra were recorded in positive SIM mode. The capillary voltage was set at +180 V, the spray voltage was at 3 kV, the source voltage offset was at +20 V, and the capillary temperature was set at $250\text{ }^{\circ}\text{C}$. The chromatographic separation was performed on a Kinetex C18 analytical column ($150\times 4.6\text{ mm}$, id. $3\text{ }\mu\text{m}$, 100 \AA) and security guard column, both supplied by Phenomenex (Torrance, CA, USA).

The analyses were performed at a flow rate of 0.3 mL/min , with solvent A (water containing 2 mM ammonium acetate) and solvent B (methanol containing 2 mM ammonium acetate and 0.1% formic acid). Elution was performed according to the following linear gradient: 15% B for 0.5 min , $15\text{--}70\%$ B from 0.5 to 2.5 min , $7\text{--}99\%$ B from 2.5 to 4.0 min and held at 99% B from 4.0 to 8.0 min . From 8 to 11.50 min , the column was equilibrated to 15% B and conditioned from 11.5 to 15.0 min at 15% B.

The injection volume was $10\text{ }\mu\text{L}$ and the column temperature was fixed at $40\text{ }^{\circ}\text{C}$. For quantitative analysis, standard curves of PEA (Sigma-Aldrich St. Louis, MO, USA) were prepared over a concentration range of $0.0001\text{--}1\text{ ppm}$ with six different concentration levels and duplicate injections at each level. All data were collected and processed using JASCO ChromNAV (v2.02.04) and Advion Data Express (v4.0.13.8).

Disease Activity Index (DAI)

The DAI scale was used to evaluate experimental colitis induction and progression. DAI was determined by scoring changes in body weight (0 = none; 1 = 1 to 5%; 2 = 5 to 10%; 3 = 10 to 20%; 4 = >20%); stool consistency (0 = normal; 2 = loose; 4 = diarrhea) and rectal bleeding (0 = normal; 2 = occult bleeding; 4 = gross bleeding), according to the criteria proposed by Cooper et al. [30]. DAI score was recorded daily (from day 0 to day 7) and the results were expressed as cumulative average scores in each experimental group.

Histopathological Analysis

After sacrifice, mouse distal colons were fixed in 4% paraformaldehyde (PFA), sectioned into 15 µm slices, and stained with hematoxylin and eosin (H&E) for macroscopic and histopathological assessment. Colonic histological damage was evaluated through a complex score, according to the criteria proposed by Li et al. [31] considering the following parameters: (i) distortion and loss of crypt architecture (0 = none; 1 = mild; 2 = moderate; 3 = severe); (ii) infiltration of inflammatory cells (0 = normal; 1 = mild infiltration; 2 = moderate infiltration; 3 = dense infiltration); (iii) muscle thickening (0 = normal; 1 = mild muscle thickening; 2 = moderate muscle thickening; 3 = marked muscle thickening); (iv) goblet cell depletion (0 = absence; 1 = presence); (v) crypt absence (0 = absence; 1 = presence). Slices were analyzed with a microscope Nikon Eclipse 80i by Nikon Instruments Europe (Nikon Corporation, Tokyo, Japan), and images were captured at 4× magnification by a high-resolution digital camera (Nikon Digital Sight DS-U1). Cumulative histological damage scores were expressed as average scores in each experimental group.

Protein Extraction and Western Blot Analysis

Proteins were extracted from colonic tissue and processed by Western blot analysis. Briefly, the samples were homogenized in ice-cold hypotonic lysis buffer (10 mM 4-(2-hydroxyethyl)-1-piperazineethanesulfonic acid (HEPES), 1.5 mM MgCl₂, 10 mM KCl, 0.5 mM phenylmethylsulphonylfluoride, 1.5 mg/mL soybean trypsin inhibitor, 7 mg/mL pepstatinA, 5 mg/mL leupeptin, 0.1 mM benzamidine and 0.5 mM dithiothreitol (DTT)). The resulting cytosolic extracts were mixed with a non-reducing gel loading buffer (50 mM Tris (hydroxymethyl) aminomethane (Tris), 10% sodiumdodecylsulfate (SDS), 10% glycerol, 2 mg bromophenol/mL) at a 1:1 ratio, and then boiled for 3 min followed by centrifugation at 10,000× *g* for 10 min. Protein concentration was determined using Bradford assay and equivalent amounts (50 µg) of each homogenate underwent electrophoresis through a polyacrylamide minigel. Proteins were transferred to nitrocellulose membranes that were saturated by incubation with 10% non-fat dry milk in 1X PBS overnight at 4°C and then incubated with either rabbit polyclonal anti-iNOS (Novus Biological, Abingdon, UK), rabbit polyclonal anti-COX-2 (Cell Signaling Technology, Danvers, MA, USA), rabbit polyclonal anti-IL-1β, rabbit polyclonal anti ZO-1, rabbit monoclonal anti-occludin (Abcam, Cambridge, UK) or mouse monoclonal anti-β-actin (Santa Cruz Biotechnology, CA, USA) for 2 h at room temperature (RT).

Membranes were then incubated with the specific secondary antibodies conjugated to horseradish peroxidase (HRP) (Dako, Milan, Italy). Immune complexes were revealed by enhanced chemiluminescence detection reagents (Amersham Biosciences, Milan, Italy) and exposed to Kodak X-Omat film (Eastman Kodak Co., Rochester, NY, USA).

Protein bands were then scanned and densitometrically analyzed with a GS-700 imaging densitometer. Results were expressed as OD (arbitrary units; mm²) and normalized on the expression of the housekeeping protein β -actin for mice and bacterial proteins, respectively.

Preparation of Blood Samples

Before being sacrificed, mice were deeply anesthetized. Blood samples were taken by cardiac puncture and collected in 5% EDTA vials, immediately prior to sacrifice. To determine nitric oxide (NO), prostaglandin E2 (PGE₂), interleukin 1 β (IL-1 β) and tumor necrosis factor- α (TNF α) levels, plasma was then isolated from the blood, immediately frozen, and stored at -80 °C until the assays.

Enzyme-Linked Immunosorbent Assay for TNF α , PGE₂ and IL-1 β

Enzyme-linked immunosorbent assay (ELISA) for PGE₂, IL-1 β and TNF α (all Thermo Fisher Scientific, MA, USA) was carried out on mouse plasma according to the manufacturer's protocol. Absorbance was measured on a microtiter plate reader. PGE₂, IL-1 β and TNF α levels were determined using standard curve methods.

NO Quantification

NO production was measured as nitrite (NO₂⁻) accumulation in murine plasma by a spectrophotometer assay based on the Griess reaction [32]. Briefly, Griess reagent (1% sulphanilamide, 0.1% naphthylethylenediamine in H₃PO₄) was added to an equal volume of plasma and the absorbance was measured at 550 nm. Nitrite concentration (nM) was thus determined using a standard curve of NaNO₂.

Myeloperoxidase Activity

Myeloperoxidase (MPO) activity was evaluated in colonic tissues to determine the extent of neutrophil infiltration and activation, as previously described [33]. After removal, mice colonic tissues were rinsed with a cold saline solution, opened, and deprived of the mucosa using a glass slide. The resulting layer was then homogenized in a solution containing 0.5% hexadecyltrimethylammonium bromide (Sigma-Aldrich) dissolved in 10 mM potassium phosphate buffer and centrifuged for 30 min at 20,000× *g* at 37 °C.

An aliquot of the supernatant was mixed with a solution of tetramethylbenzidine (1.6 mM; Sigma-Aldrich) and 0.1 mM hydrogen peroxide (Sigma-Aldrich). The absorbance was then spectrophotometrically measured at 650 nm. MPO activity was determined as the amount of enzyme degrading 1 mmol/min of peroxide at 37 °C and was expressed in milliunits per 100 mg of wet tissue weight.

Immunofluorescence Analysis

On day 7, animals were sacrificed, and distal colon was isolated then fixed in ice-cold 4% paraformaldehyde (PFA) and sectioned into 20 µm slices. Sections were blocked with bovine serum albumin and subsequently stained with rabbit anti-ZO-1 antibody (1:100 dilution *v/v*; Proteintech, Manchester, UK) or rabbit anti-occludin antibody (1:100 dilution *v/v*; Novus Biologicals, Abingdon, UK). Slices were then washed with PBS 1X and incubated in the dark with fluorescein isothiocyanate-conjugated anti-rabbit (Abcam, Cambridge, UK). Nuclei were stained with Hoechst. Sections were analyzed with a microscope (Nikon Eclipse 80i), and images were captured by a high-resolution digital camera (Nikon Digital Sight DS-U1).

Statistical Analysis

Results were expressed as the mean \pm SD of experiments. Statistical analysis was performed using parametric one-way analysis of variance (ANOVA) and multiple comparisons were performed by Bonferroni's post hoc test. p -values < 0.05 were considered statistically significant.

RESULTS

Time-Dependent Production of PEA by pNAPE-LP and Exogenous Palmitate

In an in vitro preliminary analysis, we tested the actual presence of PEA in the supernatant of pNAPE-LP strains after the boost of an ultra-low dose of exogenous palmitate. PEA release was measured at 1, 3, 6, and 12 h after the exposure to exogenous palmitate; native *Lactobacillus paracasei* (pLP) served as the control. We observed a significant PEA release only when the culture medium was enriched with 0.0003 $\mu\text{g/mL}$ of palmitate. The release of PEA reached the peak between 6 and 12 h, with a plateau detected at 12 h. In pLP, no detectable levels of released PEA were observed at the same time points, even when the medium was enriched with 0.0003 $\mu\text{g/mL}$ of palmitate (Figure 3A). Paralleling the in vitro results, the intragastric administration of pNAPE-LP and palmitate for four consecutive days resulted in a significantly increased expression of PEA in the duodenum (0.27 ± 0.19 , $p < 0.05$ vs pLP + palmitate) ileum (0.44 ± 0.24 , $p < 0.05$ vs pLP + palmitate) and colon (1.62 ± 0.42 , $p < 0.001$ vs pLP + palmitate), as compared to pLP-treated mice, with the highest PEA concentrations achieved in distal colonic samples (+123% vs pLP+ palmitate). On the contrary, no significant differences were observed in jejunal concentrations of PEA (Figure 3B).

Co-Administration of pNAPE-LP and Palmitate Improves the Severity of DSS-induced Colitis in Mice

Starting from day 4 after DSS administration (Figure 4), the disease activity index (DAI) score was significantly increased in colitis group (6.2 ± 1.45 , $p < 0.001$ vs vehicle), with a marked raise in bloody diarrhea and a significant body weight loss, as compared to control mice (Figure 4A). Parallel to this, a significant colonic shortening, and an increased spleen weight were also observed (Figure 4B–D, 3.9 ± 2.13 , 0.085 ± 0.012 ; all $p < 0.001$ vs vehicle). Co-administration of pNAPE-LP and palmitate ($0.0003 \mu\text{g}/\text{kg}$) significantly decreased DAI score, causing an overall improvement in the severity of all the above signs. A significant reduction in bloody diarrhea, an increase in body weight, an increase in colon length and a reduction in the spleen weight were indeed observed in mice receiving pNAPE-LP as compared to DSS-treated mice (Figure 4A–D, 1.8 ± 0.83 , 8.3 ± 1.33 , 0.032 ± 0.017 ; all $p < 0.001$ vs DSS). In mice receiving native *Lactobacillus Paracasei* (pLP), no significant changes in the severity of colitis were conversely observed, even in the presence of palmitate (Figure 4A–D). Additionally, administration of palmitate alone did not show any significant effect on DAI severity, colon length or spleen weight, confirming that palmitate per se did not affect the course of colitis. According to previously reported data [16,18,34], we also confirmed that the protective effects of pNAPE-LP + palmitate were almost completely abolished in the presence of the selective PPAR α antagonist (MK886), but not the PPAR γ antagonist (GW9662) (Figure 4A–D, 2.2 ± 0.83 , 8.05 ± 0.95 , 0.041 ± 0.017 ; $p < 0.001$ vs DSS), reflecting that pNAPE-LP-derived PEA exerts its beneficial effects through the selective involvement of PPAR α receptors.

pNAPE-LP and Palmitate Co-administration Improves Colon Histopathological Damage, Mucosal Neutrophils Infiltration and Decreases Inflammatory Markers Expression and Release in DSS-Treated Mice

Histopathological analysis revealed severe mucosal damage in DSS-treated mice that was characterized by marked mucosal neutrophil infiltration and a significant increase in MPO activity (Figure 4E–G, 7.2 ± 0.79 , 30.8 ± 4.6 ; $p < 0.001$ vs vehicle). The treatment with pNAPE-LP significantly ameliorated the colitis histopathological score and decreased MPO activity in comparison to DSS-treated mice (Figure 4E–G, 3.83 ± 0.95 , 13.4 ± 4.16 ; $p < 0.001$ vs DSS). No significant effects on both mucosal inflammation and MPO activity were conversely observed in DSS-treated mice receiving pLP and palmitate co-administration, nor were pNAPE-LP alone or palmitate able to significantly improve mucosal damage and neutrophil infiltration (Figure 4E–G). The protective effects of the pNAPE-LP strain were found to be dependent by selective targeting of PPAR α receptors, because they were inhibited by selective PPAR α , but not PPAR γ antagonism (Figure 4E–G, 3.86 ± 1.11 , 13 ± 4.6 ; $p < 0.001$ vs DSS). The expression of pro-inflammatory signaling molecules and cytokines and their release were evaluated in colonic tissue homogenates and plasma samples, respectively. Our results demonstrated that DSS-treatment caused a marked increase in colonic iNOS, COX-2 and IL-1 β in comparison to the vehicle group (Figure 5A–D, 14.9 ± 1.94 , 11.6 ± 1.83 , 24.1 ± 1.83 ; all $p < 0.001$ vs vehicle). Similarly, significant increases in the plasma level of NO, PGE $_2$, IL-1 β and TNF- α were observed (Figure 5E–H, 17.2 ± 2.35 , 6.05 ± 1.7 , 5.3 ± 1.73 , 7.83 ± 2.08 , respectively; all $p < 0.001$ vs vehicle). Treatment with pNAPE-LP and palmitate resulted in a significantly reduced expression and release of all the pro-inflammatory markers reported above, at

both colonic and plasmatic levels (Figure 5A–D, 2.91 ± 0.64 , 2.94 ± 0.31 , 8.82 ± 0.81 ; Figure 5E–H, 3.64 ± 1.9 , 1.55 ± 1.33 , 1.01 ± 0.45 , 1.05 ± 0.69 ; all $p < 0.001$ vs DSS).

Again, the anti-inflammatory effects were significantly inhibited in the presence of the PPAR α antagonist but not in the presence of the PPAR γ antagonist (Figure 5A–D, 3.65 ± 0.64 , 4.04 ± 2.13 , 9.65 ± 0.6 ; Figure 5E–H, 4.83 ± 1.73 , 2.05 ± 1.3 , 1.74 ± 0.74 , 2.1 ± 1.82 ; all $p < 0.001$ vs DSS), whereas administration of pNAPE-LP alone, palmitate, or pLP + palmitate failed to significantly inhibit the expression and the release of inflammatory mediators (Figure 5).

pNAPE-LP and Palmitate Co-administration Restores DSS-Induced Mucosal Integrity

Western blot and immunofluorescence analyses revealed a significant impairment of colonic mucosa integrity, as demonstrated by the significantly lower expression of zonula occludens (ZO-1) and occludin in DSS-treated, than in control mice (2.24 ± 1.44 , 3.24 ± 1.75 , 7.86 ± 3.69 , 8.33 ± 2.87 , respectively; both $p < 0.001$ vs vehicle; Figure 6). A marked recovery of mucosal integrity was observed in DSS-treated mice receiving pNAPE-LP + palmitate, with ZO-1 and occludin expression being significantly increased (14.4 ± 2.87 , 16.1 ± 3.52 , 22.3 ± 5.68 , 24.9 ± 2.87 ; both $p < 0.001$ vs DSS; Figure 6). This effect was completely abolished by MK886, but not GW9662 (14.4 ± 3.58 , 16.2 ± 4.09 , 21.5 ± 4.85 , 23.7 ± 4.33 ; both $p < 0.001$ vs DSS), further demonstrating the involvement of PPAR α receptors, while the administration of pLP + palmitate or palmitate was not able to significantly improve mucosal integrity in DSS-induced mucosal damage (both $p > 0.05$ vs DSS; Figure 6).

DISCUSSION

Our understanding of the pathophysiological role of gut microbiota underwent a paradigm shift in recent years. Considered as an innocent bystander for decades, accumulating evidence has clearly demonstrated its pivotal role in regulating several aspects of intestinal homeostasis, including mucosal integrity and inflammation [35,36]. In IBD, impaired host–microbiota interactions, resulting in a pro-inflammatory milieu, are essential for the maintenance and progression of mucosal inflammation [37,38]. The use of probiotics, by means of potential therapeutics in IBD [39], has therefore immediately captivated the scientific community as an innovative approach to control and inhibit gut inflammation [40]. However, despite the encouraging preclinical data, most probiotics are poor colonizers of the intestinal surface *in vivo*, and their bioactive metabolites are still poorly characterized.

Aside from the implicit regulation of the host–microbiota imbalance postulated in IBD, probiotics offer the unique prospect of serving as potential delivery systems of anti-inflammatory molecules at the mucosal surface [41]. Genetically engineered probiotics able to colonize and express anti-inflammatory mediators *in situ* could overcome some of the current therapeutic failings, providing a novel efficient therapeutic approach in IBD [42].

In the pioneering work by Steidler et al, genetically modified *Lactococcus (Lc.) lactis*, expressing murine IL-10, was able to prevent colitis development in IL-10 KO mice and to improve inflammation in DSS-induced colitis [41]. This approach in humans was, however, hindered by the poor survival of this probiotic in the gastrointestinal tract, given its poor bile and acid resistance, and the authors suggested novel strategies,

in order to improve the intestinal delivery of therapeutically engineered *Lc. lactis*, such as enteric coated formulations [42]. In a subsequent phase I clinical trial in Crohn's patients, the enteric-coated engineered *Lc. lactis* has been shown to improve the disease course in humans [43]. However, in this clinical study, patients received both bile acid binders and proton pump inhibitors due to *Lc. lactis* poor viability, in order to improve the colonization of the GI tract.

On the basis of such experimental paradigm, here, we demonstrated the feasibility of integrating a genetically-engineered probiotic, able to biosynthesize human NAPE-PLD, into the murine microbiota, and evaluated its effects on colonic inflammation in a well-validated mouse model of acute colitis, using *Lactobacillus paracasei* F19 spp., a widely used probiotic in clinical settings, that is featured by its peculiar genetic stability.

Lactobacillus F19 has also been chosen for its favorable technological features: it can tolerate the gastric acidic environment (pH 2.5, 1 h) and exposure to bile (20%, 2 h), and hence has good ability to colonize and persist in the human intestine. Binding of collagen by *Lactobacillus* strains has been described earlier [44], which, combined with the absence of adverse effects during human trials, even in subjects with underlying disorders, suggests that pLP is safe and effective as a probiotic in humans [45,46].

In line with this, our data confirm that the colonization by pNAPE-LP is achieved after four days of treatment, and it results in the highest concentration of PEA in the distal colon.

Our findings indicate that the oral treatment with pNAPE-LP and palmitate efficiently improves DSS-induced colitis in mice, as shown by the decreased DAI score, preservation of colonic length and the attenuation of splenomegaly. The co-administration of pNAPE-LP and palmitate also resulted in a significant histopathological improvement of colonic inflammation and neutrophil activation, as demonstrated by the reduced MPO activity. This, in turn, was mirrored by the significantly reduced expression and release of several proinflammatory molecules and cytokines.

These potent anti-inflammatory effects were dependent on the pNAPE-LP ability of expressing the NAPE-PLD gene and producing PEA under the boost of ultra-low doses of exogenous palmitate. In fact, the administration of either pLP or palmitate alone was ineffective in counteracting colonic inflammation and improving colitis course. In parallel, PEA release caused an overall stabilization of mucosal barrier integrity in colitic mice, likely exploiting its well-known gate-keeper functions [16] due to PEA-induced up-regulation of ZO-1 and occludin proteins.

We also replicated previous data showing that these effects are secondary to PPAR α receptors' activation; the co-administration with PPAR α , but not PPAR γ antagonists, was able to almost completely prevent its anti-inflammatory effects, further providing indirect evidence of the key role PEA of in mediating pNAPE-LP effects.

A number of genetically unmodified bacteria have shown potential anti-inflammatory properties in mice and, more recently, it has been proven that these effects are at least partially mediated by the endocannabinoid system. In a paper by Rossi et al., indeed, the widely used probiotic VSL#3 was able to modulate several genes encoding for

enzymes involved in endocannabinoid (EC) metabolism and to relatively modulate the expression of CB1 and CB2 at the intestinal surface [47]. A clear advantage of using engineered pNAPE-LP rather than wild-type probiotics is the possibility of selecting carrier bacteria that can increase the likelihood of reaching therapeutic doses of the appropriate compound and selectively modulating the endocannabinoid system.

Given its inability of activating the cannabinoid receptors, PEA is a very intriguing candidate-drug in IBD, because it offers the prospect of modulating the ECS without any virtual side effects [48,49]. A previous paper has also demonstrated that PEA is able to dose-dependently improve colonic inflammation both in mice and, most importantly, in human colonic tissue samples derived from patients with UC [16]. Thus, the main limiting factor to orally-administered PEA as a therapeutic in humans is largely related to its often-unpredictable tissue concentrations. The possibility of efficiently delivering and increasing the production of PEA in situ therefore represents a very promising strategy. Furthermore, PEA is a short-lived compound that is produced on demand and is rapidly metabolized to its inactive metabolites [50-52]. Several other strategies able to enhance PEA tissue delivery are under consideration, comprising the co-administration with polydatin and ultra-micronized formulation of PEA. However, given the short-lived activity of PEA, it is unclear whether any of these strategies could efficiently maintain its tissue concentration at therapeutic levels.

A possible critical advantage of genetically engineered probiotic systems is that being able to adhere to the mucosal surface and colonize the gut for prolonged periods, they could serve as a sustained source of PEA produced in situ. Because PEA is a naturally occurring acylethanolamine, deriving from endogenous mammals phospholipids, it

seems highly unlikely to trigger an immune response, even when chronically biosynthesized by heterologous sources (i.e., gut microbiota) [53]. Furthermore, the fact that PEA production from the therapeutically engineered *Lactobacillus* is responsive to the co-administration of an exogenous substrate (palmitate), and that both PEA and pLP have a very favorable safety profile, with virtually no side effects observed in human trials, adds to the safety of our system.

A limitation of our study is related to the fact that we did not explore the qualitative/quantitative changes in gut microbiota composition in mice. As previously stated, probiotics alone have shown the potential to modulate the ECS and positively impact on mucosal inflammation in IBD. However, pLP alone did not show any significant effects on mucosal inflammation in mice, and the pNAPE-LP + palmitate anti-inflammatory effects were mediated by the selective agonism at PPAR α receptor sites, exerted by PEA release in vivo. One could argue that given the high plasticity of the acylethanolamine–PPAR α axis, its anti-inflammatory effects could be attenuated for prolonged administrations. Further studies are required to determine the ideal interval and duration of booster administrations of pNAPE-LP able to maintain a sustained anti-inflammatory effect.

Taken together, the results of the present study highlight the importance of pNAPE-LP as a new therapeutic tool that, by counteracting mucosal immune cells infiltration and proinflammatory mediators release, may improve colitis. Moving forward, further research to evaluate the long-term, ecological, and environmental safety of this genetically modified organism, is ongoing in order to possibly translate this approach in humans.

Next-generation probiotics in infectious diseases: A Palmitoylethanolamide Producing *Lactobacillus paracasei* Improves *Clostridium difficile* Toxin A-Induced Colitis

ABSTRACT

Genetically engineered probiotics, able to in situ deliver therapeutically active compounds while restoring gut *eubiosis*, could represent an attractive therapeutic alternative in *Clostridium difficile* infection (CDI). Palmitoylethanolamide (PEA) is an endogenous lipid able to exert immunomodulatory activities and restore epithelial barrier integrity in human models of colitis, by binding the peroxisome proliferator-activated receptor- α (PPAR α).

The aim of this study was to explore the efficacy of a newly designed PEA-producing probiotic in a mice model of *C. difficile* toxin A (TcdA)-induced colitis. The human N-acyl-phosphatidylethanolamine-specific phospholipase D (pNAPE-LP), a key enzyme involved in the synthesis of PEA production was cloned and expressed in a *Lactobacillus paracasei*, that was intragastrically administered to mice 7 days prior the induction of the colitis. Bacteria carrying the empty vector served as negative controls (pLP).

In the presence of palmitate pNAPE-LP was able to significantly increase PEA production by 27900%, in a time- and concentration-dependent fashion. Mice treated with pNAPE-LP showed a significant improvement of colitis as measured by histological damage score, macrophage count and myeloperoxidase levels (-53, -82% and -70.4%, respectively). This was paralleled by a significant decrease both in the expression of Toll Like Receptor-4 (TLR-4) (-71%), phospho-p38 Mitogen-activated

protein kinase (phospho-p38 MAPK) (-72%), Hypoxia-inducible factor-1-alpha (HIF-1 α) (-53%), p50 (-74%) and p65 (-60%) and in the plasmatic release of Interleukin 6 (IL-6) (-86%), nitric oxide (NO) (-59%) and Vascular-Endothelial Growth Factor (VEGF) (-71%). Finally, mucosal barrier integrity was significantly improved by pNAPE-LP treatment as witnessed by the rescue of Zonula Occludens-1 (ZO-1) (+304%), Ras homolog family member A-GTP (RhoA-GTP) (+649%) and occludin expression (+160%). These protective effects were mediated by the specific release of PEA by the engineered probiotic, as they were abolished in PPAR α knock-out mice and in wild type mice treated with the pLP.

Herein, we demonstrated that pNAPE-LP has therapeutic potential in CDI by inhibiting colonic inflammation and restoring epithelial barrier integrity in mice, paving the way to next generation probiotics as a promising strategy in CDI prevention.

INTRODUCTION

Clostridium (Clostridioides) difficile infection (CDI) represents the leading cause of nosocomial diarrhea in North America and Europe and has been labeled as an urgent public health threat by the US Center for Disease Control and Prevention (CDC) [54]. The disease almost invariably follows a disruption of gut resident flora, allowing *C. difficile* colonization and germination of the colon, commonly caused by broad-spectrum antibiotic use. Recent estimates indicate that *C. difficile* strains can be found in up to 50 % of asymptomatic hospitalized patients; while in symptomatic individuals, the clinical spectrum may vary from uncomplicated diarrhea to even lethal pseudomembranous colitis, depending on strain virulence, on one hand and intestinal

microecological conditions (competitive colonization resistance from host microflora), on the other [55].

C. difficile virulence depends on two bacterial exotoxins, *C. difficile* toxin A and B (TcdA and B, respectively) [56], that are internalized into the host cells via receptor-mediated endocytosis and inhibit by glycosylation Ras homolog family member A-GTPase (RhoA-GTPase) [57]. RhoA-GTPase proteins are physiologically involved in actin cytoskeleton and tight junctions' assembly [58], resulting in the disruption of epithelial barrier, and consequently, a profound inflammatory response with release of proinflammatory cytokines and extensive neutrophil infiltration, through the activation of nuclear factor-kappa B (NF- κ B) signaling pathway [59].

Palmitoylethanolamide (PEA) is an endogenous, on demand-released N-acylethanolamine belonging to the family of bioactive autacoid local injury antagonist amides (ALIAmides), a group of lipid molecules involved in the regulation of several physiological processes, ranging from analgesia, neuroprotection and inflammation [60]. By selectively binding the peroxisome proliferator-activated receptor- α (PPAR α) [61], PEA exerts a wide-range of anti-inflammatory effects, downregulating inducible nitric oxide synthase (iNOS), cyclooxygenase-2 (COX-2) and tumor necrosis factor- α (TNF- α) expression, as well as NF- κ B signaling pathway, with downstream regulation of pro-inflammatory cytokines and immune cells infiltration in inflamed tissues.

PEA is produced by conjugation from palmitate and ethanolamine, through the N-acyl-phosphatidylethanolamine-specific phospholipase D (NAPE-PLD) [62], a key enzyme in both ALIAmides and endocannabinoid synthesis and is rapidly degraded after binding its receptor targets. Owing to its on-demand activity, PEA is safe and virtually

free from side effects, but requires high doses to achieve significant pharmacological effects. From a translational standpoint, this unfavorable pharmacokinetic profile is a major setback in PEA translatability to clinical contexts. It is therefore pivotal to develop new formulations and/or delivery systems able to increase PEA tissue exposure, enhancing its contact surface in the attempt of achieving an efficient therapeutic response.

To overcome this limitation, we developed a probiotic-based delivery system, by genetically engineering *Lactobacillus Paracasei subsp paracasei F19* with human NAPE-PLD gene (p-NAPE-LP), in order to achieve an in-situ delivery and release of PEA in the gastrointestinal tract, under the boost of ultra-low doses of exogenous palmitate. Lactobacilli are able to survive the gastrointestinal tract and colonize the large intestine, where they constitute part of the endogenous microflora. They are recognized as safe (GRAS) for human consumption, making them suitable vehicles to deliver therapeutic molecules in the large intestine. Based on this background, we tested the efficacy of daily intragastric administration of p-NAPE-LP in preventing the severity of colitis induced by intrarectal instillation of TcdA is a well-validated murine model that resembles the most important features observed in CDI in humans [63-65].

MATERIAL AND METHODS

Generation of genetically modified strains of *Lactobacillus paracasei* subsp *paracasei* F19 (pNAPE-LP)

The pTRKH3-slpGFP vector (Addgene, Watertown, Massachusetts, USA) was first modified to remove the GFP sequence at Sall/PstI restriction sites, insert T7 transcriptional terminator at BamHI/EcoRV sites, and insert linker sequence containing BsaI-BsaI at PstI/XmaI restriction sites. The cDNA of human NAPE-PLD was then inserted into the BsaI sites using In-Fusion method (Clontech, Mountain View, CA, USA). The resulting pTRKH3-slp-NAPE-PLD and parental plasmid (not expressing NAPE-PLD gene, used as negative control) constructs were transfected into the *Lactobacillus paracasei* subsp. *paracasei* F19 strain (Arla Foods, Hoersholm Denmark) by electroporation and positive clones were obtained by erythromycin (5 µg/mL) selection. Both parental plasmid (pLP) and NAPE-PLD expressing bacteria (pNAPE-LP) were amplified anaerobically in Man, Rogosa and Sharpe (MRS)-broth (Conda, Torrejón de Ardoz Madrid, Spain) and isolated in MRS agar (Conda, Torrejón de Ardoz Madrid, Spain) both supplemented with erythromycin 5 µg/mL (Sigma-Aldrich, Milan, Italy) under anaerobic conditions for 72 h at 37°C. Bacteria viability was determined by manually colonies count and the colony forming units (CFU)/mL was obtained through a colonies number correction for dilution factor.

Animals and experimental design

Six-weeks-old wild-type (WT) male C57BL/6J (Charles River, Laboratories, Italy) and PPAR α KO (Taconic, Germantown, New York, USA) mice were used for the experiments. All the procedures were approved by La Sapienza University's Ethics

Committee in compliance with the IASP and European Community (EC L358/18/12/86) guidelines on the use and protection of animals in experimental research. As depicted in Figure 7, C57BL/6J were randomly divided into four experimental groups ($n=10$ per group): (1) vehicle (control group); (2) TcdA group, (3) TcdA+pLP group and (4) TcdA+pNAPE-LP group, respectively. Both Vehicle and TcdA groups received 200 μ L MRS broth by intragastric gavage for one week, while the TcdA+pLP group was administered a daily volume of 200 μ L of MRS broth suspension containing 10^9 CFU of pLP strain with 0.0003 μ g/mL of sodium palmitate (Sigma-Aldrich, Milan, Italy). In the same conditions, the TcdA+pNAPE-LP group was administered by intragastric route with a daily volume of 200 μ L of MRS broth suspension containing 10^9 CFU of pNAPE-LP and 0.0003 μ g/mL of sodium palmitate. PPAR α KO mice were randomly divided into three experimental groups ($n=6$ per group): (1) vehicle (control group); (2) TcdA group and (3) TcdA+pNAPE-LP group respectively and treated as above. One week following probiotic administration, mice received by intrarectal route a single administration of phosphate buffered saline 1X (PBS 1X) or TcdA (50 μ g/mL dissolved in PBS 1X), according to the method described by Hirota (Hirota et al., 2012) to induce acute pseudomembranous colitis. After 4 h from the intrarectal administration, all mice used for the experimental plan were deeply anesthetized before being euthanatized and blood samples were collected by intracardiac puncture, and tissues were isolated and processed to further analyses (see below).

Extraction and quantification of in vitro and in vivo produced PEA by HPLC–MS method

Extraction and analysis of PEA released in vitro and in vivo were performed according to Gachet et al. [66], with slight modifications. Bacterial cultures were ultracentrifuged at 14,000 rpm for 10 min to separate culture medium and bacterial pellet. Culture media were freeze-dried and then resuspended in a solution containing acetonitrile with 0.1% formic acid (extraction solution). Then, the samples were ultracentrifuged (14,000 rpm, 4°C, 5 min) and the supernatant injected for the mass spectrometry analysis. Both bacterial pellet and mice colon tissues were firstly lysed using a lysis buffer and then evaporated under nitrogen stream. Residues were suspended in extraction solution, ultra-centrifuged (14,000 rpm, 4°C, 5 min), and the supernatant injected for the mass spectrometry analysis. Analyses were run on a Jasco Extrema LC-4000 system (Jasco Inc., Easton, MD) coupled to an Advion Expression mass spectrometer (Advion Inc., Ithaca, NY) equipped with an Electrospray (ESI) source. Mass spectra were recorded in positive SIM mode. The capillary voltage was set at +180V, the spray voltage was at 3kV, the source voltage offset was at +20V and the capillary temperature was set at 250°C. The chromatographic separation was performed on analytical column Kinetex C18 (150 × 4.6mm, id.3 μm, 100 Å) and security guard column both supplied by Phenomenex (Torrance, CA, USA). The analyses were performed at flow rate of 0.3mL/min, with solvent A (water containing 2mM ammonium acetate) and solvent B (methanol containing 2mM ammonium acetate and 0.1% formic acid)). Elution was performed according to the following linear gradient: 15% B for 0.5 min, 15-70% B from 0.5 to 2.5 min, 7-99% B from 2.5 to 4.0 min and held at 99% B from 4.0 to 8.0 min. From 8 min to 11.50, the column was equilibrated to 15% B and conditioned from 11.5 to 15.0 at 15% B. The injection volume was 10 μL and the column temperature was fixed at 40°C. For quantitative

analysis, standard curves of PEA (Sigma-Aldrich, Milan, Italy) were prepared over a concentration range of 0.0001-10 ppm with six different concentration levels and duplicate injections at each level. All data were collected and processed using JASCO ChromNAV (version 2.02.04) and Advion data express (4.0.13.8).

Histopathological analysis

After sacrifice, mice distal colon specimens were fixed in 4% paraformaldehyde (PFA), sectioned into 15µm slices and stained with hematoxylin and eosin (H&E) (Sigma-Aldrich, Milan, Italy) for macroscopic and histopathological assessment. Colonic histological damage was evaluated through a complex score, according to the criteria proposed [67], considering the following parameters: (1) distortion and loss of crypt architecture (0 = none; 1 = mild; 2 = moderate; 3 = severe); (2) infiltration of inflammatory cells (0 = normal; 1 = mild infiltration; 2 = moderate infiltration; 3 = dense infiltration); (3) muscle thickening (0 = normal; 1 = mild muscle thickening; 2 = moderate muscle thickening; 3 = marked muscle thickening); (4) goblet cells depletion (0 = absence; 1 = presence); (5) crypt absence (0 = absence; 1 = presence). Slices were analysed with a microscope Optika XDS-3L4 Ponteranica, BG, Italy) and images were captured at 4X magnification by a high-resolution digital camera (Nikon Digital Sight DS-U1). Cumulative histological damage score was expressed as average scores in each experimental group deriving by the observations of two independent qualified observers.

Determination of macrophages mucosal infiltration

Samples for immunohistochemical assessment of macrophages were isolated from both wt and PPAR α KO mouse distal colon. Tissues were fixed in 4% PFA, embedded

in paraffin, sectioned in 15 μ m slices and processed for immunohistochemistry. Slices were pretreated using heat-mediated antigen retrieval with a sodium citrate buffer, incubated with MAC387 (Abcam, Cambridge, UK) at RT [68], and detected using horseradish peroxidase (HRP)-conjugated compact polymer system. 3,3'-Diaminobenzidine (DAB) was used as the chromogen. Slices were then counterstained with haematoxylin, mounted with Eukitt (Sigma-Aldrich, Milan, Italy) and analyzed with a microscope (Optika XDS-3L4 Ponteranica, BG, Italy). Images were captured at 10X by a high-resolution digital camera and the data represent the median results of the two blinded assessors; in all cases, results of the assessments differed by no more than 5%. Results were quantified by ImageJ software (National Institutes of Health) and expressed as the number of macrophage marker antibody (MAC387) positive cells per area

Myeloperoxidase assay

Myeloperoxidase (MPO), a marker of polymorphonuclear leukocyte accumulation and general inflammation occurring in colonic tissues, was determined as previously described [69]. After removal, colonic tissues from both WT and PPAR α KO mice were rinsed with a cold saline solution, opened and deprived of the mucosa using a glass slide. The resulting layer was then homogenized in a solution containing 0.5% hexadecyltrimethylammonium bromide (Sigma-Aldrich, Milan, Italy) dissolved in 10mM potassium phosphate buffer and centrifuged for 30min at 20,000 \times g at 37°C. An aliquot of the supernatant was mixed with a solution of tetramethylbenzidine (1.6mM; Sigma-Aldrich, Milan, Italy) and 0.1mM hydrogen peroxide (Sigma-Aldrich, Milan, Italy). The solution was then spectrophotometrically measured at 650nm. MPO

activity was determined as the amount of enzyme degrading 1 mmol/min of peroxide at 37°C and was expressed in milliunits (mU) per 100mg of wet tissue weight.

Protein extraction and western blot analysis

Proteins were extracted from colonic tissue or bacteria pellets and processed by Western blot analysis. For protein extraction by bacterial pellet, a specific CelLytic™ lysis buffer (Sigma-Aldrich, Milan, Italy) was used according manufacturer's instructions. Tissue samples were homogenized in ice-cold hypotonic lysis buffer [10mM 4-(2-hydroxyethyl)-1-piperazineethanesulfonic acid (HEPES), 1.5mM MgCl₂, 10mM KCl, 0.5mM phenylmethylsulphonylfluoride, 1.5 µg/mL soybean trypsin inhibitor, 7mg/mL pepstatin A, 5mg/mL leupeptin, 0.1mM benzamidine and 0.5mM dithiothreitol (DTT)]. Both bacterial and tissue-deriving protein extracts were mixed with a non-reducing gel loading buffer [50mM Tris(hydroxymethyl)aminomethane (Tris), 10% sodium dodecyl sulphate (SDS), 10% glycerol, 2 mg/mL bromophenol] at a 1:1 ratio, and then boiled for 3 min followed by centrifugation at 10,000 × g for 10 min. The protein concentration was determined using Bradford assay and equivalent amounts (50µg) of each homogenate underwent electrophoresis through a polyacrilamide minigel. After the transfer the membranes were incubated with 10% non-fat dry milk in PBS overnight at 4°C and then exposed, depending on the experiments, with rabbit polyclonal anti-NAPE-PLD (Abcam, Cambridge, UK) (1:200 v/v), rabbit polyclonal anti-Toll Like Receptor-4 (TLR4) (Bioss Antibodies, Boston, USA) (1:1000 v/v), rabbit polyclonal anti-iNOS (Novus biological, Abingdon, UK) (1:1100 v/v), mouse monoclonal anti-RhoA-GTPase (Santa Cruz Biotechnology, Santa Cruz, CA, USA) (1:100 v/v), rabbit polyclonal anti-p38 Mitogen-Activated

Protein Kinase (p38 MAPK) (Bioss Antibodies, Boston, USA) (1:1000 v/v), rabbit monoclonal anti-phospho-p-38 (p-p38) MAPK (Santa Cruz Biotechnology, Santa Cruz, CA, USA) (1:1000 v/v), rabbit polyclonal anti-NF- κ B p65 (Sigma-Aldrich, Milan, Italy) (1:1000 v/v), mouse monoclonal anti-NF- κ B p50 (Santa Cruz Biotechnology, Santa Cruz, CA, USA) (1:1000 v/v), mouse monoclonal anti-Hypoxia inducible factor-1-alpha (HIF-1 α) (Novus biological, Abingdon, UK) (1:500 v/v), rabbit polyclonal anti-Glyceraldehyde 3-phosphate dehydrogenase (GAPDH) (Cell Signaling Technology, Danvers, MA, USA) (1:1000 v/v) according to standard experimental protocols. Membranes were then incubated with the specific secondary antibodies conjugated to HRP (Dako, Milan, Italy). Immune complexes were exposed to enhanced chemiluminescence detection reagents and the blots were analyzed by scanning densitometry (Versadoc MP4000; Bio-Rad, Segrate, Italy). Results were expressed as optical density (OD; arbitrary units= mm^2) and normalized against the expression of the housekeeping protein GAPDH. Immune complexes were revealed by enhanced chemiluminescence detection reagents (Amersham Biosciences, Milan, Italy) and exposed to Kodak X-Omat film (Eastman Kodak Co., Rochester, NY, USA OK). Protein bands were then scanned and densitometrically analysed with a GS-700 imaging densitometer. Results were expressed as OD (arbitrary units; mm^2) and normalized on the expression of the housekeeping protein GAPDH for mice and proteins.

Blood samples preparation

Before being sacrificed, mice were deeply anesthetized. Blood samples were taken by cardiac puncture and collected in 5% Ethylenediaminetetraacetic acid (EDTA) vials,

immediately prior to sacrifice. To determine nitric oxide (NO), Interleukin-6 (IL-6) and Vascular-Endothelial Growth Factor (VEGF) levels, plasma was then isolated from the blood, immediately frozen and stored at -80°C until the assays.

Enzyme-linked immunosorbent assay for IL-6 and VEGF

Enzyme-linked immunosorbent assay (ELISA) for IL-6, and VEGF (all from Thermo Fisher Scientific Inc., Monza, Italy) was carried out on mice plasma according to the manufacturer's protocol. Absorbance was measured on a microtiter plate reader. IL-6 and VEGF levels were determined using standard curves method.

NO quantification

NO production was measured as nitrite (NO_2^-) accumulation in murine plasma by a spectrophotometer assay based on the Griess reaction [70] (Di Rosa et al., 1990). Briefly, Griess reagent (1% sulphanilamide, 0.1% naphthylethylenediamine in H_3PO_4) was added to an equal volume of plasma and the absorbance was measured at 550nm. NO_2^- concentration (nM) was thus determined using a standard curve of NaNO_2 .

Immunofluorescence analysis for mucosal ZO-1 and occludin

Segments of distal mouse colon were isolated and fixed in ice-cold 4% PFA and sectioned into 20 μm slices. Sections were thus blocked with bovine serum albumin and subsequently stained with mouse anti-Zonula Occludens-1 (ZO-1) antibody (Bioss Antibodies, Boston, USA) (1:100 v/v) or rabbit anti-occludin antibody (Novus biological, Abingdon, UK) (1:100 v/v). Slices were then washed with PBS 1X and incubated in the dark with fluorescein isothiocyanate-conjugated anti-rabbit (Abcam,

Cambridge, UK). Nuclei were stained with 2-(4-amidinophenyl)-1H -indole-6-carboxamide (DAPI) (Thermo Fisher Scientific, Massachusetts, USA). Sections were analyzed with a microscope (Optika XDS-3FL4 Ponteranica, BG, Italy), and images were captured by a high-resolution digital camera (Nikon Digital Sight DS-U1). The expression of zonula occludens (ZO-1) and occludin were measured as relative fluorescence units (RFU) fold change versus vehicle groups.

Statistical analysis

Results are expressed as the mean \pm standard error (SEM) of n = 6, n=5 or n=4, respectively, sets of experiments in triplicate. Statistical analyses were performed using one-way analysis of variance, and multiple comparisons were performed using a Bonferroni post hoc test. *p < 0.05, **p<0.01 and ***p<0.001 was considered to indicate a statistically significant difference vs. control group and °p < 0.05, °°p<0.01 and °°°p<0.001 was considered to indicate a statistically significant difference vs. TcdA group.

RESULTS

Time- and palmitate concentration- dependent NAPE-PLD expression and PEA release by pNAPE-LP engineered bacteria in vitro.

We first evaluated in vitro the ability of pNAPE-LP engineered strains to release PEA in the bacterial supernatant under the boost of the ultra-low dose of exogenous palmitate and tested the optimal palmitate concentrations to use in our in vivo experiments. Our results demonstrated that NAPE-PLD protein expression increased in a time-dependent manner in pNAPE-LP bacteria, following culture medium supplementation with 0.000003-0.0003 $\mu\text{g/mL}$ of palmitate, reaching an expression peak between 6 and 12 h and a plateau at 12h (+89000% vs pLP) (Fig. 8 A and B), while NAPE-PLD was not detected in native pLP at the same time intervals. PEA concentrations significantly increased in the supernatant of pNAPE-LP, mirroring NAPE-PLD expression in a time and palmitate-dependent manner. PEA level peaked at 12 h (+27900% vs pLP) and reached a plateau concentration at the same time interval (Fig. 8 A and B). As anticipated, PEA levels were undetectable in pLP, even in the presence of the highest palmitate concentrations (0.0003 $\mu\text{g/L}$) (Fig.8 A and B).

In vivo NAPE-PLD expression and PEA release by pNAPE-LP engineered bacteria

At sacrifice, NAPE-PLD protein expression and PEA release were also evaluated in mice colonic tissues from the different experimental groups. Our data show that TcdA challenge, per se, increased NAPE-PLD expression and PEA release (+336% and +400%, respectively, versus vehicle), while the treatment with native pLP + palmitate

0.0003 µg/mL led to a further, but not significant increase in NAPE-PLD expression and PEA release (+21% and +8.95%, respectively, versus TcdA group).

Conversely, the treatment with pNAPE-LP + palmitate 0.0003 µg/mL resulted in a significant +85% and +72% relative increase of NAPE-PLD expression versus TcdA and pLP + palmitate 0.0003 µg/mL treated mice, respectively. In line with NAPE-PLD expression, PEA concentrations in colonic specimens from pNAPE-LP + palmitate 0.0003 µg/mL treated mice were increased up to +1233% versus vehicle and +150% versus pLP + palmitate 0.0003 µg/mL, respectively treated groups (Fig. 9A, C and E).

Treatment with pNAPE-LP and palmitate improves colonic histopathological damage, macrophage density and neutrophils infiltration in WT mice

TcdA challenge induced a severe mucosal damage evaluated at histopathological analysis performed by H&E (Fig. 10 A and C) in WT mice (+350% vs vehicle). Mucosal inflammation was featured by a markedly increased macrophage density in the colonic mucosa, as per immunohistochemical quantification of MAC387 positive cells (+450% versus vehicle) and by increased neutrophils infiltration, indirectly confirmed by the increased MPO activity (+633% versus vehicle) (Fig. 10E, G and I). A negligible and not significant improvement in terms of histological score (-6%), relative MAC387 density (-5%), and MPO activity (-9%) was observed in mice treated with native pLP + palmitate 0.0003 µg/mL. On the contrary, pNAPE-LP + palmitate 0.0003 µg/mL administration significantly improved the histological damage score (-53%), with a consequent reduction of MAC387+ cell count (-70.4%) and a significant reduction in MPO levels (-82%) compared to TcdA group in WT mice.

Treatment with pNAPE-LP and palmitate decreases pro-inflammatory markers expression and cytokine release in TcdA-treated WT mice.

The expression of pro-inflammatory signalling molecules and their release were evaluated in colonic tissue homogenates and plasma samples, respectively. Our results demonstrated that the intrarectal TcdA challenge caused a marked increase of TLR-4 (881%), phospho-p38MAPK (550%), HIF1 α (+489%) and of the markers of NF- κ B activation p50 (433%) and p65 (230%), versus vehicle in C57BL/6J mice. Immunoblot analysis also revealed a massive decrease of RhoA-GTPase protein expression in TcdA versus vehicle group (-87%) (Fig. 11 A and C). In parallel, plasmatic levels of IL-6 (+740%), NO (+245%) and VEGF (458%) were significantly increased in TcdA as compared to vehicle (Fig. 11E).

pLP + palmitate 0.0003 μ g/ml coadministration failed to improve the above-described parameters, as we observed a not significant variation in TLR-4 (-10%), phospho-p38MAPK (+6%), HIF-1 α (+5%) p50 (-4.0%), p65(-10%) and RhoA-GTPase (+9.5%) protein expression. Similarly, plasmatic pro-inflammatory mediators such as IL-6 (+5.6%), NO (-10%) and VEGF (-11%) were not significantly improved by native pLP + palmitate 0.0003 μ g/ml versus TcdA group.

Conversely, in the group of WT mice treated with pNAPE-LP + palmitate 0.0003 μ g/ml, we observed a reduced expression of pro-inflammatory signaling molecules with a significant decrease of TLR-4 (-71%), phospho-p38MAPK (-72%), HIF-1 α (-53%), p50 (-74%) and p65 (-60%) expression as compared to the TcdA group. In line with this, pNAPE-LP + palmitate 0.0003 μ g/ml also caused a significant recovery of

RhoA-GTPase expression (+649%) and a significant inhibition of the systemic release of IL-6 (-86%), NO (-59%) and VEGF (-71%).

Treatment with pNAPE-LP and palmitate improves the epithelial barrier function in TcdA- treated WT mice.

As a consequence of TcdA enterotoxicity, immunofluorescence analysis revealed a significant depletion of both ZO-1 and occludin protein expression, key factors regulating colonic mucosa integrity, as demonstrated by a severe loss of relative fluorescent units compared to vehicle.

Specifically, TcdA exposure caused a significant decrease of ZO-1 and occludin in C57BL/6J mice treated with TcdA (-78% and -77%, respectively vs vehicle) (Fig.12 A). A one-week course of pLP and palmitate did not improve both ZO-1 (+18%) and occludin (-16%) expression versus TcdA group (Fig. 12A), while pNAPE-LP + palmitate 0.0003 $\mu\text{g/mL}$ significantly improved mucosal integrity, with a relative increase in fluorescence intensity for both ZO-1 (+304%) and occludin (160%) in WT mice (Fig. 12C).

The effects of pNAPE-LP and palmitate are selectively mediated by PPAR α receptors

In line with the findings in WT animals, TcdA challenge caused a significant upregulation of colonic NAPE-PLD expression (+300%) and PEA release (+133%) also in PPAR α KO mice. The treatment with pNAPE-LP + palmitate 0.0003 $\mu\text{g/mL}$ caused a significant relative increase in NAPE-PLD tissue expression and PEA release in PPAR α KO mice, similarly to what observed in WT animals (+168% and +207%

respectively, compared to pLP + palmitate 0.0003 mg/mL treated mice (Fig. 9 B, D and F). Nonetheless, despite the increase in PEA tissue levels, the treatment with pNAPE-LP + palmitate 0.0003 mg/mL failed to display all the afore mentioned protective effects on the histological damage score, pro-inflammatory markers expression and plasmatic release and epithelial barrier function in this murine model. Indeed, under the same experimental conditions, pNAPE-LP + palmitate 0.0003 mg/mL administration failed to improve the histological damage score (-5%), macrophage density count (+1.5%) and MPO level quantification (+5%) (Fig. 10 B, F, D, H and J), in spite of the increased tissue production of PEA. Conversely to WT animals, no significant changes were detected neither in the expression of TLR-4 (+13%), RhoAGTPase (+3.7%), phospho-p38MAPK (-3.7%), HIF-1 α (+1.8%), p50 (-6.5%) and p65 (-1.5%) (Fig. 11B and D) nor in the plasmatic release of IL-6 (+3.4%), NO (-7%) and VEGF (+5%) in pNAPE-LP + palmitate 0.0003 mg/mL treated PPAR α KO mice versus the respective TcdA group (Fig. 11F), further confirming the role of PPAR α receptors in mediating PEA effects. Finally, TcdA exposure caused a significant decrease of ZO-1 and occludin in PPAR α KO mice treated with TcdA (-78% and -77%, respectively vs vehicle), but once again, the rescue of ZO-1 and occluding observed in WT animals treated with pNAPE-LP + palmitate 0.0003 μ g/ml appeared to be mediated by PPAR α receptors, since both ZO-1 (-0.89%) and occludin (+18%) signal intensity were unmodified by pNAPE-LP + palmitate 0.0003 mg/mL treatment in PPAR α KO mice (Fig. 12 B and D). Taken together, these results suggest the crucial importance of PPAR α receptors in mediating the effects of the engineered probiotic pNAPE-LP in our experimental conditions.

DUSCUSSION

With the continue rise in its incidence and recurrence, there has been an increasing interest toward the development of non-antibiotic based therapies for *C. Difficile* infection. The current treatment guidelines indeed, advise for the use of metronidazole and vancomycin as first-line treatment in CDI [71]; however, increasing concerns have been raised regarding the incidence of resistant strains and the rate of recurrence in successfully treated patients [72]. Being broad-spectrum antibiotics themselves, both metronidazole and vancomycin carry the potential to prolong the susceptibility to reinfection, by preventing the replenishment of the resident intestinal microflora and, in so doing, suppressing one of the most important protective colonization resistance factors from the host [73].

In this context, probiotics can, at least on paper, be effective in restoring the intestinal dysbiosis and play a protective role against CDI [74]. Although *Saccharomyces*, *Bifidobacterium*, and *Lactobacillus* genera all carried a protective effect against *C. difficile* [75,76], the efficacy of probiotics for CDI prevention and/or treatment is very limited. In keeping with this, we observed only a modest and not significant effect in limiting the histopathological damage and regulating the epithelial barrier integrity, following preventive administration of pLP in our murine model.

Aside from the obvious implication of regulating the host-microbiota imbalance, however, probiotics could serve as delivery systems of anti-inflammatory molecules able to limit the severity of CDI infection. Genetically engineered probiotics able to colonize and in-situ express anti-inflammatory mediators could overcome some of the therapeutic failings in CDI. Feasibility of oral therapy against CDI by means of using

engineered *Lactobacillus* able to express toxin-neutralizing antibodies was previously explored in a hamster model and showed therapeutic potential by reducing colonic inflammation and prolonging animals' survival [77]. In the current study, we explored the efficacy of an orally administered pNAPE-LP, in order to achieve an *in-situ* delivery and release of PEA in the gastrointestinal tract, under the boost of ultra-low doses of exogenous palmitate.

Our results show that pNAPE-LP was an effective strategy to produce PEA, both *in vitro* and *in vivo*. PEA is an endogenous bioactive lipid amide with pleiotropic homeostatic properties, including immune response regulation and inhibition of pain and inflammation, through the activation of PPAR α receptors [61]. These well-established immunomodulatory properties have been studied in a number of animal and human models featured by hyper-inflammation, such as osteoarthritis [78], neurodegenerative [79] and, notably, in inflammatory bowel diseases [62].

In our model, the prophylactic oral administration of pNAPE-LP was able to limit the severity of TcdA toxin-induced colitis by improving colonic mucosa histopathological damage and reducing the release of proinflammatory mediators in both colonic mucosa and plasma. The increase in PEA tissue levels was followed by a significant downregulation of p50 and p65, markers of NF- κ B activation, a key signaling pathway involved in down-stream regulating cytokine and intestinal proinflammatory mediators' release [80]. Besides, neo-angiogenesis induced by TcdA challenge *in vivo* has been recently reported as a contributing factor in CDI pathogenicity [81]. PEA release by pNAPE-LP + palmitate 0.0003 μ g/ml was followed by a significant reduction of HIF-1 α expression, through the inhibition of NF- κ B signalling pathway.

Since it has been demonstrated that HIF-1a activation prompts a rapid worsening of CDI pathology and mortality [81]. Our results highlight the importance of the control of the neo-angiogenesis as a further protective mechanism of pNAPE-LP administration. This is confirmed by the mitigation of both NO and VEGF secretion in our experimental conditions that is in line with previous observation of anti-angiogenic PEA effects in colon inflammatory conditions [82].

In parallel, PEA release caused an overall stabilization of mucosal barrier integrity, likely exploiting its well-known gate-keeper functions due to up-regulation of ZO-1 and occludin proteins, on one hand and the significant rescue of RhoA GTPase, on the other. PEA is also known for its ‘entourage effect’ on the endocannabinoid system (ECS), being able to potentiate the effect of prototypical endocannabinoids, but not carrying their potential side effects [83]. Interestingly, the non-psychotropic cannabinoid Cannabidiol (CBD) was able to prevent the cytotoxic damage caused by TcdA in in vitro cultured Caco-2 cells [84]. The observed increase in mucosal integrity and reduced cellular permeability in this study were mediated by the involvement of the cannabinoid-1 (CB-1) receptor. CBD is a very low-affinity CB1 ligand, that can nonetheless still affect CB1 receptor activity and the ECS in vivo in an indirect manner. Although it has been suggested that CBD is well tolerated and safe in humans at high doses and with chronic use, in vitro and in vivo studies showed potential drug metabolism interactions, cytotoxicity and decreased CB receptor activity [85,86].

On the contrary, PEA offers the prospect of modulating the ECS without any virtual side effects, owing to its inability of activating the CB receptors [87]. PEA belongs to the Autacoid Local Injury Antagonist (ALIA) amides family, a group of shortly-lived

lipids that is produced on demand and rapidly metabolized to their inactive metabolites [88]. Hence, the main limiting factor to its clinical transability in humans is PEA often-unpredictable tissue concentrations following oral administration.

Here, we demonstrated the feasibility of integrating into the murine microbiota a genetically engineered probiotic, able to topically biosynthesize PEA, overcoming such limitations.

We used the *Lactobacillus Paracasei subsp paracasei F19*, a widely used probiotic in clinical settings [89] that is featured by its peculiar genetic stability and its ability to colonize and persist in the human intestine [90]. Analogously to PEA, the *Lactobacillus Paracasei subsp paracasei F19* is considered safe for human consumption and during human trials, it showed the absence of adverse effects, even in subjects with underlying disorders, adding to the safety of our system.

One limitation of the current study is that NAPE-PLD gene is a key enzyme responsible for the production of several other bioactive lipids, including oleoyl-ethanolamine (OEA) and anandamide (AEA) and PEA production is often coupled by a relative increase of these bioactive compounds. Although we did not test their levels in our model, the evidence that the protective effects of pNAPE-LP were abolished in PPAR α KO mice supports the idea that PEA release is the key factor in mediating such effects. Nonetheless, these so-called ‘entourage’ effects on the ECS are not to be excluded a priori when considering the potential therapeutic effects of pNAPE-LP.

Another potential setback is that we explored an acute intestinal disease model by intrarectally-injecting mice with TcdA enterotoxin. This is a highly reproducible and well-validated model to replicate the pathological findings of CDI; however, it carries

the setback of not being able to explore pNAPE-LP anti-inflammatory effects for prolonged administrations and/or the secondary changes to gut microflora that would have undoubtedly strengthened our results in human pathology.

Despite these limitations, the results of the present study highlight the safety and effectiveness of pNAPE-LP that, by counteracting mucosal inflammation and restoring the epithelial barrier function, can improve TcdA-induced colitis in mice. Although further research is needed to evaluate the long-term, ecological and environmental safety of this genetically modified organism in order to translate this approach in humans, this evidence supports, for the first time, the role of PEA and this genetically engineered probiotic in counteracting CDI in mice.

NEXT-GENERATION PROBIOTICS IN OBESITY AND METABOLIC SYNDROME

ABSTRACT

Oleoylethanolamine (OEA) is an N-acylethanolamide produced on-demand by the enzyme N-acylphosphatidylethanolamine- preferring phospholipase D (NAPE-PLD). Being a key member of the larger family of bioactive autacoid local injury antagonist amides (ALIAmides), OEA displays a number of actions that are protective against obesity and related disorders, including the control of satiety and the regulation of the fat acids beta-oxidation in the adipose tissue. Despite its safety profile, however, high OEA doses are required in vivo to exert its therapeutic activity.

To overcome OEA pharmacokinetic limitations, we developed a NAPE-PLD expressing *Lactobacillus paracasei* F19 (pNAPE-LP) able to produce OEA under the boost of ultra-low (and non-toxic) oleate supply. We tested this formulation in obese mice treated with high-fat diet (HFD), investigating the effects of pNAPE-LP + oleate on weight, glycemic and lipid profile and on histological severity of liver steatosis. Moreover, we evaluated the effects of pNAPE-LP and oleate on gut microbiome composition.

The coadministration of pNAPE-LP and oleate led to time- and palmitate-concentration dependent release of OEA, resulting in a significant weight loss in HFD treated mice, with a parallel improvement in blood glucose and lipid levels and significant improvement in liver steatosis. Furthermore, at the end of the treatment, microbiome analysis revealed a restore in the imbalance between Firmicutes and Bacteroidetes ratio with an increased abundance for the strains *Lactobacillus* and

Prevotella species. These effects were strictly dependent on the ability of pNAPE-LP of integrating within the host microbiota and release the biotherapeutic in situ, since we did not observe any effects with the treatment with the native probiotic.

pNAPE-LP combined with ultra-low oleate supply stands as a new method to increase the in situ intestinal delivery of OEA as a new therapeutic in weight control and metabolic syndrome.

BACKGROUND & AIM

The metabolic syndrome is defined by the concomitant occurrence of several known cardiovascular risk factors, comprising insulin resistance, hypertension, dyslipidemia and obesity. These disorders are strictly co-dependent and share common pathophysiological mechanisms and pathways [91]. Among these, obesity represents one of the most critical contributing factors in the development and progression of metabolic syndrome and related chronic diseases, such as type 2 diabetes, atherosclerosis and non-alcoholic fatty liver disease [92-95]; with vast economic burden [96, 97]. Lifestyle and behavioral modifications, such as dietary restriction, are the cornerstone of the management of metabolic syndrome, albeit they often fail in achieving long-term and sustainable success, particularly in morbidly obese patients at higher risk of complications [98]. In this setting, pharmacological approaches should be taken into consideration to achieve body weight control and prevent and/or mitigate the long-term effects of metabolic syndrome. The endocannabinoid system (ECS) has been one of the most extensively studied pharmacological targets for its therapeutic potential in preventing obesity [99].

Being a pleiotropic endogenous signaling pathway, targeting the ECS bears the intriguing potential of modulating at once several aspects implied in the pathophysiology of the metabolic syndrome and its complications [100].

Indeed, the ECS is able of positively regulating metabolism and body composition in obesity by modulating food intake at hypothalamic level, while increasing, at the same time, peripheral lipogenesis and insulin sensitivity. For these reasons, Rimonabant, a type 1 cannabinoid (CB1) receptor antagonist, has been among the first pharmacological agents to be approved by the Food and Drug Administration (FDA) for the management of severe obesity [101,102]. Nonetheless, despite its promising therapeutic effects, it has been withdrawn from the market because of serious psychiatric side effects, particularly depression and suicide ideation [103]. Thus, novel strategies exploiting the beneficial pleiotropic effects of the ECS without increasing the risk of central side effects, driven by CB1 receptors, are utterly awaited.

Oleoylethanolamine (OEA) is an N-acylethanolamide produced on-demand by the enzyme N-acylphosphatidylethanolamine- preferring phospholipase D (NAPE-PLD) [104]. OEA belongs to the larger family of the bioactive autacoid local injury antagonist amides (ALIAmides), which are endocannabinoid-related compounds voided of the potential central side effects of classical cannabinoids, given their inability of activating the cannabinoid receptors (CBRs) [105]. OEA is, in fact, a high-affinity ligand of the intracellular Peroxisome Proliferator-Activated Receptors (PPAR) - α [106-108]. PPAR- α is a key regulator of lipid metabolism and energy homeostasis [108-109]. Indeed, fibrates retain their antihyperlipidemic and antiatherogenic functions, via PPAR- α agonism [110-112]. OEA is a more effective

inducer of PPAR- α receptors than other natural substrates (such as oleic acid) and a 500 to 900 times more potent agonist than fibrates [113]. Aside from the protective cardio-metabolic peripheral effects, OEA is also able to decrease food intake and appetite sensation, with consequent reduction of body weight in animal models and human trials [114]. For these reasons, OEA has been recently approved as a food supplement by the FDA given the positive effects in decreasing body mass index (BMI) by 7–8% with no reported side effects, aside from nausea, in clinical trials [115, 116]. However, the main issue limiting OEA therapy is its rapid metabolism along the gastrointestinal (GI) tract. Indeed, pharmacokinetic studies show that when administered orally, radiolabeled OEA was rapidly metabolized with only 0.48% of the given dose found at tissue level [115].

Using *Lactobacillus paracasei subsp paracasei F19* (pLP) engineered with human N-acylphosphatidylethanolamine-specific phospholipase D-(NAPE-PLD) gene, we aimed at generating an in-situ drug-delivery probiotic system, able to selectively release OEA in the GI tract, under the boost of ultra-low dose of exogenous oleate.

Given the high genetic stability of this widely used probiotic, we tested whether the engineered NAPE-expressing LP (pNAPE-LP) was effectively able to release OEA and assessed the *in vivo* effects of orally administered pNAPE-LP and oleate on (i) weight and food intake, (ii) plasmatic levels of blood glucose and lipids (iii) histopathological severity of liver steatosis and (iv) microbiome composition in obese mice treated with high-fat diet (HFD).

MATERIALS AND METHODS

*Generation of genetically-modified strains of *Lactobacillus paracasei* subsp *paracasei* F19*

The pTRKH3-slpGFP vector (Addgene) was first modified to remove the GFP sequence at Sall/PstI restriction sites, insert T7 transcriptional terminator at BamHI/EcoRV sites, and insert linker sequence containing BsaI-BsaI at PstI/XmaI restriction sites. The cDNA of human NAPE-PLD was then inserted into the BsaI sites using In-Fusion method (Clontech). The resulting pTRKH3-slp-NAPE-PLD construct was transfected into the *Lactobacillus Paracasei* by electroporation and positive clones were obtained by erythromycin (5 µg/mL) selection. Probiotics pLP (LP strain with empty expression plasmid) and pNAPE-LP (LP strain expressing human NAPE*pld* gene) were amplified anaerobically in Man, Rogosa and Sharpe (MRS)-broth (Conda, Torrejón de Ardoz Madrid, Spain) and isolated in MRS agar (Conda, Torrejón de Ardoz Madrid, Spain) both supplemented with erythromycin 5 µg/ml (Sigma-Aldrich, Milan, Italy) under anaerobic conditions for 72 h at 37 °C. Bacteria viability was determined by manually colonies count and the colony forming units (CFU)/ml was obtained through a colonies number correction for dilution factor.

In vitro assessment of NAPE-PLD expression and quantification of bacterial-derived OEA release

To test the ability of pNAPE-LP to release OEA in presence of oleate, respectively, 0.8-1.2 x 10⁹ CFU/ml of bacteria have been supplemented with increasing concentrations of oleate (0.0003, 0.00003 and 0.000003 µg/l) in the culture medium. Bacterial samples were ultra-centrifuged at 14,000 rpm for 10 min to obtain the

supernatants (culture medium) and pellets (bacteria) at 1, 3, 6 and 12 h after challenge with oleate. Extraction and analysis were performed according to Gachet et al [66] with slight modifications. Briefly, an amount of 250 μ l of supernatant was extracted with the same volume of ACN with 0.1% formic acid (extraction solution), vortexed for 1 min and placed at 4°C for 10 min, to facilitate the precipitation of proteins. Then, the samples were then centrifuged (14,000 rpm, 4°C, 5 min) and the supernatant injected for the mass spectrometry analysis. For the lysis of the bacterial pellet, 200 μ l of extraction solution were added to each sample and vortexed for 1 min. Samples were kept to -20°C for 10 min and then in ultrasound bath for 30 min (2 cycles of 15 minutes each, with 5 minutes of break). Subsequently, the samples were centrifuged (14,000 rpm, 4°C, 5 min) and the supernatant injected for the mass spectrometry analysis. Analyses were run on a Jasco Extrema LC-4000 system (Jasco Inc., Easton, MD) coupled to an Advion Expression mass spectrometer (Advion Inc., Ithaca, NY) equipped with an Electrospray (ESI) source. Mass spectra were recorded in positive SIM mode. The capillary voltage was set at +180 V, the spray voltage was at 3 kV, the source voltage offset was at +20 V and the capillary temperature was set at 250°C. The chromatographic separation was performed on analytical column Kinetex C18 (150 \times 4.6 mm, id.3 μ m, 100 Å) and security guard column both supplied by Phenomenex (Torrance, CA, USA). The analyses were performed at flow rate of 0.3 mL/min, with solvent A (water containing 2 mM ammonium acetate) and solvent B (methanol containing 2 mM ammonium acetate and 0.1% formic acid). Elution was performed according to the following linear gradient: 15% B for 0.5 min, 15-70% B from 0.5 to 2.5 min, 7-99% B from 2.5 to 4.0 min and held at 99% B from 4.0 to 8.0 min. From 8 min to 11.50, the column was equilibrated to 15% B and conditioned from

11.5 to 15.0 at 15% B. The injection volume was 10 μ L and the column temperature was fixed at 40°C. For quantitative analysis, standard curves of OEA (Sigma-Aldrich St. Louis, MO, USA) were prepared over a concentration range of 0.0001-1 ppm with six different concentration levels and duplicate injections at each level. All data were collected and processed using JASCO ChromNAV (version 2.02.04) and Advion data express (4.0.13.8). OEA concentration (μ g/ml) in pNAPE-LP-derived supernatants was determined and compared to non-expressing NAPE-PLD bacteria at 1, 3, 6 and 12 hours. In parallel, NAPE-PLD protein expression was determined in pNAPE-LP pellets by using B-PER bacterial protein extraction reagent (Thermo Fisher Scientific, Massachusetts, USA) and western blot analysis at the same time points.

Animals and experimental design

All experiments involving animals were carried out according to Sapienza University's Ethics Committee. Animal care was in compliance with the IASP and European Community (EC L358/1 18/12/86) guidelines on the use and protection of animals in experimental research. Six-weeks-old male C57BL/6J mice (Charles River, Lecco, Italy) were used for the experiments. All mice were maintained on a 12-hour light/dark cycle in a temperature-controlled environment with access to food and water *ad libitum*. We used an accelerated high-fat diet (HFD) protocol [117] to induce the onset of obesity/overweight at 4–6 weeks of diet ingestion [118]. In the initial set of experiments assessing the effect of HFD on body weight and metabolic disorder onset, mice were fed with a standard chow diet containing 6.2% fat (SD group, n = 10; Charles River, Lecco, Italy), or with a high-fat diet containing 72% fat (HFD, n = 10; modified DIO 70% kcal fat diet with 2% additional corn oil, TestDiet, Richmond, IN)

for 12 weeks. Weekly body weight was measured to monitor overweight progression. Glucose tolerance test, HOMA index (homeostatic model assessment), fasting baselines of glucose, insulin, cholesterol, and triglyceride were measured in each mouse at week 12. In a second set of experiments, we tested whether 8-weeks of oleate-pNAPE-LP treatment reverted the HFD-induced metabolic and behavioral dysfunction in mice fed with HFD for 12 weeks in comparison with pLP-oleate (0.0003 $\mu\text{g}/\text{Kg}$) treatment. One group of mice (vehicle, $n = 10$) continued on a standard chow diet for the entire duration of the study, receiving a daily intragastric gavage with MRS broth without probiotic. The other three groups of mice ($n = 10$ mice per group) received an HFD for 12 weeks prior to the beginning of probiotic treatment and remained on this diet for the entire duration of the study (8 weeks). Two of these groups received a daily intragastric gavage with pLP (pLP+oleate group) or pNAPE-LP (pNAPE-LP+oleate group) combined with oleate (0.0003 $\mu\text{g}/\text{Kg}$), respectively, while the last group of mice (HFD group) continued on an HFD without any supplementary treatment. Probiotic treatment consisted in 0.1 ml of bacteria suspension containing $0.8\text{-}1.2 \times 10^9$ CFU/ml of pLP or pNAPE-LP supplemented by oleate (0.0003 $\mu\text{g}/\text{Kg}$) for 8 weeks. Food intake and body weight were determined weekly. At the end of the study, glucose tolerance test, HOMA index (homeostatic model assessment), fasting baselines of glucose, insulin, cholesterol, and triglyceride were measured again, and then mice were euthanized and blood and tissues were collected. At euthanasia, epididymal fat pads were collected, weighed immediately, and expressed as an average ratio of total mouse body weight for each group. Feces were collected before and during bacterial treatment in either set of experiments.

Evaluation of body weight and food intake

Weekly body weight was recorded for each animal during the entire duration of the study. As healthy adult mice continued to grow throughout the study period, we compared the average weights of SD and HFD groups each week by *t-test* to assess the obesity/overweight onset. Also, we reported the gain in body weight for each group during the entire duration of probiotic treatment and showed the average weight gain at the end of the treatment as a percentage of initial body weight [initial weight (g)/total weight (g)]X100. This verifies that weight gain was not influenced by initial animal weight. Weekly food intake was measured by adding pre-weighed food pellets to each cage and then reweighing the remaining pellets. Cumulative food intake for each experimental group was reported weekly during the 8 weeks under probiotic treatment.

Glucose tolerance test

To mimic the human glucose tolerance test, mice fasted for 6 h during the onset of the light cycle. This fasting period is more physiological if compared to humans because mice are active during the light-dark phase. Briefly, blood was drawn by cutting the tail with a scalpel to obtain fasting blood glucose values by Multicare in glucometer (Gima S.p.A., Milan, Italy). Following an intraperitoneal injection of glucose solution (1 g/kg in a 10 ml/kg volume), blood glucose measurements at 15-, 30-, 60-, and 90-minute time points were repeated. Glucose tolerance was evaluated by generating a curve of blood glucose levels (mg/dl) and measuring the related area-under-curve (AUC). Glucose tolerance impairment is indicated by the larger area under curve (AUC) values.

Insulin level assessment

We performed to collect serum samples for fasting insulin levels measurement together with the glucose tolerance test. Before the intraperitoneal injection of glucose solution, baseline blood was collected into a capillary tube. Capillary tubes were spinned into a microhematocrit centrifuge at 12,000 g for 10 min to split serum and red blood cells. Serum samples have been frozen at -20°C for later measurements and, then, fasting insulin was measured by ELISA (Ultra-Sensitive Mouse Insulin ELISA Kit, Crystal Chem, Elk Grove Village (IL), USA).

Homeostatic model assessment (HOMA)

Homeostatic model assessment (HOMA) values were calculated as an estimate of insulin sensitivity, using the formula $\text{fasting plasma glucose (mmol/L)} \times \text{insulin } (\mu\text{U/ml})/22.5$ as previously described [119]. Higher values of HOMA indicate reduced insulin sensitivity.

Cholesterol and triglycerides levels measurement

Fasting baselines of cholesterol and triglycerides (mg/dl) were measured together with fasting blood glucose measurement by Multicare in glucometer (Gima S.p.A., Milan, Italy).

Histological analysis

Liver tissues were fixed in paraformaldehyde, processed in paraffin blocks, embedded and sectioned at $5 \mu\text{m}$, and stained with hematoxylin and eosin using a standard procedure. The cellular structure and lipid accumulation in tissue samples were

observed and photographed ($\times 200$, original magnification) under a microscope (Olympus, BX43; Olympus Co., Tokyo, Japan).

Fecal microbiota community determination by shotgun sequencing

Fecal samples were collected in a sterilized Eppendorf tube and stored at $-20\text{ }^{\circ}\text{C}$ until processing or $-80\text{ }^{\circ}\text{C}$ for long-term storage. DNA concentration was quantified via Qubit (ThermoFisher Scientific) and DNA extraction from the stool samples was performed using the MagBind Stool DNA according to the manufacturer's instruction (Omega Bio-Tek). The libraries were prepared using CeleroTM DNA-Seq Library Preparation Kit (Tecan, Männedorf, CH), according to the manufacturer's instructions. Both input and the final libraries were quantified by Qubit 2.0 Fluorometer (Invitrogen, Carlsbad, CA) and quality tested by Agilent 2100 Bioanalyzer High Sensitivity DNA assay (Agilent technologies, Santa Clara, CA). After the Qubit quantification and quality test, the library was sequenced on NovaSeq 6000 in paired-end 150 bp, producing a number of reads per sample.

Statistical analysis

Results were expressed as mean \pm SEM of experiments. Statistical analysis was performed using parametric one-way analysis of variance (ANOVA) and multiple comparisons were performed by Bonferroni's post hoc test. p values <0.05 were considered significant. Metagenomic studies were performed by shotgun sequencing (WGS) and analyzed by the GAIA platform (v 2.02) (<https://metagenomics.sequentiabiotech.com/>) [120] to obtain taxonomy tables at different levels. Through the R phyloseq package (v 1.36.0), the alpha-diversity was computed with the indexes Shannon and Chao1, and the beta-diversity was also

computed with the Bray-Curtis dissimilarity index for the overall taxonomic composition among samples. DESeq2 (v 1.32.0) was used to perform pairwise differential abundance analyses between the different groups at the 20-week endpoint. Analyses are based on the threshold of significance $p < 0.05$. The overall statistical analysis was done on program R (version 4.1.0), using ggplot2 (v 3.3.5), ggbur (v 0.4.0), reshape2 (v 1.4.4) packages.

RESULTS

Time and oleate concentration-dependent OEA production by pNAPE-LP expressing bacteria.

In preliminary setup experiments in vitro, we tested in the bacterial supernatant whether pNAPE-LP strains were effectively able to release OEA in the presence of exogenous oleate. We measured OEA concentrations and NAPE-PLD protein expression at 1, 3, 6 and 12 hours after the exposure to exogenous oleate; lactobacilli carrying the empty vector (pLP) served as control.

In pNAPE-LP bacteria, the expression of NAPE-PLD significantly increased only when culture medium was enriched with 0.000003-0.0003 $\mu\text{g/ml}$ of oleate, with a peak of expression between 6 and 12 h (Fig. 13B). Similarly, the concentration of OEA was significantly increased in the supernatant of pNAPE-LP in the same experimental conditions (Fig. 13A). No significant changes in the expression of NAPE-PLD and in the release of OEA were observed at the same time points in native bacteria (pLP), even at highest oleate concentrations (Fig.13). These findings confirm that enzymatic expression NAPE-PLD is controlled by the co-administration of oleate, since OEA release from pNAPE-LP was absent at baseline.

The co-administration of pNAPE-LP and oleate reduces body weight and modulates satiety in obese mice via the in-situ production of OEA

Six weeks after the start of the HFD, we observed a progressive trend toward increasing body weight in C57BL6J mice (+23% $p < 0.05$ at week 6), reaching a peak between week 10 and 12 as compared to mice fed with the Standard Diet (SD) (+30.4%

and +32%, both $p < 0.01$ vs SD at 10 and 12 weeks, respectively) (Figure 14A). Paralleling this, a significant increase in endymal fat pads was also observed (+243% vs SD, $p < 0.0001$; figure 14D).

The treatment with pNAPE-LP and oleate induced a progressive and significant weight loss compared to HFD mice starting from week 4 after probiotic treatment. After 8 weeks of treatment, the normalized body weight loss for the pNAPE-LP and oleate group was -324% as compared to untreated mice, with mean body weight values comparable to those of the control group ($p = \text{NS}$ vs SD at week 20) (Figure 14A and B). Importantly, the effects on weight were not related to an adverse health effect of treatment with pNAPE-LP, since probiotic supplementation did not increase fecal pellets over the course of the experimental plan, witnessing the absence of GI distress in treated mice (Figure 15). Indeed, such effects were the consequence of a progressively reduced food intake in pNAPE-LP and oleate group as compared to untreated mice (-10.74% at the final time point 8 weeks, $p < 0.0001$) (Figure 14C)

In mice receiving the native *Lactobacillus Paracasei* (pLP), no significant body weight changes were observed, even in the presence of oleate (figure 14). Additionally, administration of oleate alone failed to improve body weight, confirming that oleate *per se* did not exhibit orexigenic effects.

The co-administration of pNAPE-LP and oleate improves metabolic profile and reduces liver steatosis in HFD-treated mice via the in-situ production of OEA.

Histopathological analysis of liver specimens using H&E staining demonstrated an increased intrahepatic accumulation of triglycerides of HFD treated mice. Treatment with pNAPE-LP and oleate for 8 weeks was able to significantly reduce hepatic

triglyceride accumulation. Indeed, histological examination showed a significant decrease in triglyceride accumulation in mice treated with pNAPE-LP oleate, but not in the other treatment groups (figure 16).

Paralleling the improvement in liver steatosis, serum levels of cholesterol and triglyceride levels were improved following the treatment with pNAPE-LP and oleate (-33.7% and -31.2% vs HFD, respectively; both $p < 0.001$) (figure 17 E, F).

To assess the presence of insulin resistance, we tested glycemic profile following the glucose tolerance test, as well as fasting insulin and the HOMA-IR values. HFD-treated mice showed apparent signs of insulin resistance with a markedly increased glucose peak at 20 minutes following the glucose tolerance test (+60.3% $p < 0.01$ vs SD) (Figure 17 A, B) and higher levels of fasting insulin and HOMA-IR values as compared to mice fed with the standard diet (+609% and +707.8%, $p < 0.05$ and $p < 0.0001$ vs SD; respectively) (Figure 17 C, D).

Treatment with pNAPE-LP and oleate improved glucose tolerance in HFD mice compared to vehicle or pLP groups. The area under the curve (AUC) for glucose was significantly reduced by the treatment with pNAPE-LP + oleate (-36.8% vs HFD, $p < 0.01$). Also, both fasting insulin levels and HOMA-IR index showed a remarkable improvement in the pNAPE-LP and oleate group (-86.5% and -65.6%, $p < 0.01$ and $p < 0.001$ vs HFD; respectively) (Figure 17).

Again, none of the positive effects on the metabolic profile were not observed in mice treated with either pLP or oleate alone, witnessing that these effects were selectively dependent by the release of OEA by pNAPE-LP under the boost of ultra-low doses of oleate (Figure 17).

Effects of pNAPE-LP and oleate on gut microbiota profile in HFD-treated mice

At the end of our experimental plan (week 20), the gut microbiota profile of the HFD group showed an imbalance in the ratio between Firmicutes/Bacteroidetes phyla (F/B), as compared to the controls with an average of 0.96. At genus level, this imbalance mirrored a significant increase in *Blautia*, *Coprococcus*, and *Tynzerella* and a decrease in *Lactobacillus*, *Prevotella* and *Parabacteroides* in the HFD diet group as compared to controls. The treatment with pNAPE-LP + oleate led to a decrease in the imbalance of the F/B ratio, with an average value as 0.46 (Figure 18A) and induced an increased representation for the genera *Lactobacillus* sp., *Bacteroides*, and *Prevotella* (Figure 18B). In the figure 18D, it is depicted the Log₂ fold-changes (Log₂FC) obtained by comparing HFD vs pNAPE-LP and oleate treated group. Following pNAPE-LP treatment, we observed an increase for the genera *Eisenbergella* (1.58) and *Ruminococcus* (1.04), and a decrease for *Parabacteroides* (-2.96), *Escherichia* (-3.89), unknown *Bacteroidales* (o) (-1.35) and *Lactobacillaceae* (f) (-5.86) as compared to HFD mice.

The analysis at species level showed an increase in the relative abundance for *Lactobacillus acidophilus*, *Lactobacillus gasseri*, *Lactobacillus paracasei*, *Prevotella* sp. in pNAPE-LP treated mice. Interestingly, this effect was not apparent in the group treated with native *Lactobacillus* (pLP) and oleate group. As depicted in Figure 19A, indeed we observed that the strains *Lactobacillus paracasei* showed a major percentage abundance for the pNAPE-LP and oleate group than pLP.

Finally, we built a heatmap with the relative abundance obtained with DESeq2 at the significant species strain, with the replicates for the different experimental conditions.

In the HFD group, the graph revealed a cluster (Figure 20A), with an abundance of species of the phylum Firmicutes and a reduction for Bacteroidetes; in fact, we found an increase in *Ruminococcus* sp, *Tynzerella*, *Veillonella* and *Blautia* sp., and a reduction for the strains *Lactobacillus acidophilus*, *Lactobacillus fermentum*, *Prevotella*, *Akkermansia* sp.

To further analyze the structure of the bacterial community, we performed the principal coordinate analysis (PCoA) based on Bray-Curtis distance (Figure 20B). The results revealed cluster distributions, and two principal component scores, representing 43.6% and 17.8% of total changes. In fact, confirming the results of the heatmap, we observed a clustering among the pNAPE-LP group and control group, signifying that following the treatment with the engineered probiotic the composition of the gut microbiota resembled that of non-obese mice. In contrast, the pLP and HFD groups showed a greater dispersion away from the control group, witnessing the persistent perturbation in gut microbiota species, following a HFD regimen.

CONCLUSIONS

The term *globesity* has been coined by the World Health Organization (WHO) to reflect the huge economic and healthcare burden represented by obesity and metabolic syndrome complications worldwide [121]. There is an urgent call for new pharmaceuticals able to counteract weight gain and most importantly, target obesity related-disorders such as insulin resistance and type 2 diabetes, hyperlipidemia and non-alcoholic fatty liver disease [96,97,122]. In this context, OEA represents an ideal candidate because it combines its orexigenic effects with the peripheral agonism at PPAR- α receptors, key therapeutic targets for their antihyperlipidemic properties [114]. The FDA has indeed recently approved OEA supplements in obese patients, based on the evidence that it is able to reduce BMI values in clinical trials, without any serious side effects [123]. However, limiting its potential therapeutic application stands the rapid catabolism of OEA and other ALIAmides in the GI tract. Indeed, less than 1% of the oral doses of OEA actually reaches its target tissue [116]. This accounts for conflicting results reported in clinical trials in vivo, with no effects observed on body weight and satiety in 50 obese patients [124]. Of note, a concentration of at least 300nM is required to exert these protective cardiometabolic effects [125].

To overcome this unfavorable pharmacokinetic profile, we genetically modified a *Lactobacillus paracasei* F19 to express the human NAPE-PLD gene and respond to the co-administration of oleate with the in-situ production of OEA.

Our results demonstrate that our probiotic platform was effectively able to respond in a time- and oleate-dependent manner with the release of OEA. This in turn, was paralleled by a progressive decrease in body weight and epididymal fat in HFD treated

mice. The effects on weight control were directly related to the progressively reduced food intake in mice treated with pNAPE-LP, yielding to body weight values comparable to those of the control group on standard diet by the end of the experimental plan. Mirroring the decrease in food intake and weight, we observed a progressive improvement in mice's metabolic profile with reduced levels of cholesterol and triglycerides. Furthermore, the glucose peak after tolerance test and fasting insulin levels were markedly reduced, indicating a significant improvement of insulin resistance. This also resulted in the histopathological improvement of liver steatosis.

These potent orexigenic and positive metabolic effects were strictly dependent on the in-situ production of OEA under the boost of ultra-low doses of exogenous oleate, by the engineered probiotic. In fact, the administration of either pLP or oleate alone was ineffective in reducing body weight and improving the metabolic profile.

OEA belongs to the larger family of ALIAmides, endocannabinoid-related compounds which are released and act as on-demand signaling molecules, displaying their therapeutic effects on non-conventional cannabinoid receptors [105-106]. Owing to its inability of activating the cannabinoid receptors, OEA is a very intriguing candidate-drug because it is voided of potential central side effects, like the ones observed for rimonabant; a promising and effective anti-obesity drug, withdrawn from the market for the increased risk of psychiatric disorders [103, 109]. OEA orexigenic effects are attributed to the modulation of the release of hypothalamic neurotransmitters that inhibit food intake and increase satiety, such as oxytocin [126]. The main receptor target by which OEA modulates food intake is the PPAR α receptors, which OEA

activates with higher affinity compared to fibrates and other naturally- occurring agonists, such as oleic acid itself [110,127]. Indeed, in our experimental conditions, the ultra-low doses of oleate administered were unable to exert these protective effects, resulting in no significant differences with the control group.

Aside from PPAR α receptors, however, OEA also recognizes other important pharmacological targets involved in energy homeostasis, such as the G-coupled receptor GPR119, which is in turn able to increase the release of Glucagon-like peptide 1 (GLP-1), one of the most important gut-derived peptides modulating satiety signals [128, 129]. Furthermore, OEA also targets the Transient Receptor Potential Vanilloid 1 (TRPV1) expressed on vagal afferents and exerts analgesic and anorexic effects [130]. Combined with the effects on central neuropeptides and appetite regulation, OEA agonism on PPAR α also reduces dyslipidemia and liver steatosis by up-regulating the expressions of several genes involved in fatty acids uptake, utilization, and catabolism, including peroxisomal and mitochondrial fatty acid β -oxidation [110].

A number of studies have linked intestinal dysbiosis and obesity. Reproducing previous results reported in Literature, we indeed observed that a prolonged HFD markedly disrupts the F/B ratio of resident microbiota. Based on this evidence, it has been postulated that probiotics (e.g. *Lactobacillus* spp. and *Bifidobacterium* spp.) may elicit anti-obesity effects by modulating gut microbial community and influencing host metabolism [131-132]. *Lactobacillus paracasei* F19 was the chosen probiotic platform for its ability of being a good colonizer of the human intestine combined with the absence of adverse effects during human trials, even in subjects with underlying disorders; suggesting its safety and effectiveness as a probiotic [45,46].

In line with this, our data confirm that the colonization by pNAPE-LP was effectively achieved since by the end of the treatment the relative abundance of *Lactobacilli* strains significantly increased compared to the HFD group. The microbiota profile of pNAPE-LP tended to cluster with the SD-fed mice, while HFD and pLP-treated groups showed a greater dispersion from the control group. Interestingly, the group treated with the native probiotic (pLP) did not show a significant increase in *Lactobacilli* colonization at the end of the treatment, as compared to untreated mice. This demonstrates that, despite being a good colonizer, *Lactobacillus paracasei* F19 failed to successfully engraft in a perturbed microbiota, like the one observed following a prolonged high fat diet. This reflects the evidence from real-life practice showing that probiotic therapy may have null, if not conflicting effects, in certain populations of patients, as a consequence of their inability of establishing a niche within the resident gut microbiota [133].

The observation that only the engineered probiotic, but not the native *Lactobacillus paracasei* was able to increase the relative abundance of *Lactobacilli*, leads to hypothesize that the release of OEA might also positively influence its engraftment within the host microbiota, maximizing the therapeutic impact of pNAPE-LP treatment.

Overall, the results of the present study suggest that pNAPE-LP may represent a new therapeutic tool in obesity and metabolic syndrome by modulating intestinal dysbiosis while also releasing OEA at therapeutic concentrations within the gut milieu; with sustained effects on weight control, insulin sensitivity, dyslipidemia and liver steatosis.

REFERENCES

1. Hill C., Guarner F., Reid G., Gibson G. R., Merenstein D. J., Pot B., et al. The international scientific association for probiotics and prebiotics consensus statement on the scope and appropriate use of the term probiotic. *Nat. Rev. Gastroenterol. Hepatol.* 2014; 11 506–514. doi:10.1038/nrgastro.2014.66.
2. Mimee M, Nadeau P, Hayward A, et al. An ingestible bacterial-electronic system to monitor gastrointestinal health. *Science.* 2018;360(6391):915-918. doi:10.1126/science.aas9315.
3. Cui M, Pang G, Zhang T, et al. Optotheranostic Nanosystem with Phone Visual Diagnosis and Optogenetic Microbial Therapy for Ulcerative Colitis At-Home Care. *ACS Nano.* 2021;15(4):7040-7052. doi:10.1021/acsnano.1c00135.
4. Riglar DT, Giessen TW, Baym M, Kerns SJ, Niederhuber MJ, Bronson RT, Kotula JW, Gerber GK, Way JC, Silver PA. 2017. Engineered bacteria can function in the mammalian gut long-term as live diagnostics of inflammation. *Nat Biotechnol* 35:653–658. doi:10.1038/nbt.3879.
5. Wang L, Liao Y, Yang R, et al. An engineered probiotic secreting Sjl6 ameliorates colitis via Ruminococcaceae/butyrate/retinoic acid axis. *Bioeng Transl Med.* 2021;6(3):e10219. Published 2021 Apr 2. doi:10.1002/btm2.10219.
6. Esposito G, Pesce M, Seguella L, et al. Engineered *Lactobacillus paracasei* Producing Palmitoylethanolamide (PEA) Prevents Colitis in Mice. *Int J Mol Sci.* 2021;22(6):2945. Published 2021 Mar 14. doi:10.3390/ijms22062945.
7. Hamady ZZ, Scott N, Farrar MD, et al. Xylan-regulated delivery of human keratinocyte growth factor-2 to the inflamed colon by the human anaerobic commensal bacterium *Bacteroides ovatus*. *Gut.* 2010;59(4):461-469. doi:10.1136/gut.2008.176131.
8. Barra M, Danino T, Garrido D. Engineered Probiotics for Detection and Treatment of Inflammatory Intestinal Diseases. *Front Bioeng Biotechnol.* 2020;8:265. Published 2020 Mar 31. doi:10.3389/fbioe.2020.00265.
9. Naydich AD, Nangle SN, Bues JJ, et al. Synthetic Gene Circuits Enable Systems-Level Biosensor Trigger Discovery at the Host-Microbe Interface. *mSystems.* 2019;4(4):e00125-19. Published 2019 Jun 11. doi:10.1128/mSystems.00125-19.
10. Hesselink, J.M.K.; Kopsky, D.J.; Witkamp, R.F. Palmitoylethanolamide (PEA)—‘Promiscuous’ anti-inflammatory and analgesic molecule at the interface between nutrition and pharma. *PharmaNutrition* 2014, 2, 19–25, doi:10.1016/j.phanu.2013.11.127.
11. Al Houayek, M.; Botteman, P.; Subramanian, K.V.; Lambert, D.M.; Makriyannis, A.; Cani, P.; Muccioli, G.G. N -Acylethanolamine-hydrolyzing acid amidase inhibition increases colon N-palmitoylethanolamine levels and counteracts murine colitis. *FASEB J.* 2015, 29, 650–661, doi:10.1096/fj.14-255208.
12. Hussain, Z.; Uyama, T.; Tsuboi, K.; Ueda, N. Mammalian enzymes responsible for the biosynthesis of N -acylethanolamines. *Biochim. et Biophys. Acta (BBA)-Mol. Cell Biol. Lipids* 2017, 1862, 1546–1561, doi:10.1016/j.bbalip.2017.08.006.
13. Zhu, C.; De Solorzano, C.O.; Sahar, S.; Realini, N.; Fung, E.; Sassone-Corsi, P.; Piomelli, D. Proinflammatory Stimuli Control N-Acylphosphatidylethanolamine-Specific Phospholipase D Expression in Macrophages. *Mol. Pharmacol.* 2011, 79, 786–792, doi:10.1124/mol.110.070201.

14. Borrelli, F.; Romano, B.; Petrosino, S.; Pagano, E.; Capasso, R.; Coppola, D.; Battista, G.; Orlando, P.; Di Marzo, V.; Izzo, A.A. Palmitoylethanolamide, a naturally occurring lipid, is an orally effective intestinal anti-inflammatory agent. *Br. J. Pharmacol.* 2015, *172*, 142–158, doi:10.1111/bph.12907.
15. O’Sullivan, S.E. Cannabinoids go nuclear: Evidence for activation of peroxisome proliferator-activated receptors. *Br. J. Pharmacol.* 2007, *152*, 576–582, doi:10.1038/sj.bjp.0707423.
16. Esposito, G.; Capoccia, E.; Turco, F.; Palumbo, I.; Lu, J.; Steardo, A.; Cuomo, R.; Sarnelli, G.; Steardo, L. Palmitoylethanolamide improves colon inflammation through an enteric glia/toll like receptor 4-dependent PPAR- α activation. *Gut* 2014, *63*, 1300–1312, doi:10.1136/gutjnl-2013-305005.
17. Couch, D.G.; Cook, H.; Ortori, C.; Barrett, D.; Lund, J.N.; O’Sullivan, S.E. Palmitoylethanolamide and Cannabidiol Prevent Inflammation-induced Hyperpermeability of the Human Gut In Vitro and In Vivo—A Randomized, Placebo-controlled, Double-blind Controlled Trial. *Inflamm. Bowel Dis.* 2019, *25*, 1006–1018, doi:10.1093/ibd/izz017.
18. Sarnelli, G.; Gigli, S.; Capoccia, E.; Iuvone, T.; Cirillo, C.; Seguela, L.; Nobile, N.; D’Alessandro, A.; Pesce, M.; Steardo, L.; et al. Palmitoylethanolamide Exerts Antiproliferative Effect and Downregulates VEGF Signaling in Caco-2 Human Colon Carcinoma Cell Line Through a Selective PPAR- α -Dependent Inhibition of Akt/mTOR Pathway. *Phytotherapy Res.* 2016, *30*, 963–970, doi:10.1002/ptr.5601.
19. Löwenberg, M.; D’Haens, G. Novel Targets for Inflammatory Bowel Disease Therapeutics. *Curr. Gastroenterol. Rep.* 2013, *15*, 311, doi:10.1007/s11894-012-0311-3.
20. Sarnelli, G.; D’Alessandro, A.; Iuvone, T.; Capoccia, E.; Gigli, S.; Pesce, M.; Seguela, L.; Nobile, N.; Aprea, G.; Maione, F.; et al. Palmitoylethanolamide Modulates Inflammation-Associated Vascular Endothelial Growth Factor (VEGF) Signaling via the Akt / mTOR Pathway in a Selective Peroxisome Proliferator-Activated Receptor Alpha (PPAR- α)-Dependent Manner. *PLoS ONE* 2016, *11*, e0156198.
21. Russo, R.; Cristiano, C.; Avagliano, C.; De Caro, C.; La Rana, G.; Raso, G.M.; Canani, R.B.; Meli, R.; Calignano, A. Gut-brain Axis: Role of Lipids in the Regulation of Inflammation, Pain and CNS Diseases. *Curr. Med. Chem.* 2018, *25*, 3930–3952, doi:10.2174/0929867324666170216113756.
22. Gabrielsson, L.; Mattsson, S.; Fowler, C.J. Palmitoylethanolamide for the treatment of pain: Pharmacokinetics, safety and efficacy. *Br. J. Clin. Pharmacol.* 2016, *82*, 932–942, doi:10.1111/bcp.13020.
23. Djordjević, G. Positive Selection, Cloning Vectors for Gram-Positive Bacteria Based on a Restriction Endonuclease Cassette. *Plasmid* 1996, *35*, 37–45, doi:10.1006/plas.1996.0004.
24. Djordjevic, G.M.; Klaenhammer, T.R. Inducible gene expression systems in *Lactococcus lactis*. *Mol. Biotechnol.* 1998, *9*, 127–139, doi:10.1007/bf02760814.
25. Mättö, J.; Fondén, R.; Tolvanen, T.; Von Wright, A.; Vilpponen-Salmela, T.; Satokari, R.; Saarela, M. Intestinal survival and persistence of probiotic *Lactobacillus* and *Bifidobacterium* strains administered in triple-strain yoghurt. *Int. Dairy J.* 2006, *16*, 1174–1180, doi:10.1016/j.idairyj.2005.10.007.

26. Chassaing, B.; Aitken, J.D.; Malleshappa, M.; Vijay-Kumar, M. Dextran Sulfate Sodium (DSS)-Induced Colitis in Mice. *Curr. Protoc. Immunol.* 2014, *104*, 15.25.1–15.25.14, doi:10.1002/0471142735.im1525s104.
27. Kim, J.J.; Shajib, S.; Manocha, M.M.; Khan, W.I. Investigating Intestinal Inflammation in DSS-induced Model of IBD. *J. Vis. Exp.* 2012, e3678, doi:10.3791/3678.
28. De Filippis, D.; d'Amico, A.; Cipriano, M.; Petrosino, S.; Orlando, P.; Di Marzo, V.; Iuvone, T.; Endocannabinoid Research, Group. Levels of endocannabinoids and palmitoylethanolamide and their pharmacological manipulation in chronic granulomatous inflammation in rats. *Pharmacol. Res.* 2010, *61*, 321–328.
29. Gachet, M.S.; Rhyn, P.; Bosch, O.G.; Quednow, B.B.; Gertsch, J. A quantitative LC-MS/MS method for the measurement of arachidonic acid, prostanoids, endocannabinoids, N-acyl ethanolamines and steroids in human plasma. *J. Chromatogr. B* 2015, *976-977*, 6–18, doi:10.1016/j.jchromb.2014.11.001.
30. Cooper, H.S.; Murthy, S.N.; Shah, R.S.; Sedergran, D.J. Clinicopathologic study of dextran sulfate sodium experimental murine colitis. *Lab. Investig.* 1993, *69*, 238–249.
31. Li, R.; Kim, M.-H.; Sandhu, A.K.; Gao, C.; Gu, L. Muscadine Grape (*Vitis rotundifolia*) or Wine Phytochemicals Reduce Intestinal Inflammation in Mice with Dextran Sulfate Sodium-Induced Colitis. *J. Agric. Food Chem.* 2017, *65*, 769–776, doi:10.1021/acs.jafc.6b03806.
32. Di Rosa, M.; Radomski, M.; Carnuccio, R.; Moncada, S. Glucocorticoids inhibit the induction of nitric oxide synthase in macrophages. *Biochem. Biophys. Res. Commun.* 1990, *172*, 1246–1252.
33. Cassini-Vieira, P.; Moreira, C.F.; da Silva, M.F.; da Silva Barcelos, L. Estimation of Wound Tissue Neutrophil and Macrophage Accumulation by Measuring Myeloperoxidase (MPO) and N-Acetyl- β -D-glucosaminidase (NAG) Activities. *Bio-Protoc.* 2015, *5*, e1662, doi:10.21769/BioProtoc.1662.
34. Sarnelli, G.; Pesce, M.; Seguela, L.; Lu, J.; Efficie, E.; Tack, J.; De Palma, F.D.E.; D'Alessandro, A.; Esposito, G. Impaired Duodenal Palmitoylethanolamide Release Underlies Acid-Induced Mast Cell Activation in Functional Dyspepsia. *Cell. Mol. Gastroenterol. Hepatol.* 2021, *11*, 841–855, doi:10.1016/j.jcmgh.2020.10.001.
35. Hammer, H.F. Gut Microbiota and Inflammatory Bowel Disease. *Dig. Dis.* 2011, *29*, 550–553, doi:10.1159/000332981.
36. Lane, E.R.; Zisman, T.L.; Suskind, D.L. The microbiota in inflammatory bowel disease: Current and therapeutic insights. *J. Inflamm. Res.* 2017, *10*, 63–73, doi:10.2147/jir.s116088.
37. Gioacchini, G.; Rossi, G.; Carnevali, O. Host-probiotic interaction: New insight into the role of the endocannabinoid system by in vivo and ex vivo approaches. *Sci. Rep.* 2017, *7*, 1261, doi:10.1038/s41598-017-01322-1.
38. Nishida, A.; Inoue, R.; Inatomi, O.; Bamba, S.; Naito, Y.; Andoh, A. Gut microbiota in the pathogenesis of inflammatory bowel disease. *Clin. J. Gastroenterol.* 2018, *11*, 1–10, doi:10.1007/s12328-017-0813-5.
39. Abraham, B.P.; Quigley, E.M. Probiotics in Inflammatory Bowel Disease. *Gastroenterol. Clin. North Am.* 2017, *46*, 769–782, doi:10.1016/j.gtc.2017.08.003.

40. Ganji-Arjenaki, M.; Rafieian-Kopaei, M. Probiotics are a good choice in remission of inflammatory bowel diseases: A meta analysis and systematic review. *J. Cell. Physiol.* 2018, *233*, 2091–2103, doi:10.1002/jcp.25911.
41. Steidler, L.; Hans, W.; Schotte, L.; Neiryneck, S.; Obermeier, F.; Falk, W.; Fiers, W.; Remaut, E. Treatment of Murine Colitis by Lactococcus lactis Secreting Interleukin-10. *Science* 2000, *289*, 1352–1355, doi:10.1126/science.289.5483.1352.
42. Zurita-Turk, M.; Del Carmen, S.; Santos, A.C.; Pereira, V.B.; Cara, D.C.; Leclercq, S.Y.; dM de LeBlanc, A.; Azevedo, V.; Chatel, J.-M.; Leblanc, J.G.; et al. Lactococcus lactis carrying the pValac DNA expression vector coding for IL-10 reduces inflammation in a murine model of experimental colitis. *BMC Biotechnol.* 2014, *14*, 73, doi:10.1186/1472-6750-14-73.
43. Braat, H.; Rottiers, P.; Hommes, D.W.; Huyghebaert, N.; Remaut, E.; Remon, J.; van Deventer, S.J.; Neiryneck, S.; Peppelenbosch, M.P.; Steidler, L. A Phase I Trial with Transgenic Bacteria Expressing Interleukin-10 in Crohn's Disease. *Clin. Gastroenterol. Hepatol.* 2006, *4*, 754–759, doi:10.1016/j.cgh.2006.03.028.
44. Miljkovic, M.; Thomas, M.; Serror, P.; Rigottier-Gois, L.; Kojic, M. Binding activity to intestinal cells and transient colonization in mice of two Lactobacillus paracasei subsp. paracasei strains with high aggregation potential. *World J. Microbiol. Biotechnol.* 2019, *35*, 85, doi:10.1007/s11274-019-2663-4.
45. Zampieri, N.; Pietrobelli, A.; Biban, P.; Soffiati, M.; Dall'agnola, A.; Camoglio, F.S. Lactobacillus paracasei subsp. paracasei F19 in Bell's stage 2 of necrotizing enterocolitis. *Minerva Pediatr.* 2013, *65*, 353–360.
46. Lavilla-Lerma, L.; Pérez-Pulido, R.; Martínez-Bueno, M.; Maqueda, M.; Valdivia, E. Characterization of functional, safety, and gut survival related characteristics of Lactobacillus strains isolated from farmhouse goat's milk cheeses. *Int. J. Food Microbiol.* 2013, *163*, 136–145, doi:10.1016/j.ijfoodmicro.2013.02.015.
47. Rossi, G.; Gioacchini, G.; Pengo, G.; Suchodolski, J.S.; Jergens, A.E.; Allenspach, K.; Gavazza, A.; Scarpona, S.; Berardi, S.; Galosi, L.; et al. Enterocolic increase of cannabinoid receptor type 1 and type 2 and clinical improvement after probiotic administration in dogs with chronic signs of colonic dysmotility without mucosal inflammatory changes. *Neurogastroenterol. Motil.* 2020, *32*, e13717, doi:10.1111/nmo.13717.
48. Petrosino, S.; Di Marzo, V. The pharmacology of palmitoylethanolamide and first data on the therapeutic efficacy of some of its new formulations. *Br. J. Pharmacol.* 2017, *174*, 1349–1365, doi:10.1111/bph.13580.
49. Nestmann, E.R. Safety of micronized palmitoylethanolamide (microPEA): Lack of toxicity and genotoxic potential. *Food Sci. Nutr.* 2017, *5*, 292–309, doi:10.1002/fsn3.392.
50. Petrosino, S.; Cordaro, M.; Verde, R.; Moriello, A.S.; Marcolongo, G.; Schievano, C.; Siracusa, R.; Piscitelli, F.; Peritore, A.F.; Crupi, R.; et al. Oral Ultramicronized Palmitoylethanolamide: Plasma and Tissue Levels and Spinal Anti-hyperalgesic Effect. *Front. Pharmacol.* 2018, *9*, 249, doi:10.3389/fphar.2018.00249.
51. Pesce, M.; D'Alessandro, A.; Borrelli, O.; Gigli, S.; Seguella, L.; Cuomo, R.; Esposito, G.; Sarnelli, G. Endocannabinoid-related compounds in gastrointestinal diseases. *J. Cell. Mol. Med.* 2017, *22*, 706–715, doi:10.1111/jcmm.13359.

52. Pesce, M.; Esposito, G.; Sarnelli, G. Endocannabinoids in the treatment of gastrointestinal inflammation and symptoms. *Curr. Opin. Pharmacol.* 2018, *43*, 81–86, doi:10.1016/j.coph.2018.08.009.
53. Cani, P.; Plovier, H.; Van Hul, M.; Geurts, L.; Delzenne, N.M.; Druart, C.; Everard, A. Endocannabinoids—At the crossroads between the gut microbiota and host metabolism. *Nat. Rev. Endocrinol.* 2016, *12*, 133–143, doi:10.1038/nrendo.2015.211.
54. Lessa, F.C., Winston, L.G., and McDonald, L.C. (2015). Burden of *Clostridium difficile* infection in the United States. *N Engl J Med* 372, 2369-2370.
55. Napolitano, L.M., and Edmiston, C.E., Jr. (2017). *Clostridium difficile* disease: Diagnosis, pathogenesis, and treatment update. *Surgery* 162, 325-348.
56. Schäffler, H., and Breitrück, A. (2018). *Clostridium difficile* - From Colonization to Infection. *Front Microbiol* 9, 646.
57. Chen, S., Sun, C., Wang, H., and Wang, J. (2015). The Role of Rho GTPases in Toxicity of *Clostridium difficile* Toxins. *Toxins (Basel)* 7, 5254-5267.
58. Terry, S., Nie, M., Matter, K., and Balda, M.S. (2010). Rho signaling and tight junction functions. *Physiology (Bethesda)* 25, 16-26.
59. Kim, J.M., Lee, J.Y., Yoon, Y.M., Oh, Y.K., Youn, J., and Kim, Y.J. (2006). NF-kappa B activation pathway is essential for the chemokine expression in intestinal epithelial cells stimulated with *Clostridium difficile* toxin A. *Scand J Immunol* 63, 453-460.
60. Petrosino, S., and Di Marzo, V. (2017). The pharmacology of palmitoylethanolamide and first data on the therapeutic efficacy of some of its new formulations. *Br J Pharmacol* 174, 1349-1365.
61. Sarnelli, G., Gigli, S., Capoccia, E., Iuvone, T., Cirillo, C., Seguella, L., Nobile, N., D'alessandro, A., Pesce, M., Steardo, L., Cuomo, R., and Esposito, G. (2016b).
62. Pesce, M., D'alessandro, A., Borrelli, O., Gigli, S., Seguella, L., Cuomo, R., Esposito, G., and Sarnelli, G. (2018). Endocannabinoid-related compounds in gastrointestinal diseases. *J Cell Mol Med* 22, 706-715.
63. Hirota, S.A., Iablokov, V., Tulk, S.E., Schenck, L.P., Becker, H., Nguyen, J., Al Bashir, S., Dingle, T.C., Laing, A., Liu, J., Li, Y., Bolstad, J., Mulvey, G.L., Armstrong, G.D., Macnaughton, W.K., Muruve, D.A., Macdonald, J.A., and Beck, P.L. (2012). Intrarectal instillation of *Clostridium difficile* toxin A triggers colonic inflammation and tissue damage: development of a novel and efficient mouse model of *Clostridium difficile* toxin exposure. *Infect Immun* 80, 4474-4484.
64. Markham, N.O., Bloch, S.C., Shupe, J.A., Laubacher, E.N., Washington, M.K., Coffey, R.J., and Lacy, D.B. (2020). Murine intrarectal instillation of purified recombinant *C. difficile* toxins enables mechanistic studies of pathogenesis. 2020.2008.2030.274738.
65. Sun, X., and Hirota, S.A. (2015). The roles of host and pathogen factors and the innate immune response in the pathogenesis of *Clostridium difficile* infection. *Mol Immunol* 63, 193-202.
66. Gachet, M.S., Rhyn, P., Bosch, O.G., Quednow, B.B., and Gertsch, J. (2015). A quantitative LC-MS/MS method for the measurement of arachidonic acid, prostanoids, endocannabinoids, N-acyl ethanolamines and steroids in human plasma. *J Chromatogr B Analyt Technol Biomed Life Sci* 976-977, 6-18.

67. Li, R., Kim, M.H., Sandhu, A.K., Gao, C., and Gu, L. (2017). Muscadine Grape (*Vitis rotundifolia*) or Wine Phytochemicals Reduce Intestinal Inflammation in Mice with Dextran Sulfate Sodium-Induced Colitis. *J Agric Food Chem* 65, 769-776.
68. Thoree, V., Skepper, J., Deere, H., Pele, L.C., Thompson, R.P., and Powell, J.J. (2008). Phenotype of exogenous microparticle-containing pigment cells of the human Peyer's patch in inflamed and normal ileum. *Inflamm Res* 57, 374-378.
69. Mullane, K.M., Kraemer, R., and Smith, B. (1985). Myeloperoxidase activity as a quantitative assessment of neutrophil infiltration into ischemic myocardium. *J Pharmacol Methods* 14, 157-167.
70. Di Rosa, M., Radomski, M., Carnuccio, R., and Moncada, S. (1990). Glucocorticoids inhibit the induction of nitric oxide synthase in macrophages. *Biochem Biophys Res Commun* 172, 1246-1252.
71. McDonald, L.C., Gerding, D.N., Johnson, S., Bakken, J.S., Carroll, K.C., Coffin, S.E., Dubberke, E.R., Garey, K.W., Gould, C.V., Kelly, C., Loo, V., Shaklee Sammons, J., Sandora, T.J., and Wilcox, M.H. (2018). Clinical Practice Guidelines for *Clostridium difficile* Infection in Adults and Children: 2017 Update by the Infectious Diseases Society of America (IDSA) and Society for Healthcare Epidemiology of America (SHEA). *Clin Infect Dis* 66, 987-994.
72. Johnson, S. (2009). Recurrent *Clostridium difficile* infection: a review of risk factors, treatments, and outcomes. *J Infect* 58, 403-410.
73. Baines, S.D., and Wilcox, M.H. (2015). Antimicrobial Resistance and Reduced Susceptibility in *Clostridium difficile*: Potential Consequences for Induction, Treatment, and Recurrence of *C. difficile* Infection. *Antibiotics (Basel)* 4, 267-298.
74. Na, X., and Kelly, C. (2011). Probiotics in *clostridium difficile* Infection. *J Clin Gastroenterol* 45 Suppl, S154-158.
75. Mills, J.P., Rao, K., and Young, V.B. (2018). Probiotics for prevention of *Clostridium difficile* infection. *Curr Opin Gastroenterol* 34, 3-10.
76. Liu, D., Zeng, L., Yan, Z., Jia, J., Gao, J., and Wei, Y. (2020). The mechanisms and safety of probiotics against toxigenic *clostridium difficile*. *Expert Rev Anti Infect Ther* 18, 967-975.
77. Andersen, K.K., Strokappe, N.M., Hultberg, A., Truusalu, K., Smidt, I., Mikelsaar, R.H., Mikelsaar, M., Verrips, T., Hammarström, L., and Marcotte, H. (2016). Neutralization of *Clostridium difficile* Toxin B Mediated by Engineered *Lactobacilli* That Produce Single-Domain Antibodies. *Infect Immun* 84, 395-406.
78. Britti, D., Crupi, R., Impellizzeri, D., Gugliandolo, E., Fusco, R., Schievano, C., Morittu, V.M., Evangelista, M., Di Paola, R., and Cuzzocrea, S. (2017). A novel composite formulation of palmitoylethanolamide and quercetin decreases inflammation and relieves pain in inflammatory and osteoarthritic pain models. *BMC Vet Res* 13, 229.
79. Beggiano, S., Tomasini, M.C., and Ferraro, L. (2019). Palmitoylethanolamide (PEA) as a Potential Therapeutic Agent in Alzheimer's Disease. *Front Pharmacol* 10, 821.
80. Wullaert, A. (2010). Role of NF-kappaB activation in intestinal immune homeostasis. *Int J Med Microbiol* 300, 49-56.
81. Huang, J., Kelly, C.P., Bakirtzi, K., Villafuerte Gálvez, J.A., Lyras, D., Mileto, S.J., Larcombe, S., Xu, H., Yang, X., Shields, K.S., Zhu, W., Zhang, Y., Goldsmith, J.D., Patel, I.J., Hansen, J., Huang, M., Yla-Herttuala, S., Moss, A.C., Paredes-Sabja, D.,

- Pothoulakis, C., Shah, Y.M., Wang, J., and Chen, X. (2019). Clostridium difficile toxins induce VEGF-A and vascular permeability to promote disease pathogenesis. *Nat Microbiol* 4, 269-279.
82. Sarnelli, G., D'alessandro, A., Iuvone, T., Capoccia, E., Gigli, S., Pesce, M., Seguella, L., Nobile, N., Aprea, G., Maione, F., De Palma, G.D., Cuomo, R., Steardo, L., and Esposito, G. (2016a). Palmitoylethanolamide Modulates Inflammation-Associated Vascular Endothelial Growth Factor (VEGF) Signaling via the Akt/mTOR Pathway in a Selective Peroxisome Proliferator-Activated Receptor Alpha (PPAR- α)-Dependent Manner. *PLoS One* 11, e0156198.
 83. Davis, M.P., Behm, B., Mehta, Z., and Fernandez, C. (2019). The Potential Benefits of Palmitoylethanolamide in Palliation: A Qualitative Systematic Review. *Am J Hosp Palliat Care* 36, 1134-1154.
 84. Gigli, S., Seguella, L., Pesce, M., Bruzzese, E., D'alessandro, A., Cuomo, R., Steardo, L., Sarnelli, G., and Esposito, G. (2017). Cannabidiol restores intestinal barrier dysfunction and inhibits the apoptotic process induced by Clostridium difficile toxin A in Caco-2 cells. *United European Gastroenterol J* 5, 1108-1115.
 85. Bergamaschi, M.M., Queiroz, R.H., Zuardi, A.W., and Crippa, J.A. (2011). Safety and side effects of cannabidiol, a Cannabis sativa constituent. *Curr Drug Saf* 6, 237-249.
 86. Iffland, K., and Grotenhermen, F. (2017). An Update on Safety and Side Effects of Cannabidiol: A Review of Clinical Data and Relevant Animal Studies. *Cannabis Cannabinoid Res* 2, 139-154.
 87. Ambrose, T., and Simmons, A. (2019). Cannabis, Cannabinoids, and the Endocannabinoid System-Is there Therapeutic Potential for Inflammatory Bowel Disease? *J Crohns Colitis* 13, 525-535.
 88. Okamoto, Y., Morishita, J., Tsuboi, K., Tonai, T., and Ueda, N. (2004). Molecular characterization of a phospholipase D generating anandamide and its congeners. *J Biol Chem* 279, 5298-5305.
 89. Di Cerbo, A., and Palmieri, B. (2013). Lactobacillus Paracasei subsp. Paracasei F19; a farmacogenomic and clinical update. *Nutr Hosp* 28, 1842-1850.
 90. Higl, B., Kurtmann, L., Carlsen, C.U., Ratjen, J., Först, P., Skibsted, L.H., Kulozik, U., and Risbo, J. (2007). Impact of water activity, temperature, and physical state on the storage stability of Lactobacillus paracasei ssp. paracasei freeze-dried in a lactose matrix. *Biotechnol Prog* 23, 794-800.
 91. Huang PL. A comprehensive definition for metabolic syndrome. *Dis Model Mech*. 2009 May-Jun;2(5-6):231-7. doi: 10.1242/dmm.001180. PMID: 19407331; PMCID: PMC2675814.
 92. Van Gaal, L., Mertens, I. & De Block, C. Mechanisms linking obesity with cardiovascular disease. *Nature* 444, 875–880 (2006). <https://doi.org/10.1038/nature05487>
 93. Lois K., Kumar S. Obesity and diabetes. *Endocrinol Nutr*, 56 (4) (2009), pp. 38-42
 94. Hossain P., B. Kavar, M. El Nahas Obesity and diabetes in the developing world—a growing challenge *N Engl J Med*, 356 (3) (2007), pp. 213-215
 95. Fabbrini E, Sullivan S, Klein S. Obesity and nonalcoholic fatty liver disease: biochemical, metabolic, and clinical implications. *Hepatology*. 2010 Feb;51(2):679-89. doi: 10.1002/hep.23280. PMID: 20041406; PMCID: PMC3575093.

96. Popkin BM, Kim S, Rusev ER, Du S, Zizza C. Measuring the full economic costs of diet, physical activity and obesity-related chronic diseases. *Obes Rev.* 2006;7(3):271–93.
97. Müller-Riemenschneider, F., Reinhold, T., Berghöfer, A. *et al.* Health-economic burden of obesity in Europe. *Eur J Epidemiol* **23**, 499 (2008). <https://doi.org/10.1007/s10654-008-9239-1>
98. Zhang X., Qi Q., Zhang C., Smith S.R., Hu F.B., Sacks F.M., Bray G.A., Qi L. FTO Genotype and 2-Year Change in Body Composition and Fat Distribution in Response to Weight-Loss Diets: The POUNDS LOST Trial. *Diabetes.* 2012; 61:3005–3011. doi: 10.2337/db11-1799.
99. Muccioli GG, Naslain D, Bäckhed F, Reigstad CS, Lambert DM, Delzenne NM, Cani PD. The endocannabinoid system links gut microbiota to adipogenesis. *Mol Syst Biol.* 2010 Jul; 6:392. doi: 10.1038/msb.2010.46. PMID: 20664638; PMCID: PMC2925525.
100. André, A, & Gonthier, M.-P. (2010). The endocannabinoid system: Its roles in energy balance and potential as a target for obesity treatment *The International Journal of Biochemistry & Cell Biology*, 42(11), 1788-1801.
101. Després J-P, Golay A, Sjöström L for the Rimonabant in Obesity–Lipids Study Group. Effects of rimonabant on metabolic risk factors in overweight patients with dyslipidemia. *N Engl J Med.* 2005; 353: 2121-2134
102. Pi-Sunyer FX, Aronne LJ, Heshmati HM, Devin J, Rosenstock J, for the RIO-North America Study Group. Effect of rimonabant, a cannabinoid-1 receptor blocker, on weight and cardiometabolic risk factors in overweight or obese patients: RIO-North America: a randomized controlled trial. *JAMA.* 2006; 295: 761-775
103. King, A. Neuropsychiatric adverse effects signal the end of the line for rimonabant. *Nat Rev Cardiol* 7, 602 (2010). <https://doi.org/10.1038/nrcardio.2010.148>
104. Brown, J. D., Karimian Azari, E, & Ayala, J. E. (2017). Oleoylethanolamide: A fat ally in the fight against obesity. *Physiology & Behavior*, 176, 50-58.
105. Bellocchio, L., Cervino, C., Pasquali, R., & Pagotto, U. (2008). The endocannabinoid system and energy metabolism. *Journal of Neuroendocrinology*, 20(6), 850-857.
106. Misto, A., Provensi, G., Vozella, V., Passani, M. B., & Piomelli, D. (2018). Mast cell-derived histamine regulates liver ketogenesis via oleoy-lethanolamide signaling. *Cell Metabolism*, 29, 1-12.
107. Oveisi, F. (2004). Oleoylethanolamide inhibits food intake in free-feeding rats after oral administration. *Pharmacological Research*, 49(5), 461-466.
108. Guzman, M., Lo verme, J., Fu, J., Oveisi, F., Blazquez, C., & Piomelli, D. (2004). Oleoylethanolamide stimulates lipolysis by activating the nuclear receptor peroxisome proliferator-activated receptor α (PPAR- α). *Journal of Biological Chemistry*, 279(27), 27849-27854.
109. Fu, J., Gaetani, S., Oveisi, F., Lo verme, J., Serrano, A., Rodriguez de Fonseca, F., Piomelli, D. (2003). Oleoylethanolamide regulates feeding and body weight through activation of the nuclear receptor PPAR- α . *Nature*, 425(6953), 90-93.

110. Kersten, S., & Wahli, W. (2000). Peroxisome proliferator activated receptor agonists. *New Approaches to Drug Development*, 32, 141-151
111. Mandarci, S., Miiller, M., & Kersten, S. (2004). Peroxisome proliferator-activated receptor a target genes. *Cellular and Molecular Life Sciences CMLS*, 61(4), 393-416.
112. Stienstra, R., Duval, C., Miiller, M., & Kersten, S. (2007). PPARs, obesity, and inflammation. *PPAR research*, 2007, 1-10.
113. Hansen, H. S., Rosenkilde, M. M., Holst, J. J., & Schwartz, T. W. (2012). GPR119 as a fat sensor. *Trends In Pharmacological Sciences*, 33(7), 374-381.
114. Laleh P, Yaser K, Alireza O. Oleoylethanolamide: A novel pharmaceutical agent in the management of obesity-an updated review. *J Cell Physiol*. 2019 Jun;234(6):7893-7902. doi: 10.1002/jcp.27913. Epub 2018 Dec 7. PMID: 30537148.
115. Laleh, P., Yaser, K., Abolfazl, B., Shahriar, A., Mohammad, A. J., Nazila, F., & Alireza, O. (2018). Oleoylethanolamide increases the expression of PPAR-A and reduces appetite and body weight in obese people: A clinical trial. *Appetite*, 128, 44-49.
116. Nielsen, M. J., Petersen, G., Astrup, A., & Hansen, H. S. (2004). Food intake is inhibited by oral oleoylethanolamide. *Journal of Lipid Research*, 45(6), 1027-1029.
117. Cani PD, Amar J, Iglesias MA, Poggi M, Knauf C, Bastelica D, Neyrinck AM, Fava F, Tuohy KM, Chabo C, Waget A, Delmée E, Cousin B, Sulpice T, Chamontin B, Ferrières J, Tanti JF, Gibson GR, Casteilla L, Delzenne NM, Alessi MC, Burcelin R. Metabolic endotoxemia initiates obesity and insulin resistance. *Diabetes*. 2007 Jul;56(7):1761-72. doi: 10.2337/db06-1491. Epub 2007 Apr 24. PMID: 17456850.
118. Stenkamp-Strahm, Chloe M. et al. "Prolonged high fat diet ingestion, obesity, and type 2 diabetes symptoms correlate with phenotypic plasticity in myenteric neurons and nerve damage in the mouse duodenum." *Cell and Tissue Research* 361 (2015): 411 - 426.
119. Ding, S., Chi, M. M., Scull, B. P., Rigby, R., Schwerbrock, N. M., Magness, S., Jobin, C., & Lund, P. K. (2010). High-fat diet: bacteria interactions promote intestinal inflammation which precedes and correlates with obesity and insulin resistance in mouse. *PloS one*, 5(8), e12191. <https://doi.org/10.1371/journal.pone.0012191>
120. Paytuví, E Battista, F Scippacercola, RA Cigliano, W Sanseverino GAIA: an integrated metagenomics suite. *BioRxiv* (2019).
121. Lifshitz F, Lifshitz JZ. Globesity: the root causes of the obesity epidemic in the USA and now worldwide. *Pediatr Endocrinol Rev*. 2014 Sep;12(1):17-34. PMID: 25345082.
122. Jones BJ, Bloom SR. The New Era of Drug Therapy for Obesity: The Evidence and the Expectations. *Drugs*. 2015 Jun;75(9):935-45. doi: 10.1007/s40265-015-0410-1. PMID: 25985865; PMCID: PMC4464860.
123. Brown, J. D., McAnally, D., Ayala, J. E., Burmeister, M. A., Morta, C., Smith L., & Ayala, J. E. (2018). Oleoylethanolamide modulates glucagon-like peptide-1 receptor agonist signaling and enhances Exendin-4- mediated weight loss in obese mice. *American Journal of Physiology-Regulatory, Integrative and Comparative Physiology*, 315(4), 595-608.

124. Mangine, G. T., Gonzalez, A. M., Wells, A. J., McCormack, W. P., Fragala, M. S., Stout, J. R., & Hoffman, J. R. (2012). The effect of a dietary supplement (N-oleyl-phosphatidyl-ethanolamine and epigallocatechin gallate) on dietary compliance and body fat loss in adults who are overweight: A double-blind, randomized control trial. *Lipids in Health and Disease*, 11(1), 127-135.
125. Fu, J., Astarita, G., Gaetani, S., Kim, J., Cravatt, B. F., Mackie, K., & Piomelli, D. (2007). Food intake regulates oleoylethanolamide formation and degradation in the proximal small intestine. *Journal of Biological Chemistry*, 282(2), 1518-1528.
126. van Raalte DH, Li M, Pritchard PH, Wasan KM. Peroxisome proliferator-activated receptor (PPAR)-alpha: a pharmacological target with a promising future. *Pharm Res*. 2004 Sep;21(9):1531-8. doi: 10.1023/b:pham.0000041444.06122.8d. PMID: 15497675.
127. Sanderson, L. M., de Groot, P. J., Hooiveld, G. J. E. J., Koppen, A., Kalkhoven, E., Miiller, M., & Kersten, S. (2008). Effect of synthetic dietary triglycerides: A novel research paradigm for nutrigenomics. *PLoS One*, 3(2), 1-11.
128. Moss, C. E., Glass, L. L., Diakogiannaki, E., Pais, R., Lenaghan, C., Smith, D. M., ... Reimann, F. (2016). Lipid derivatives activate GPR119 and trigger GLP-1 secretion in primary murine L-cells. *Peptides*, 77, 16-20.
129. Lauffer, L. M., lakoubov, R., & Brubaker, P. L. (2009). GPR119 is essential for oleoylethanolamide-induced glucagon-like peptide-1 secretion from the intestinal enteroendocrine L-cell. *Diabetes*, 58(5), 1058-1066.
130. Wang, X., Miyares, R. L., & Ahern, G. P. (2005). Oleoylethanolamide excites vagal sensory neurones, induces visceral pain and reduces short-term food intake in mice via capsaicin receptor TRPV1. *The Journal of Physiology*, 564(2), 541-547.
131. Pedersen HK, Gudmundsdottir V, Nielsen HB, Hyotylainen T, Nielsen T, Jensen BA, Forslund K, Hildebrand F, Prifti E, Falony G, Le Chatelier E, Levenez F, Doré J, Mattila I, Plichta DR, Pöhö P, Hellgren LI, Arumugam M, Sunagawa S, Vieira-Silva S, Jørgensen T, Holm JB, Trošt K; MetaHIT Consortium, Kristiansen K, Brix S, Raes J, Wang J, Hansen T, Bork P, Brunak S, Oresic M, Ehrlich SD, Pedersen O. Human gut microbes impact host serum metabolome and insulin sensitivity. *Nature*. 2016 Jul 21;535(7612):376-81. doi: 10.1038/nature18646. Epub 2016 Jul 13. PMID: 27409811.
132. John GK, Mullin GE. The Gut Microbiome and Obesity. *Curr Oncol Rep*. 2016 Jul;18(7):45. doi: 10.1007/s11912-016-0528-7. PMID: 27255389.
133. Lebeer, S., Vanderleyden, J. & De Keersmaecker, S. Host interactions of probiotic bacterial surface molecules: comparison with commensals and pathogens. *Nat Rev Microbiol* 8, 171–184 (2010). <https://doi.org/10.1038/nrmicro2297>

FIGURES AND LEGENDS

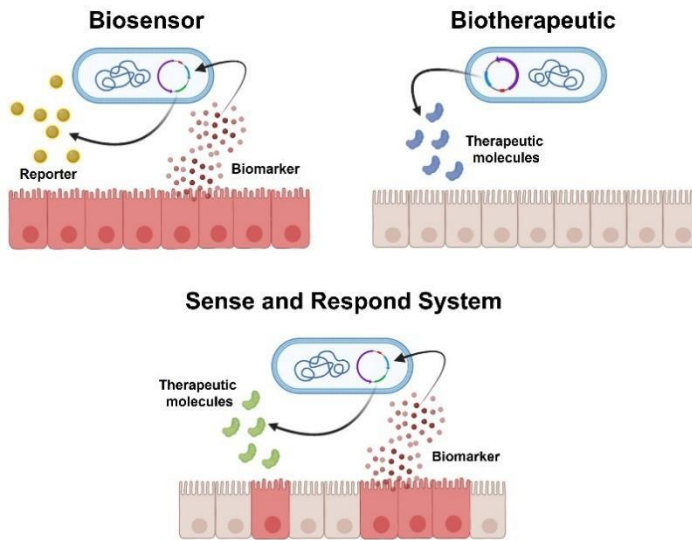


Figure 1. Main approaches in probiotics engineering. Biosensors can induce the expression of a reporter (usually a fluorescent marker) upon detecting specific biomarkers. Biotherapeutics are able to produce at the mucosal surface a therapeutic molecule either constitutively or following the activation of an exogenous substrate (inducible systems). Sense and respond systems incorporate the technology of biosensors, by responding to specific biomarkers with the production of a therapeutic molecule.

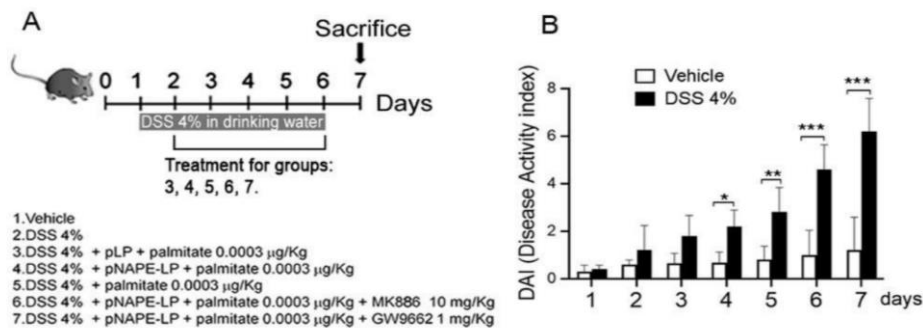


Figure 2. Experimental plan and colitis induction (A) Representative scheme showing our experimental protocol. Vehicle group received no treatment and served as internal control. All other mice groups were administered dextran sulfate sodium (DSS 4% w/v, MW 36,000 to 50,000, Sigma Aldrich, Italy) in drinking water for six consecutive days (starting from day 1). Starting from day 2, mice were randomly divided into the following groups (n = 10 each): (1) no further treatment (DSS 4%); (2) pLP+ palmitate (0.0003 $\mu\text{g}/\text{Kg}$), (3) pNAPE-LP + palmitate (0.0003 $\mu\text{g}/\text{Kg}$) (4) palmitate alone (0.0003 $\mu\text{g}/\text{Kg}$) (5) pNAPE-LP + palmitate (0.0003 $\mu\text{g}/\text{Kg}$) with the selective PPAR α antagonist MK886 (10 mg/Kg) and (6) pNAPE-LP + palmitate (0.0003 $\mu\text{g}/\text{Kg}$) with the selective PPAR γ antagonist GW966 (1 mg/Kg), respectively. All treatments were given daily from day 2 until day 6 by intragastric gavage, while PPAR α and PPAR γ antagonists were administered intraperitoneally from day 2 to day 6. (B) Kinetic of colitis induction showing DAI measurements from day 0 to 7 in DSS-treated mice.

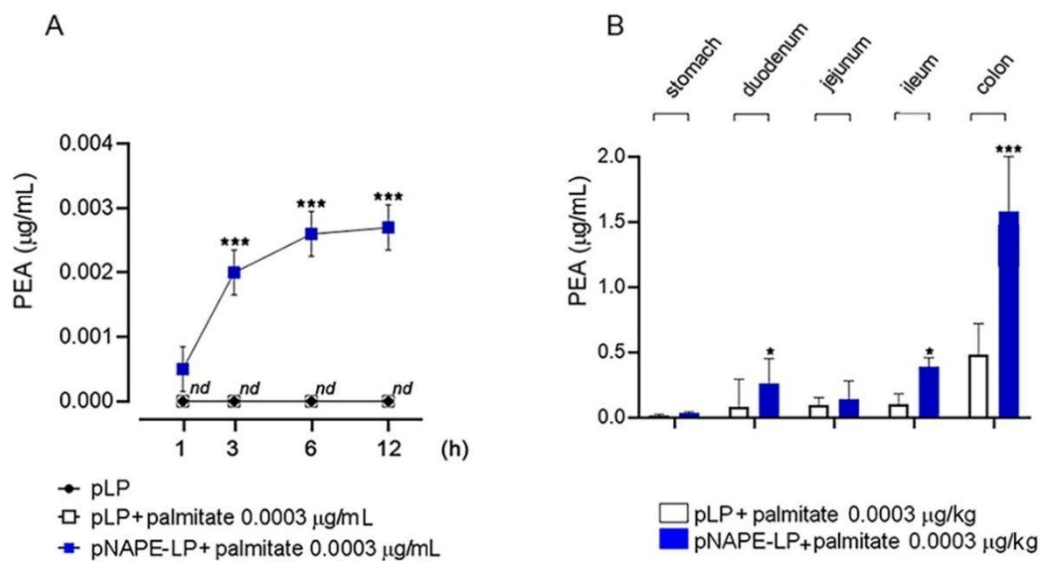


Figure 3. Palmitoylethanolamide (PEA) is time-dependently released by engineered NAPE-LP probiotic under palmitate boost. (A) Released PEA levels were evaluated in bacterial supernatant at 1, 3, 6, and 12 h by HPLC–MS and the results are expressed as the mean \pm SD of $n = 4$ experiments performed in triplicate. In comparison with pLP in absence of palmitate supply, exogenous palmitate (0.0003 $\mu\text{g}/\text{mL}$) time-dependently increased PEA release from pNAPE-LP probiotics, both *** $p < 0.001$ vs pLP and pLP in presence of palmitate 0.0003 $\mu\text{g}/\text{mL}$. No detectable amount of PEA was revealed by pLP even in the presence of 0.0003 $\mu\text{g}/\text{mL}$ supplementation of exogenous palmitate. (B) PEA tissue concentrations evaluated in tissue homogenates from stomach, duodenum, jejunum, ileum and colon in mice treated with pNAPE-LP + palmitate 0.0003 $\mu\text{g}/\text{kg}$ or pLP + palmitate 0.0003 $\mu\text{g}/\text{kg}$ by HPLC–MS. Results are expressed, for each two groups as the mean \pm SD of $n = 6$ experiments performed in triplicate. A significantly increased tissue concentration of PEA was observed in the duodenum and ileum of pNAPE-LP + palmitate 0.0003 $\mu\text{g}/\text{kg}$ -treated mice as compared to pLP + palmitate 0.0003 $\mu\text{g}/\text{kg}$ (+200% and +148%, respectively, both * $p < 0.05$), while the highest tissue concentration was reached in the colon with a 123% increase vs pLP + palmitate 0.0003 $\mu\text{g}/\text{kg}$ (***) $p < 0.0001$).

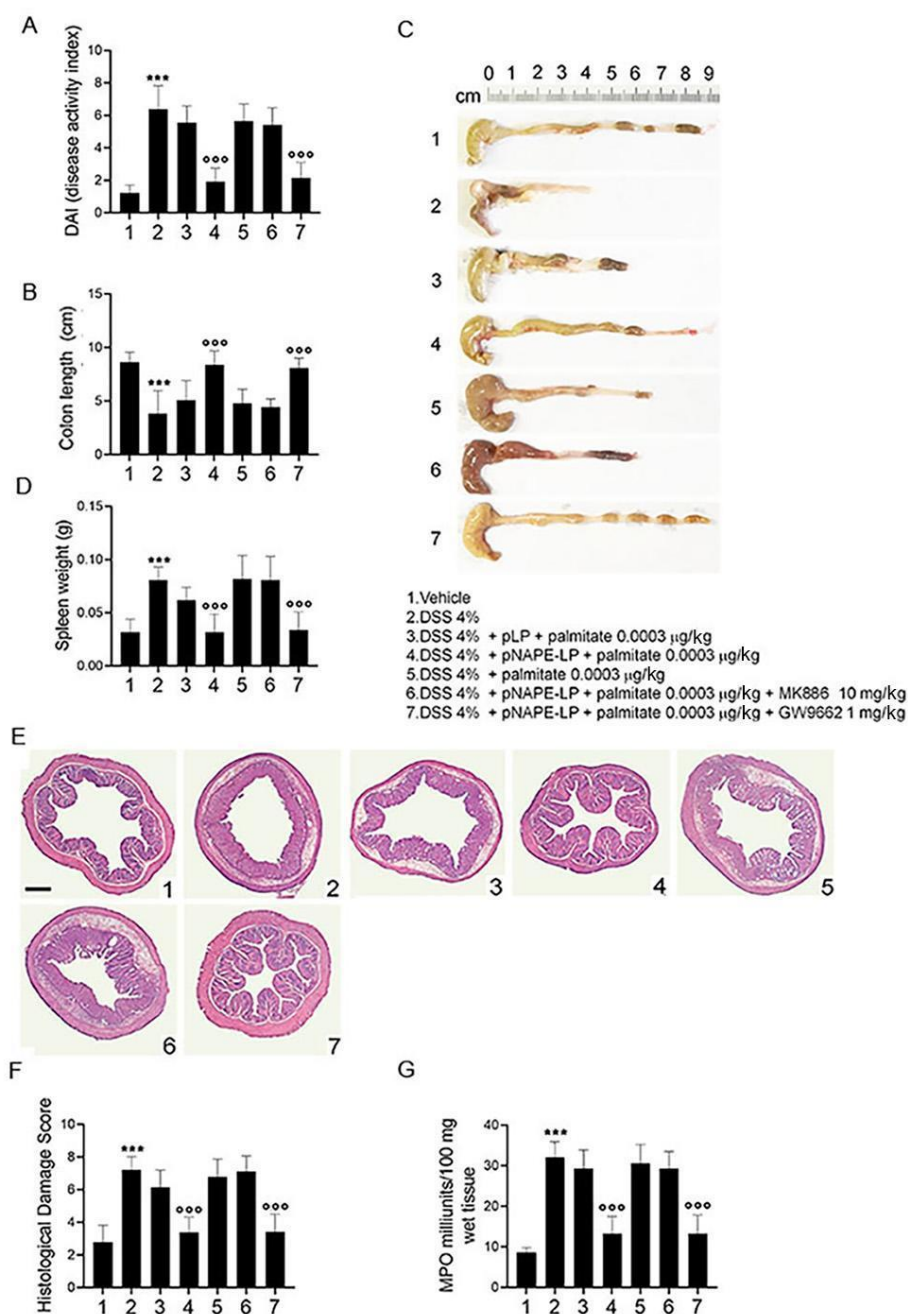


Figure 4. Engineered pNAPE-LP + palmitate ameliorates macroscopic signs of colitis, prevents colonic histological damage and neutrophil infiltration in DSS-treated mice. PPAR α -dependent effects of pNAPE-LP + palmitate treatment on (A) DAI score, (B,C) colonic length and (D) spleen weight in DSS-exposed mice. (E) Representative images of hematoxylin and eosin (H&E) stained distal colon sections and (F) relative histological damage score showing the effect of pNAPE-LP + palmitate on DSS-induced colonic injury; magnification 4 \times ; scale bar: 200 μ m. (G) Myeloperoxidase (MPO) activity quantification as indirect evidence of neutrophils infiltration. Results are expressed as the mean \pm SD of $n = 5$ experiments. *** $p < 0.001$ versus vehicle; ^{ooo} $p < 0.001$ versus DSS-treated mice.

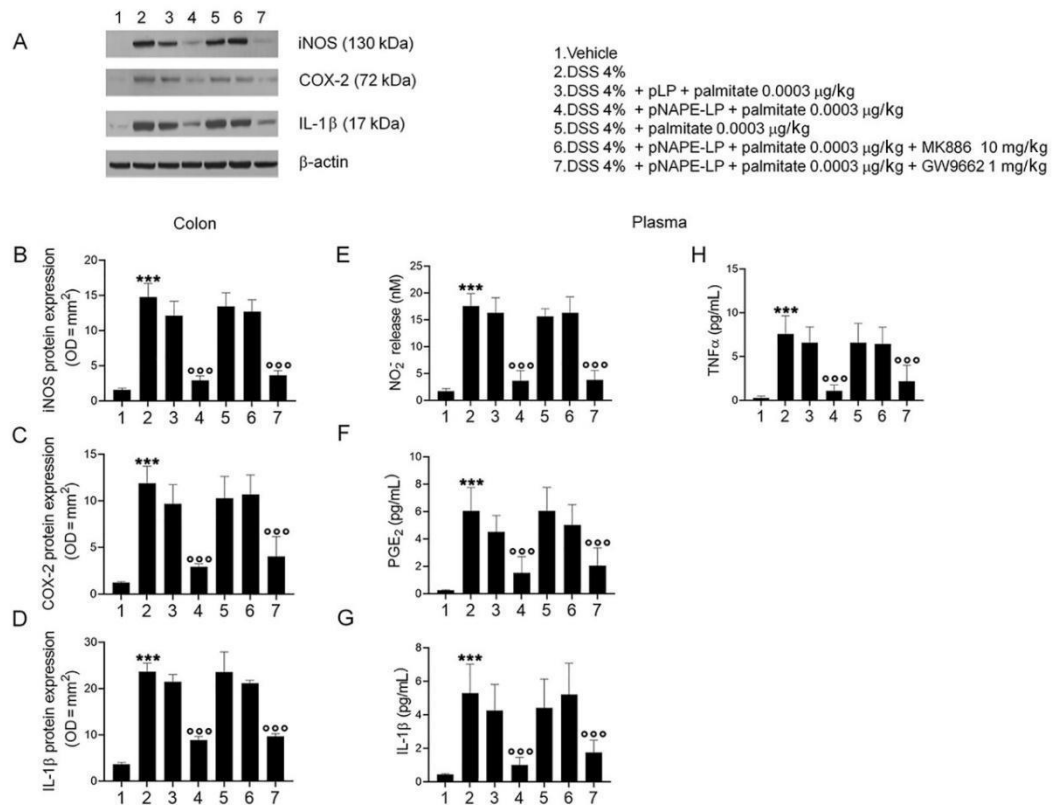


Figure 5. PEA release by pNAPE-LP + palmitate decreases pro-inflammatory mediators' expression in the mouse colon and their release in the plasma through a selective PPAR α involvement in DSS-treated mice. The administration of pNAPE-LP associated to palmitate (0.0003 µg/kg) induced a significant reduction in iNOS, COX-2 and IL-1 β protein expression, as well as NO, PGE₂, IL-1 β and TNF α levels through PPAR α -dependent involvement in mice colon and plasma. (A) Western blot analysis of iNOS, COX-2 and IL-1 β protein expression and (B–D) relative densitometric analysis (arbitrary units normalized on the expression of the housekeeping protein β -actin). (E–H) Respective quantification of NO₂⁻, PGE₂, IL-1 β and TNF α levels in mice plasma showing the effects of pNAPE-LP associated to palmitate (0.0003 µg/kg), given alone or in the presence of MK886 (10 mg/kg) or GW9662 (1 mg/kg) in the colonic tissue of DSS-treated mice. Results are expressed as the mean \pm SD of $n = 5$ experiments performed in triplicate. *** $p < 0.001$ versus vehicle; ^{ooo} $p < 0.001$ versus DSS-treated mice.

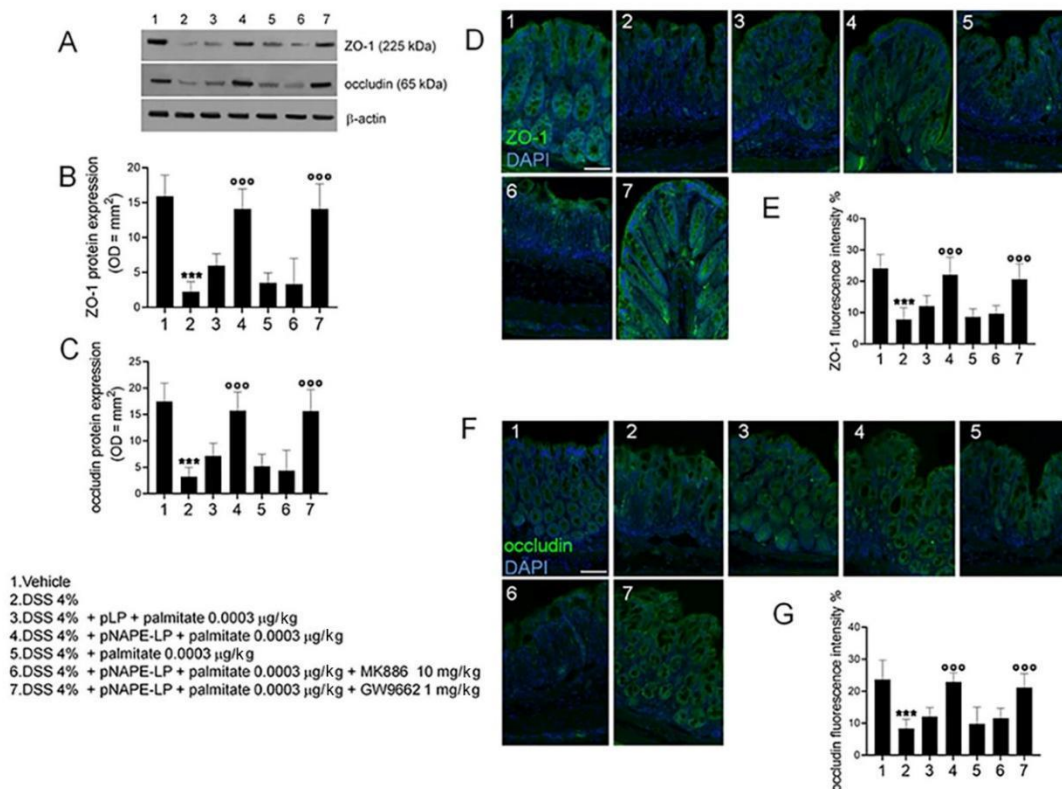


Figure 6. PEA released from pNAPE-LP + palmitate prevents the loss of tight junction proteins ZO-1 and occludin and colonic barrier disruption. A) Immunoreactive bands and (B,C) relative densitometric analyses (arbitrary units normalized on the expression of the housekeeping protein β-actin), as well as immunofluorescence staining and their respective quantification corresponding to (D,E) ZO-1 and (F,G) occludin, showing the effects of pNAPE-LP combined to palmitate (0.0003 µg/kg), given alone or in the presence of MK886 (10 mg/kg) or GW9662 (1 mg/kg) on colonic mucosa of DSS-treated mice. Palmitate alone (0.0003 µg/kg) failed to significantly affect ZO-1 and occludin expression in colonic mucosa. Nuclei were also investigated using DAPI staining. Results are expressed as the mean ± SD of $n = 5$ experiments performed in triplicate. *** $p < 0.001$ versus vehicle; °°° $p < 0.001$ versus DSS-treated mice. Scale bar = 100 µm; magnification 10×.

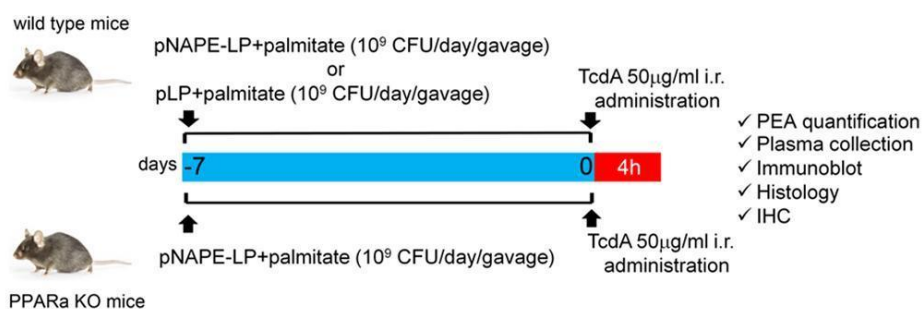


Figure 7. Experimental plan. Both wild type and PPARα KO mice received a daily prophylactic gavage administration of either pNAPE-LP (10⁹ CFU) or pLP (10⁹ CFU) 200µL suspensions with sodium palmitate (0.0003 µg/ml). At day 7, animals received a single intrarectal instillation of TcdA (50µg/ml). Animals were euthanized 4 hours later and PEA quantification and other molecular/histological analyses were thus carried on post-mortem isolated colonic tissue or related samples.

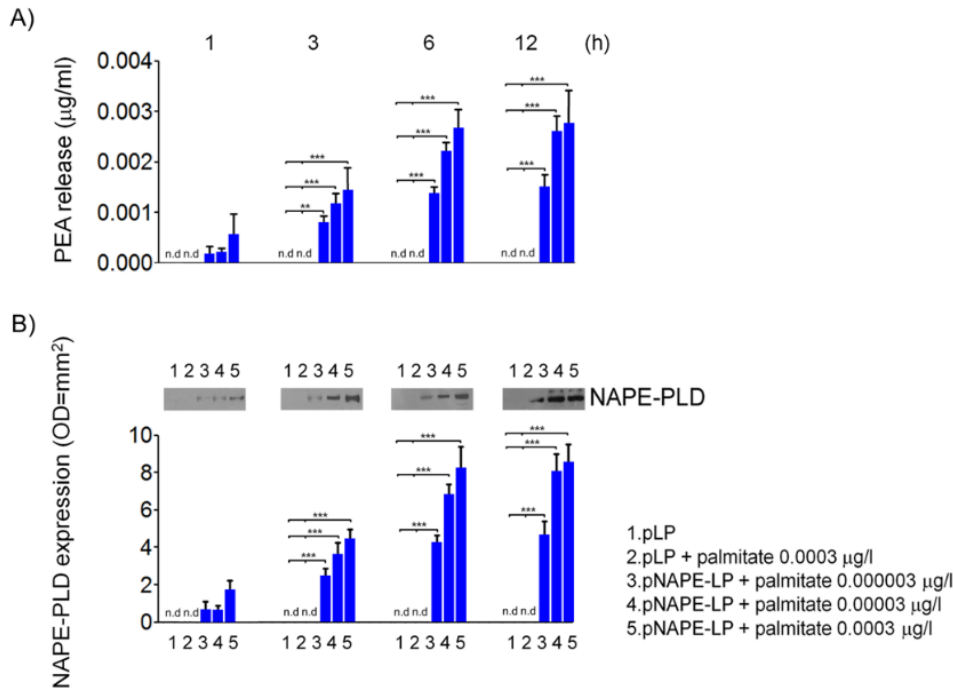


Figure 8. PEA is released in vitro by engineered NAPE-PLD *Lactobacillus paracasei* under palmitate dose and time dependent boost. A) PEA release was evaluated in bacterial supernatants at 1, 3, 6, 12h respectively by HPLC-MS and the results are expressed as mean±SEM of n=4 experiments performed in triplicate. Compared with pLP in absence of palmitate supply, exogenous palmitate (0.000003-0.0003 µg/l) dose- and time-dependently increased PEA release from pNAPE-LP probiotics, ***p<0.001, **p<0.01 vs both pLP and pLP in presence of palmitate 0.0003 µg/L. PEA levels were undetectable in pLP supernatants, even in the presence of the highest tested doses of exogenous palmitate (0.0003 µg/L). In the same conditions, (B) Western blot analysis of NAPE-PLD expression and relative densitometric analysis of immunoreactive bands, show that NAPE-PLD protein expression is time (1,3,6,12h) and palmitate-concentration (0.000003-0.0003 µg/l) dependent in pNAPE-LP engineered bacteria, whereas no expression was noticeable in pLP alone at the different time points, even in the presence of the highest palmitate doses (0.0003 µg/L). ***p<0.001 vs both pLP and pLP + palmitate 0.0003 µg/L. n.d = non-detectable.

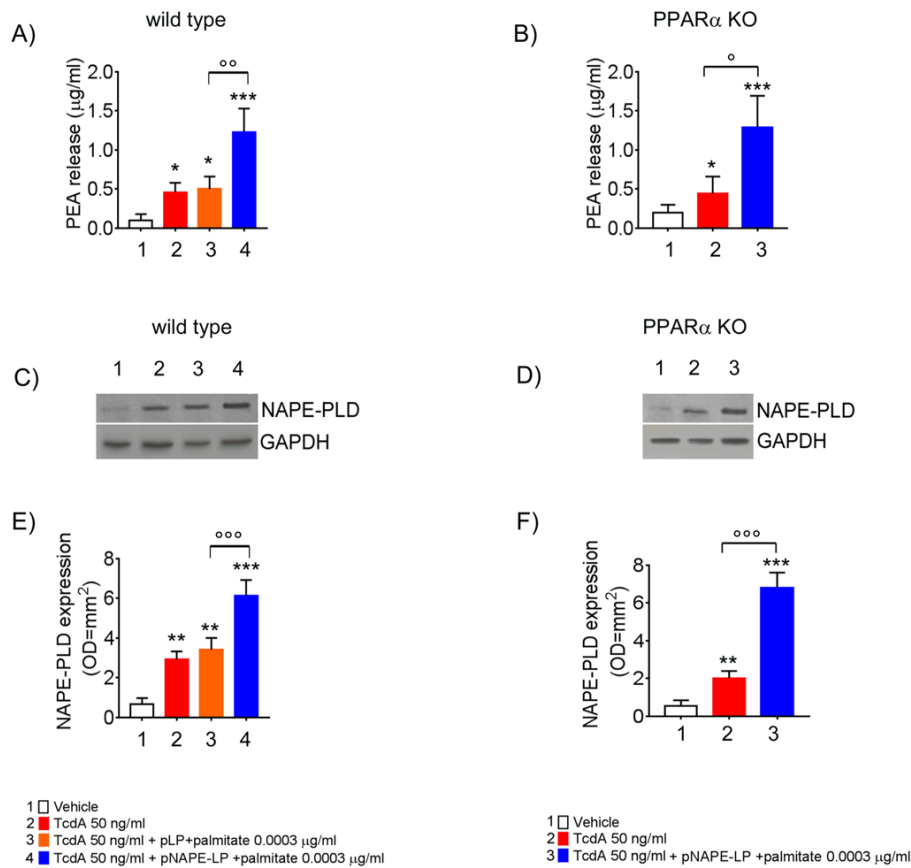


Figure 9. PEA is released in vivo by engineered NAPE-PLD probiotic under palmitate dose and time dependent boost. PEA levels were measured in both wild type (A) and PPAR α KO mice (B) colon by HPLC-MS and results are expressed as mean \pm SEM of n=6 experiments performed in triplicate. TcdA challenge caused PEA increase in both mice types (* p <0.05 versus respective controls). Figure A and B show that pNAPE-LP + palmitate (0.0003 μ g/Kg), resulted in a significantly increased PEA release as compared to vehicle (both *** p <0.001 vs vehicle) and TcdA-treated groups in both wild type and PPAR α KO mice ($^{\circ\circ}$ p <0.001 and $^{\circ}$ p <0.01 and $^{\circ}$ p <0.05 versus respectively TcdA groups). Fig. 2 also shows western blot analysis of NAPE-PLD expression and relative densitometric analysis of immunoreactive bands in both wild type (C) and PPAR α KO mice (D) colon and their relative densitometric quantification (E and F). Results are expressed as mean \pm SEM of n=6 experiments performed in triplicate. TcdA challenge caused an increased expression of NAPE-PLD in both mice types (** p <0.01 versus respective controls). pNAPE-LP and palmitate (0.0003 μ g/Kg) supply, resulted in a significantly higher NAPE-PLD protein expression in the colon of both untreated mice types (both *** p <0.001 vs vehicle) (C-D, E-F), and in both wild type and PPAR α KO mice treated with TcdA (both $^{\circ\circ}$ p <0.001 versus respectively TcdA groups).

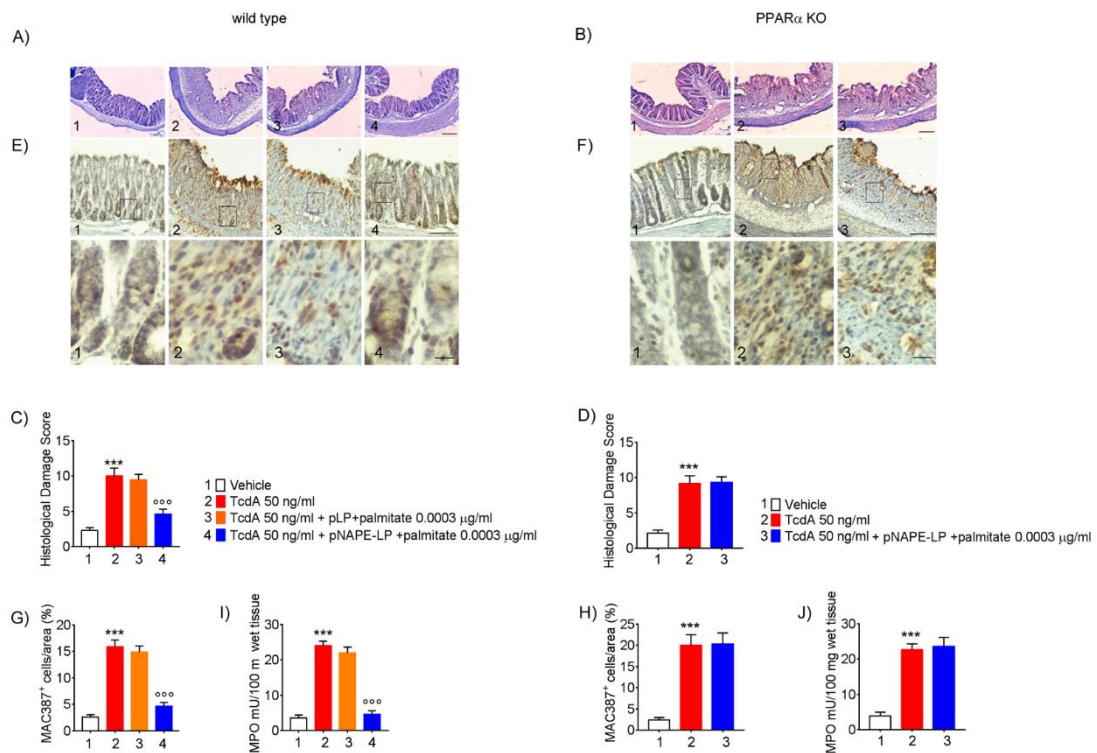


Figure 10. Prophylactic administration of pNAPe-LP and ultra-low palmitate dose accounts for histological damage attenuation with macrophage and neutrophils infiltration reduction in TcdA challenged mice. Haematoxylin and eosin (H&E) stained distal colonic specimens and (A-B) relative histological damage score showing the protective and PPAR α -dependent effect of pNAPe-LP/palmitate treatment on TcdA-induced colonic injury (C-D) in both wild type and PPAR α mice (magnification 4X, scale bar: 100 μ m). Figure also shows the effect of pNAPe-LP/palmitate association on the immunohistochemical expression of MAC387 positive cell (marker of macrophage density) in distal colonic sections deriving from wild type and PPAR α KO mice (E-F) (magnification 10X, scale bar: 100 μ m) and its relative quantification (G-H), as well as the myeloperoxidase (MPO) activity quantification (indirect evidence of neutrophils infiltration) in both mice types (J-K). Results are expressed as mean \pm SEM of n=5 experiments. ***p<0.001 versus vehicle; $^{\circ\circ\circ}$ p<0.001 versus TcdA-treated mice.

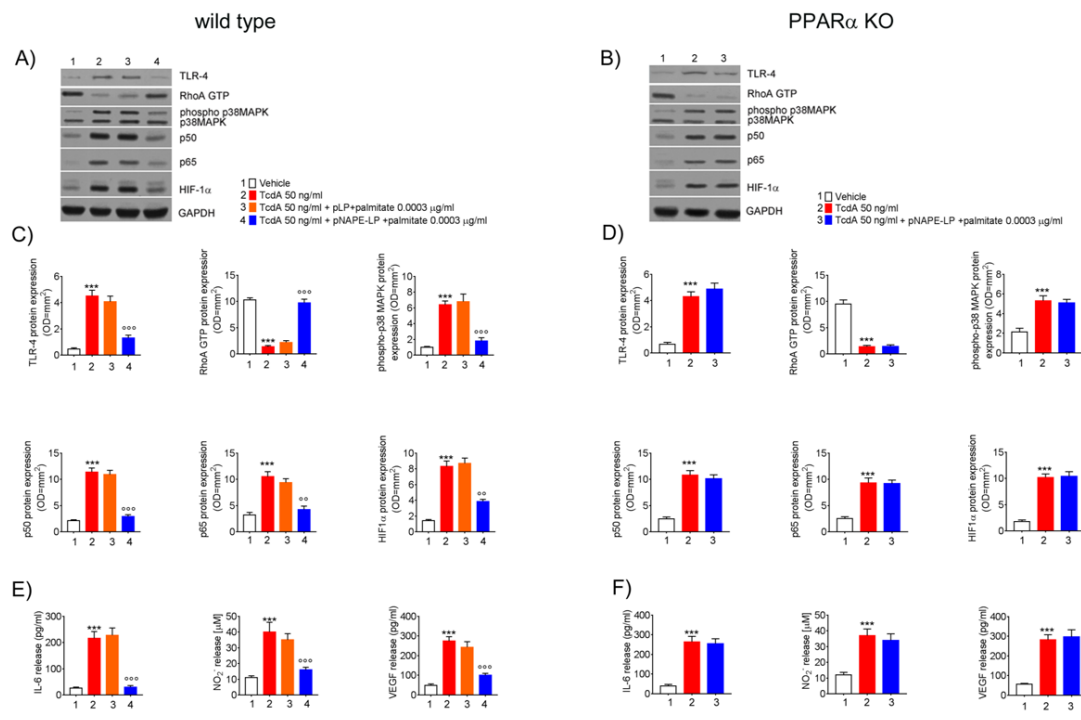


Figure 11. Prophylactic administration of pNAPE-LP and ultra-low palmitate administration on pro-inflammatory signaling molecules expression and release in mice colon. Immunoreactive bands showing TLR-4, RhoA GTP, phosphorylated/unphosphorylated -p38 MAPK, NF- κ B-related p50 and p65 and HIF-1 α protein expression in both wild type (A) and PPAR α KO (B) mice following TcdA challenge and their relative PPAR α -dependent decrease following pNAPE-LP/palmitate co-administration. Relative densitometric analysis (C-D) of each protein (arbitrary units normalized on the expression of the housekeeping protein GAPDH). Results were expressed as mean \pm SEM of n = 6 experiments performed in triplicate. ***p < 0.001 versus vehicle; and ^{oo}p < 0.001 and ^op < 0.01 versus TcdA. Figure also shows the effect of pNAPE-LP on TcdA challenged wild type (E) and PPAR α KO mice (F) in terms of release of IL-6, nitric oxide (NO) and VEGF in the plasma. Results were expressed as mean \pm SEM of n = 6 experiments performed in triplicate. ***p < 0.001 versus vehicle; and ^{oo}p < 0.001 versus TcdA.

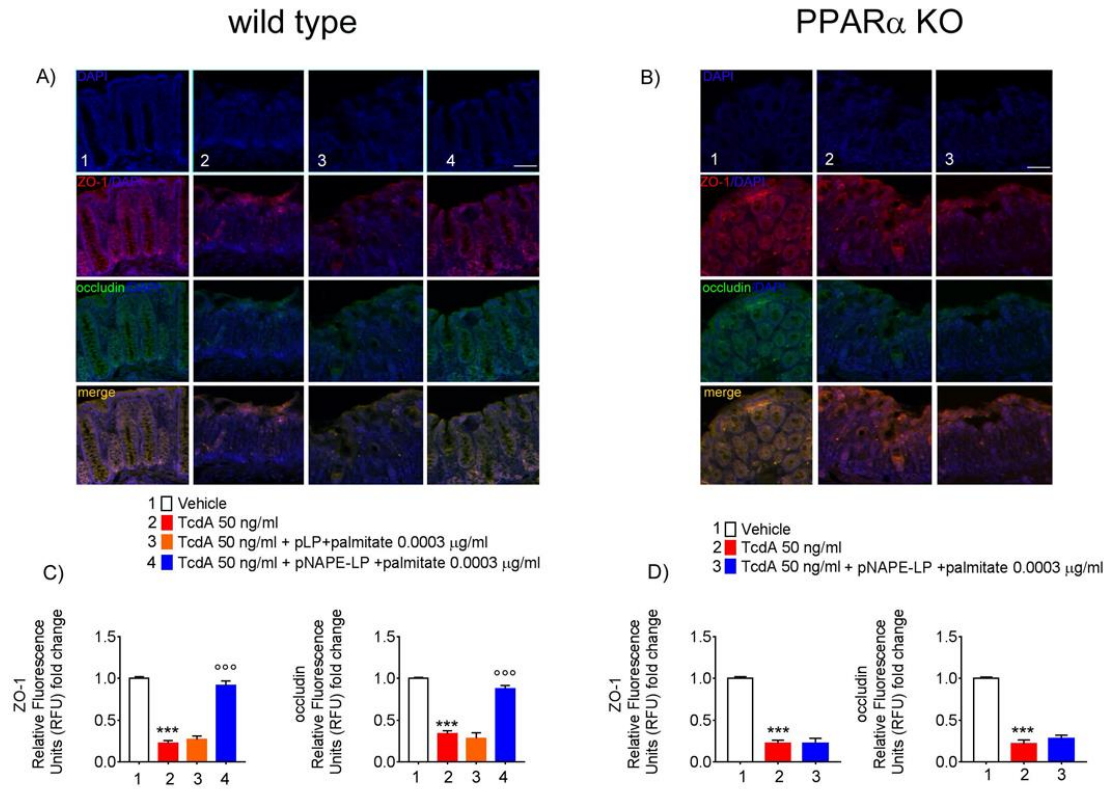


Figure 12. PEA released from pNAPE-LP and ultra-low palmitate co-administration restores TcdA-induced colon-barrier disruption, through the upregulation of tight junction proteins ZO-1 and occluding. Representative immunofluorescence images showing the expression of ZO-1 (red), occludin (green) and their merge (yellow) in both wild type (A) and PPAR α KO (B) mice colonic specimen with their respective quantification (C and D) showing the PPAR α -dependent protective effects of pNAPE-LP combined to palmitate (0.0003 μ g/Kg) co-administration. Nuclei were also investigated using DAPI staining. Results are expressed as mean \pm SEM of n=5 experiments performed in triplicate. *** p<0.001 versus vehicle; °°°p<0.001 versus DSS-treated mice. Scale bar = 100 μ m; magnification 10X. Scale bar: 100 μ m.

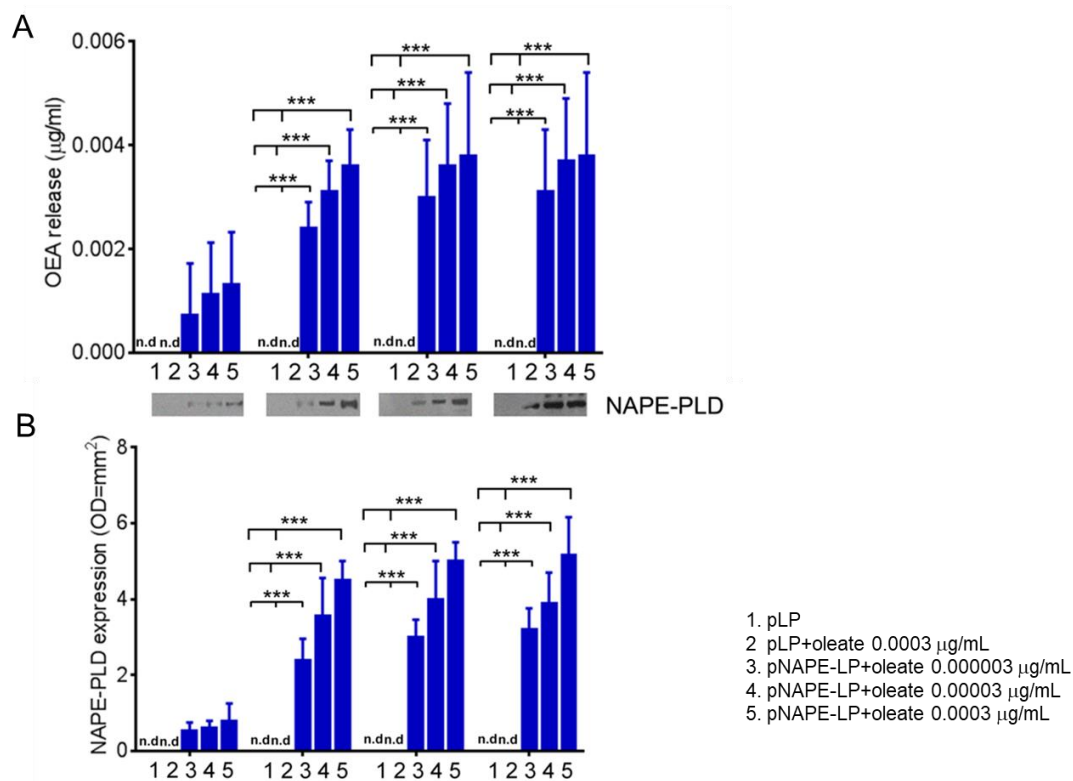


Figure 13. OEA is released in vitro by engineered NAPE-PLD *Lactobacillus paracasei* under oleate dose and time dependent boost. A) OEA release was evaluated in bacterial supernatants at 1, 3, 6, 12h respectively by HPLC-MS and the results are expressed as mean±SEM of n=4 experiments performed in triplicate. Compared with pLP in absence of oleate supply, exogenous oleate (0.000003-0.0003 µg/l) dose- and time-dependently increased OEA release from pNAPE-LP probiotics, ***p<0.001 vs both pLP and pLP in presence of oleate 0.0003 µg/L. OEA levels were undetectable in pLP supernatants, even in the presence of the highest tested doses of exogenous oleate (0.0003 µg/L). In the same conditions, (B) Western blot analysis of NAPE-PLD expression and relative densitometric analysis of immunoreactive bands, show that NAPE-PLD protein expression is time (1,3,6,12h) and oleate-concentration (0.000003-0.0003 µg/l) dependent in pNAPE-LP engineered bacteria, whereas no expression was noticeable in pLP alone at the different time points, even in the presence of the highest oleate doses (0.0003 µg/L). ***p<0.001 vs both pLP and pLP + oleate 0.0003 µg/L. n.d = non-detectable.

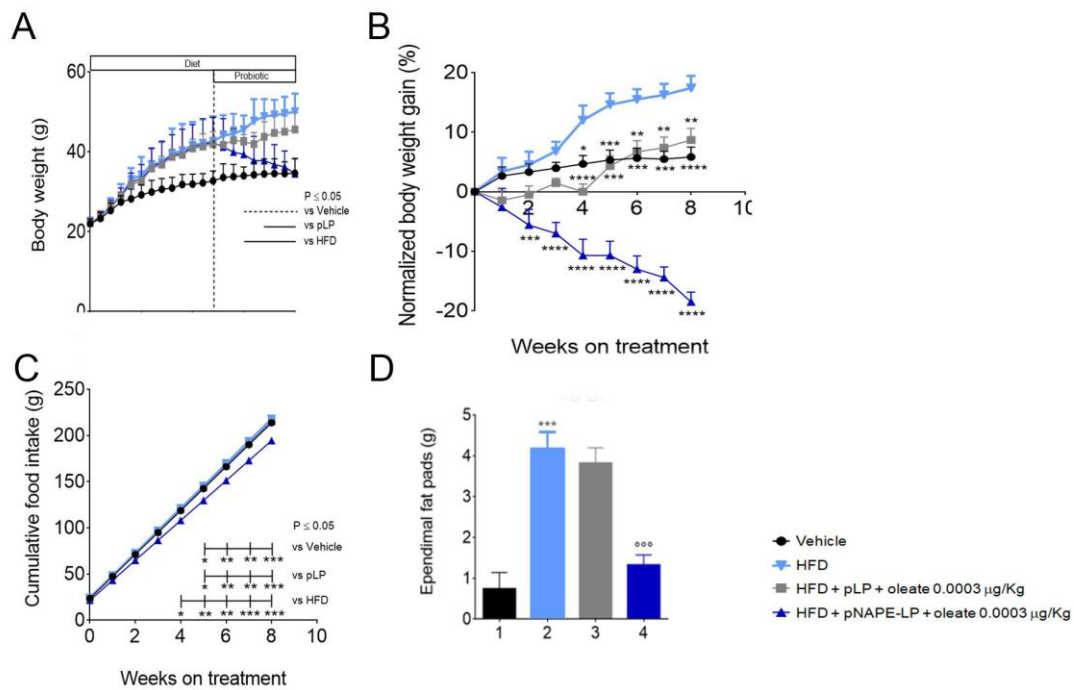


Figure 14. The co-administration of pNAPE-LP and oleate reduces body weight and modulates satiety in obese mice via the in-situ production of OEA. (A) Following probiotic treatment, a progressive weight loss was observed in HFD mice treated with pNAPE-LP combined with oleate (0.0003 µg/Kg), but not in the other groups (2-way ANOVA, for interaction $P=0.1420$, time $P=0.9438$, and treatment $P<0.0001$). (B) Cumulative effect of probiotic treatments on the gain in body weight after 8 weeks of treatment (1-way ANOVA, $*P<0.05$ and $****P<0.0001$ vs HFD group) (C) Treatment with pNAPE-LP associated with oleate (0.0003 µg/Kg) also resulted in a decrease cumulative food intake in HFD mice compared to the other groups (2-way ANOVA, for treatment and time $P<0.0001$) and (D) in epididymal fat mass (1-way ANOVA, $***P<0.001$ vs vehicle group; $^{\circ\circ}P<0.001$ vs HFD group). Results are expressed as mean \pm SEM, $n=8$ per group. Solid bars and dashed bars indicate time points with significant or not significant differences between pNAPE-LP and other groups, respectively (2-way ANOVA, $P < 0.05$ by Bonferroni's multiple comparison test).

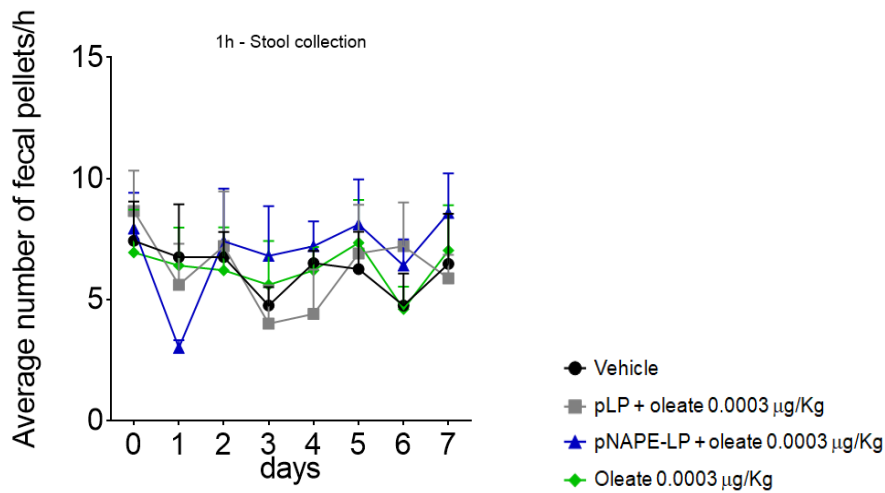


Figure 15. Probiotic treatment does not induce GI symptoms. Gut motility was monitored by 1h-stool collection test and average number of fecal pellets were measured once a day for 7 days. There was no significant difference between groups until the day 7 of treatment. Results are shown as mean±SEM.

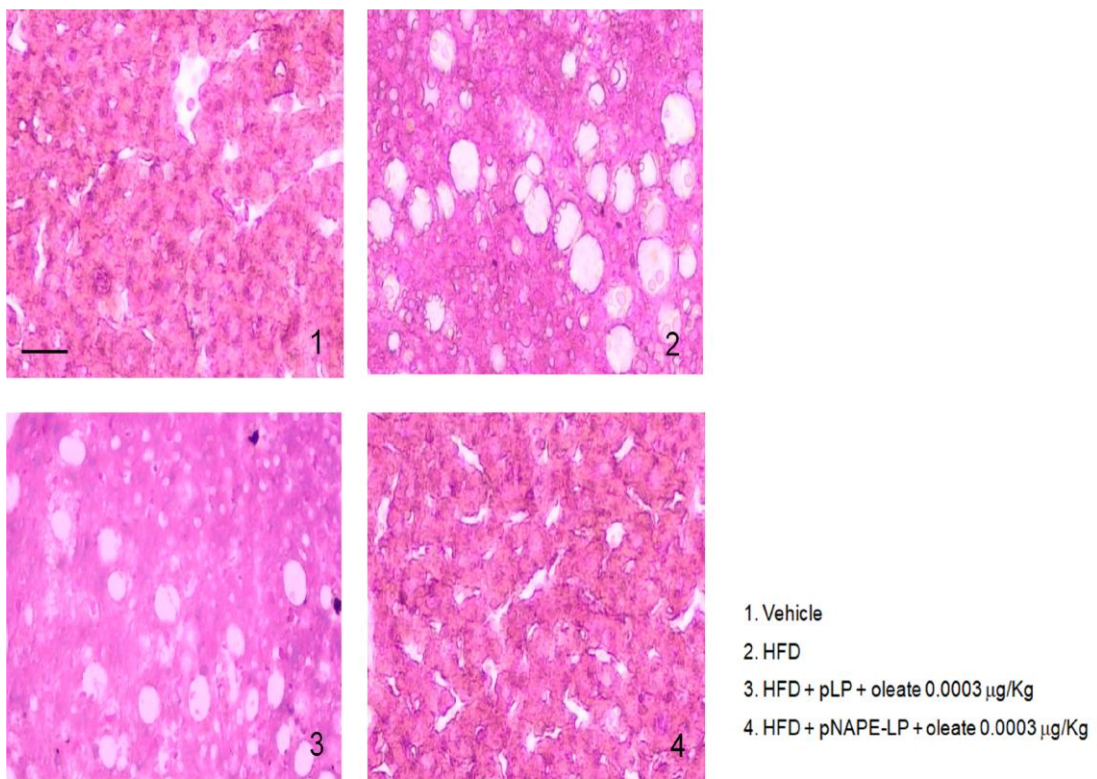


Figure 16. Treatment with pNAPE-LP associated with oleate reduces intrahepatic triglyceride accumulation. Hemotoxylin and eosin (H&E) staining of liver sections showed a decrease in triglycerides accumulation in the liver of HFD mice after oleate-combined pNAPE-LP treatment, but not in the other treatment groups.

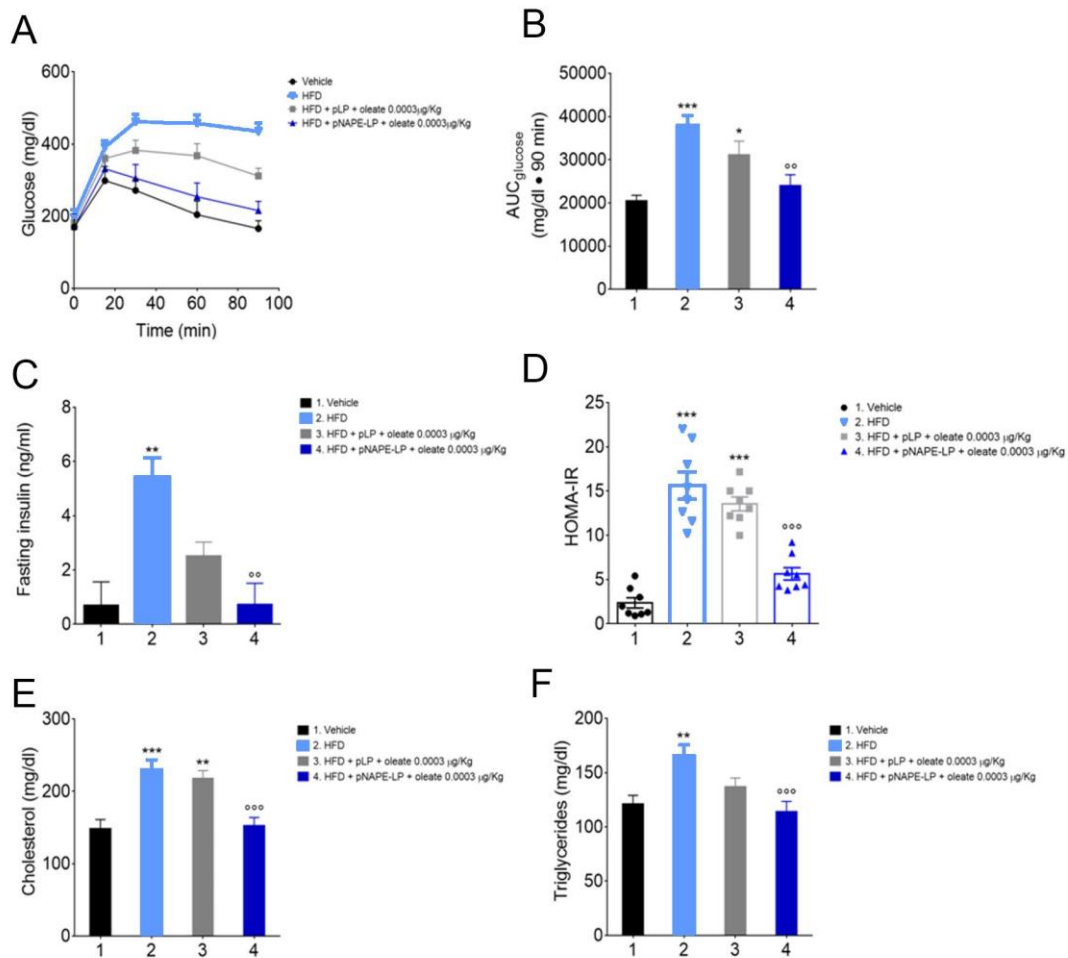


Figure 17. The co-administration of pNAPE-LP and oleate improves metabolic profile in HFD-treated mice via the in-situ production of OEA. Oleate-combined pNAPE-LP treatment improved glucose tolerance in HFD mice compared with vehicle or pLP/oleate groups. (A-B) Quantitative analysis showed that glucose peak and AUC differed markedly among the other groups (1-way ANOVA, * $P < 0.1$ and *** $P < 0.001$ vs vehicle group; ° $P < 0.01$ vs HFD group). (C) Lower fasting insulin levels (D) and a HOMA index improvement were detected after the treatment with oleate-combined pNAPE-LP in HFD mice (1-way ANOVA, ** $P < 0.01$ and *** $P < 0.001$ vs vehicle group; °° $P < 0.01$ and °°° $P < 0.001$ vs HFD group). (E) Basal cholesterol and (F) triglycerides levels were lower in pNAPE-LP/oleate-treated HFD mice compared with the other treatment groups (1-way ANOVA, ** $P < 0.01$ and *** $P < 0.001$ vs vehicle group; °°° $P < 0.001$ vs HFD group). Results are expressed as mean \pm SEM, $n = 8$ per group. Solid bars and dashed bars indicate time points with significant or not significant differences between pNAPE-LP and other groups, respectively (2-way ANOVA, $P < 0.05$ by Bonferroni's multiple comparison test).

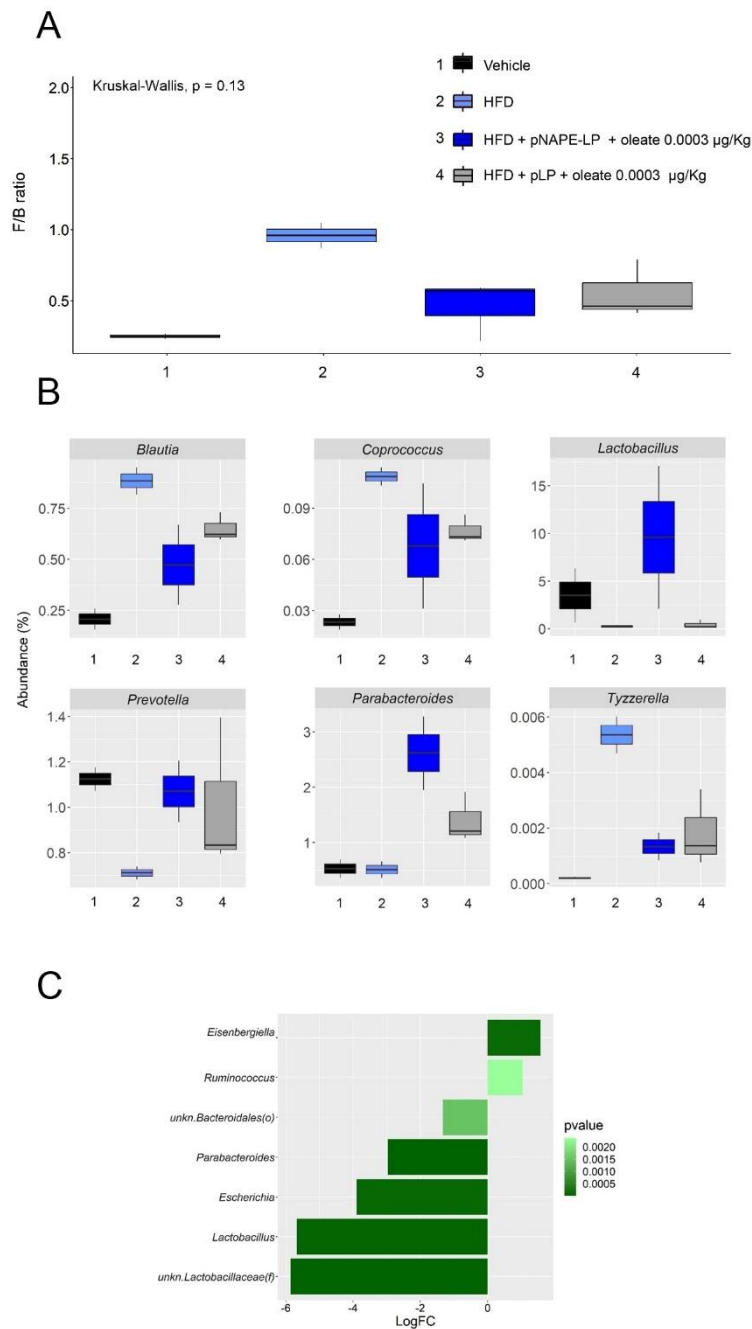


Figure 18. Effects of pNAPE-LP and oleate treatment on gut microbiota composition. (A) Analysis at phylum level: at week 20, a significant imbalance in the F/B ratio was observed in HFD mice as compared to mice fed with a standard diet (SD), while treatment with pNAPE-LP + oleate led to a decrease in the imbalance of the F/B ratio, with an average value as 0.46 (B) Analysis at genus level: a significant increase in *Blautia*, *Coprococcus*, and *Tynzerella* and a decrease in *Lactobacillus*, *Prevotella* and *Parabacteroides* in the HFD group vs SD; while pNAPE-LP treated mice displayed an increased representation for the genera *Lactobacillus*, *Bacteroides*, and *Prevotella*, (C) Log₂ fold-changes (Log₂FC) obtained by comparing HFD vs pNAPE-LP and oleate treated group at the end of our experimental plan.

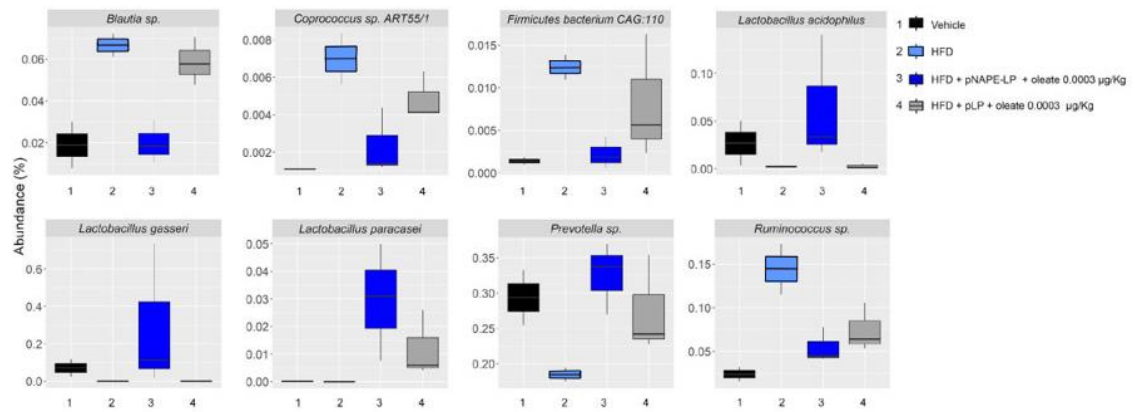


Figure 19. Metagenomic studies by shotgun sequencing (WGS) at species level. The analysis at species level showed an increase in the relative abundance for *Lactobacillus acidophilus*, *Lactobacillus gasseri*, *Lactobacillus paracasei*, *Prevotella sp.* in pNAPE-LP treated mice. This effect was not apparent in the group treated with native *Lactobacillus* (pLP) and oleate group.

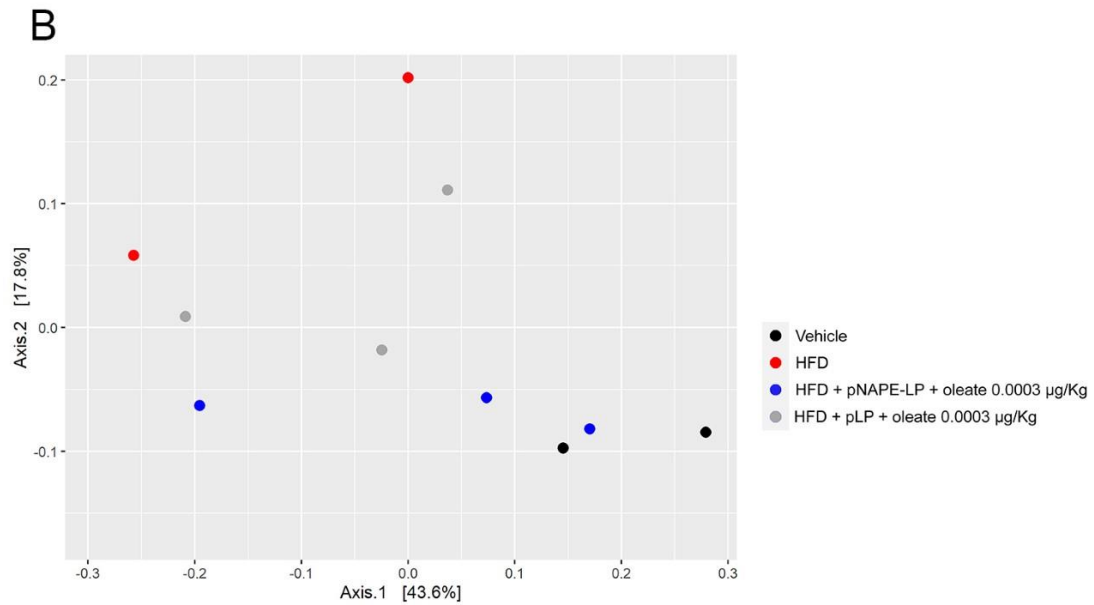


Figure 20. (A) Heatmap with the relative abundance obtained with DESeq2 at the significant species strain, with the replicates for the different experimental conditions. In the HFD group, the graph revealed a cluster with an abundance of *Ruminococcus* sp, *Tynzerella*, *Veillonella* and *Blautia* sp., and a reduction for the strains *Lactobacillus acidophilus*, *Lactobacillus fermentum*, *Prevotella*, *Akkermansia* sp. (B) Principal coordinate analysis (PCoA) based on Bray-Curtis distance. The results revealed cluster distributions, and two principal component scores, representing 43.6% and 17.8% of total changes. pLP and HFD groups showed a greater dispersion away from the control group, while the pNAPE-LP group tended to cluster with the control group.